CONCEPTUALIZING WIND VARIABILITY IN DELAWARE

by

Matthew C. Brianik

A thesis submitted to the Faculty of the University of Delaware in partial fulfillment of the requirements for the degree of Master of Science in Geography

Spring 2017

CONCEPTUALIZING WIND VARIABILITY IN DELAWARE

by

Matthew C. Brianik

Approved: _____
Dana Veron, Ph.D.
Professor in charge of thesis on behalf of the Advisory Committee

Approved: _____
Delphis Levia, Ph.D.
Chair of the Department of Geography

Approved: _____
Mohsen Badiey, Ph.D.
Acting Dean of the College of Earth, Ocean, and Environment

Approved: _____

Ann L. Ardis, Ph.D.
Senior Vice Provost for Graduate and Professional Education

ACKNOWLEDGMENTS

I would like to personally thank the group of people that advised, motivated and encouraged me throughout the process of completing this degree.

First of all thank you to Dr. Dana E. Veron, my advisor who pushed me harder than I wanted at times and never let me settle for anything but my best.

A big thank you goes out to Dr. David Legates who helped me master many of the statistical and technical skills used so heavily in this project.

Thank you Dr. John Madsen for all the help and being on my committee.

Thank you to my lab group, especially Dr. Joseph Brodie for his continual availability, and Alex Schroth for all the coding help.

Thank you to the UD Geography Department for accepting me as a Master's Degree Candidate, and my classmates for all the support and encouragement.

Thank you my fellow graduate students, it's hard to believe our time here is up, but I will always remember sharing these wonderful times with all of you.

Thank you to my family, especially my Mom and Dad who always did their best to support me to do my best; this has never stopped. You are the best parents I could ever ask for, and I hope I made you proud.

Thank you to my Fiancé, Pamela (soon to be Brianik) who in many ways motivated, encouraged and supported me throughout this process and always reminded me to keep the faith and trust that all is well and in God's hands.

Finally, I would like to dedicate this thesis to my family; the one I come from, the one I'm joining and the one I'm making, you are what gets me up in the morning.

TABLE OF CONTENTS

LIST OF TABLES

LIST OF FIGURES

ABSTRACT

This study explores ways to conceptualize the variability of winds in southern Delaware by analyzing annual wind observations from 29 weather observation stations. Wind speeds were interpolated to a standard height of 114 meters using the Log Law by determining the surface roughness at each station using the Danish Wind Industry Land Roughness Criteria. This criteria specifies the height of vegetation and various terrain aspects surrounding a weather observation station and provides a corresponding roughness length to aid in the calculation of winds aloft accounting for local wind speed influences.

These station data then were analyzed using several different techniques and subsequently interpolated to a 4.73-km grid using inverse distance weighting. Values of the mean, median, mean-median difference, standard deviation, upper and lower quartile, and quartile deviation were calculated for each grid point and mapped. This led to the characterization of four distinct regions of wind in southern Delaware – the Bay, Coastal, Inland, and Southwest corridors – the identification of which was assisted by auto- and cross-correlations between and among the stations to identify station-to-station similarity. The applicability of the Normal and Weibull distributions, as well as wind roses, for each of the four regions also was examined.

Results indicate in the assessment of wind power resource availability, particularly in areas with highly variable winds, reliance on the mean wind speed and the assumptions implicit in the mean about the normal distribution of the wind speeds may cause some biases, due to the degree of skewness in wind speed data. Consequently, the mean-median difference may prove to be a more useful tool in assessing the applicability of the accuracy of the mean wind speed in representing

winds over a given area. Moreover, the Weibull distribution better represents wind speeds than the Normal distribution and the quartile deviation is better than the standard deviation at describing variable wind patterns. As expected, the Coastal and Bay corridors represented the best sites for potential wind farms while the southwest corner of the state may also be useful for on-shore wind farms.

Chapter 1

BACKGROUND

This project was designed to shed light on a common ambiguity within the wind energy industry related to wind resource assessment. Within the wind energy industry wind speeds are typically represented by annual averages. This method does not accurately represent seasonal variability within the winds and this lack of information may mislead developers' primary assessments of the wind resource at a specific location. This project aims to clarify aspects of wind variability through a variety of analytical techniques and developed metrics.

1.1 Growth of Wind Energy in the US

Earliest references to wind energy and its capabilities date back to before the second century AD and Hero of Alexandria (Manwell et al. 2010). Since this time, wind energy has been exploited for travel in sailing ships, agriculture in grind mills and, within the last century, for generating electrical power. The use of wind for power generation in the United States (US) dates back to the late 1880s when Charles Brush developed the first noteworthy electrical generator powered by a wind mill (Manwell et al. 2010). Sadly, the wind energy sector's method of generating electricity and its many advantages were somewhat ignored in America from Brush's time until the 1970s when California invested in wind energy in response to the 1970s oil crisis (US Department of Energy (USDOE) 2008). Wind energy expanded in California to over 1.2 gigawatts (GW) of installed capacity which, at the time, was

over 90% of the installed wind capacity in the world. This wind generation expansion in the US lasted until 1986 when government incentives expired and the European market took the lead in wind energy production. Wind energy in the US showed little growth until recent years (as early as 2005) when new federal and state incentives coupled with advances in turbine technology made wind energy more financially attractive once again (United States Department of Energy (USDOE) 2008). This is evidenced by the decrease in the levelized cost in the US of wind energy in good and excellent sites by over 33% between 2008-2013 (USDOE 2015).

Wind energy in the US has been making strides over the last decade to catch up with Europe's wind industry. Between 2008 and 2013, $13 billion (B) US dollars has been invested annually in wind warm development (USDOE 2015). In 2015, wind power investment was $14.5B with 8.6 GW of newly installed capacity, representing 41% of all new power generation additions (Wiser and Bolinger 2015). In 2016, an additional 8.2 GW with a value of $13.8B in investment was installed with 79% of this capacity being completed in the final quarter of 2016, the second strongest installation quarter on record as shown in Figure 1.1 (America Wind Energy Association (AWEA) 2017). Total US wind energy capacity is 82.2 GW located throughout the US including Guam and Puerto Rico with 47 new projects recently commissioned in the 4th quarter of 2016 (AWEA 2017). Within the US, 12 states have 10% or more of their energy produced via wind power (Wiser and Bolinger 2015). The US offshore wind industry is budding with the recent installation of the United States' first offshore wind farm at Block Island (AWEA 2017), and future project commitments such as the South Fork 90 MW wind farm recently proposed by New

York Governor Andrew Cuomo approved to be completed by 2022 representing a committed investment of $740 million (Koeneman 2017).

Currently the wind resource in the United States has been extensively mapped by the National Renewable Energy Laboratory (Fields et al. 2016) located in Golden Colorado. NREL is part of the USDOE Office of Energy Efficiency and Renewable Energy and provides substantial resources for prospective wind developers and power companies with respect to wind resources and their related topics (Fields et al. 2016).

1.2 Current Maps and Methods

NREL has mapped the entire US wind resource at 80-meter (m) heights with a 2.5-kilometer (km) resolution and has even completed individual state analysis for 19 states as recently as 2010 (Wind Exchange 2010). Figure 1.2 shows an NREL map of the 80-m wind resource available within Delaware while Figure 1.3 shows the offshore wind resource available off the coast of Delaware at 90-m height. These resource maps are state of the art and of the highest quality available within the wind energy market, and are created via combining observational and model based data to generate wind maps showing annual representative wind speeds (Fields et al. 2016).

One dilemma for current NREL projections is that the initial 80-m wind speed assessment is becoming obsolete. 80-m hub heights are becoming outdated as developers design new wind turbines with hub heights in excess of 100 m to take advantage of faster wind speeds higher aloft in the atmosphere (Wind Exchange 2010), a prime example of this being MidAmerica energy beginning construction on the tallest turbine tower in the US in 2016 which when completed will have a tower height over 110 m (MidAmerica 2017). NREL has generated capacity projections

using current industry standards up to heights of 110 m and 140 m, but has not yet revised the available wind resource maps.

Another issue in wind resource assessment is that wind variability is not yet characterized spatially in a generalized manner. This may be because in preliminary site analysis, the annual mean wind speed provides an indication of where the highest generation potential exists (NYSERDA 2010). This may be enough to satisfy industry professionals' financial reservations in preliminary project spending in that industry professionals in large part desire to spend no more than 1% of total project cost on resource assessment (Fields et al. 2016).

However, this does not provide much information about the distribution of wind speeds. Wind speeds can be highly variable, on numerous time scales. For example, an average daily wind speed of 5 m/s can mask the temporal distribution of those wind speeds. Consider Station A where the wind is 2.0 m/s for half the time and 8.0 m/s for the other half while Station B has evenly distributed wind speeds of 4.0 m/s and 6.0 m/s. For both Station A and Station B, the average wind speed is 5.0 m/s and, using just the average wind speed metrics, they have identical wind characteristics (Figure 1.4). In practice, however, the difference between these two stations is substantial and the potential output from a wind Turbine at each of these locations may vary greatly. That is why after a preliminary site is identified, wind farm developers install wind monitoring towers, often at great expense, to measure the actual winds at the site (NYSERDA 2010). These data are then used along with the details of the proposed turbines, to calculate actual power generation (Fields et al. 2016).

Since one of the largest obstacles facing the wind energy industry is accounting for variability within the wind resource (NYSERDA 2010, USDE 2015), it is of interest to explore techniques that would allow wind developers to have a preliminary assessment of the wind variability, potentially as a map, when performing initial site selection. Accounting for variability of wind speeds during the planning phase of wind farm installation will improve prediction of wind farm generation potential and may assist with the integration of wind into the electrical grid (Office of Efficiency & Renewable Energy (OERE), 2016). Thus, characterization of wind variability might enhance penetration of wind power generation into national and regional electricity generation.

There are many ways to characterize wind speeds and their variability. The most common form of displaying wind speeds is mean wind speeds represented annually, as is the case in Archer and Jacobson (2003), or for a specific sub-annual time period such as monthly mean wind speeds (Garmashov and Polonskii 2011). Using the mean as a reference, both of these studies, as is the industry norm (Holttinen 2008), represented variability using standard deviation.

Power spectral analysis is another technique used to characterize variability in wind speeds and has been used extensively in predicting power generation fluctuations cause by wind variability within existing wind farms. This is shown in the analysis conducted by Sorensen et al. (2002) of modeled wind farm production, and the analysis of two separate wind farms over the course of a 10-day period conducted by Apt (2007). Autoregressive integrated moving average models (ARIMA) are used to identify shorter time period variability and have experienced success, although are only applicable to smaller time scales as demonstrated by Yunus et al. (2016) in their

ARIMA study of modeled 10-minute wind speed data in three locations located in the Baltic Sea. Other statistical approaches have also been employed such as empirical orthogonal function analysis, showcased by Davy et al. (2010) in their analysis of 2 years' worth of modeled data, and principal components analysis, used by Klink and Willmott (1988) to analyze annual wind speeds of 68 weather observation stations across the United States.

The numerous techniques studies for quantifying wind variability hint at the reality that wind erraticism is still in need of clarification. Therefore, in this project I explore developing a new way of analyzing and characterizing local and regional winds such that wind variability can be easily understood, and taken into account earlier in the assessment process of potential wind farm sites. Within this study, one year's worth of wind speed and directional data was taken from 29 weather observation stations located within the lower 2 counties of Delaware.

This data was then analyzed using the following statistics, which fall into three classes Basic, dispersion, and similarity: mean, median, wind rose plots, upper quartile and lower quartile; standard deviation, quartile deviation, mean-median difference, skewness, and Weibull and Normal distributions; Pearson correlation and autocorrelation statistics.

1.3 Study Area

Although Delaware is one of the smallest states in the United States, it still boasts one of the densest weather monitoring networks in the nation, the Delaware Environmental Observing System (DEOS 2016). As a result, Delaware is an ideal location to test new methods for assessing various meteorological phenomena, including wind variability.

The research area chosen for this study (Figure 1.4) is comprised of Kent County and Sussex County Delaware, the southernmost two counties in the State. This area was chosen because it is a coastal plain environment possessing generally lower relief and more uniform topography. New Castle County, the northern county in the state transitions into the Piedmont with higher relief terrain, and was excluded from this study due to associated meteorological complications induced by this topography (Delaware-Map 2015). Along the coast in Sussex County, Delaware, notable urban/suburban development exists although this decreases considerably away from the coast, where the prominent land classification is farmland.

1.4 Spatial Variations in the Wind

The research area was expected to subdivide according to known influences on the wind into three major types. The sub-areas were initially identified as Bay, Coastal and Inland and each had a corresponding roughness coefficient based off the terrain features present. Roughness coefficients are a measure of surface obstruction and serve to limit wind speeds such that areas with high roughness coefficients will have lower wind speeds than areas with lower coefficients (Manwell et al. 2010). It was expected that roughness effects on Bay winds will be less than Inland winds and therefore Bay observed wind speeds were expected to be higher than Inland wind speeds with Coastal wind speeds between the two. An additional point of interest in this study was how local winds would be effected via the predominant winds in the region. Generally winds in the Delaware region are characterized by northwesterly winds that dominate in the winter months while southerly winds are more prevalent in the summer season, see Figure 1.6 (Hughes and Veron 2015). Additionally, along the

coast and bordering locations within the Bay and Inland areas, sea breeze effects have a daily influence on wind speeds and direction (Hughes and Veron 2015).

1.5 Project Summary

This study explored many different methods of assessing wind variability on multiple scales using observed wind data from three different observing networks. The stations were assessed individually, and then grouped geographically, to observe spatial variations in the wind field. Correlations among stations were explored. Finally maps of various analyses were produced using ArcGIS to further refine our understanding of the characteristics of the wind resource available in southern Delaware.

Using results from this study, two metrics for quantitatively defining wind variability are proposed for use in future wind farm siting and planning: mean-median difference (MMD) and quartile deviation (QD). These metrics would enable planners to better evaluate average wind speed for a given site by providing simple and easily calculated statistics thus enhancing planning efforts. The MMD metric provides an assessment of how representative mean wind speed is for a given site. For example, when the MMD is positive (as is usually the case), the peak of the distribution is shifted (i.e., longer tail) toward higher wind speeds. Since the mean is more sensitive to the higher outliers, the difference between the mean and the median is indicative of the degree to which the wind distribution is asymmetric. Thus, the greater the MMD, the more asymmetric the distribution.

The QD metric is useful in that it provides the dispersion of wind speed around the median. The QD is chosen over the standard deviation because it is less sensitive to outliers since distributions of hourly wind speeds are typically asymmetric

due to irregular distributions inherent in wind speeds. Thus, the QD is a measure of the range of wind speeds and, can consequently yield insight into the relative consistency of power output in a given area.

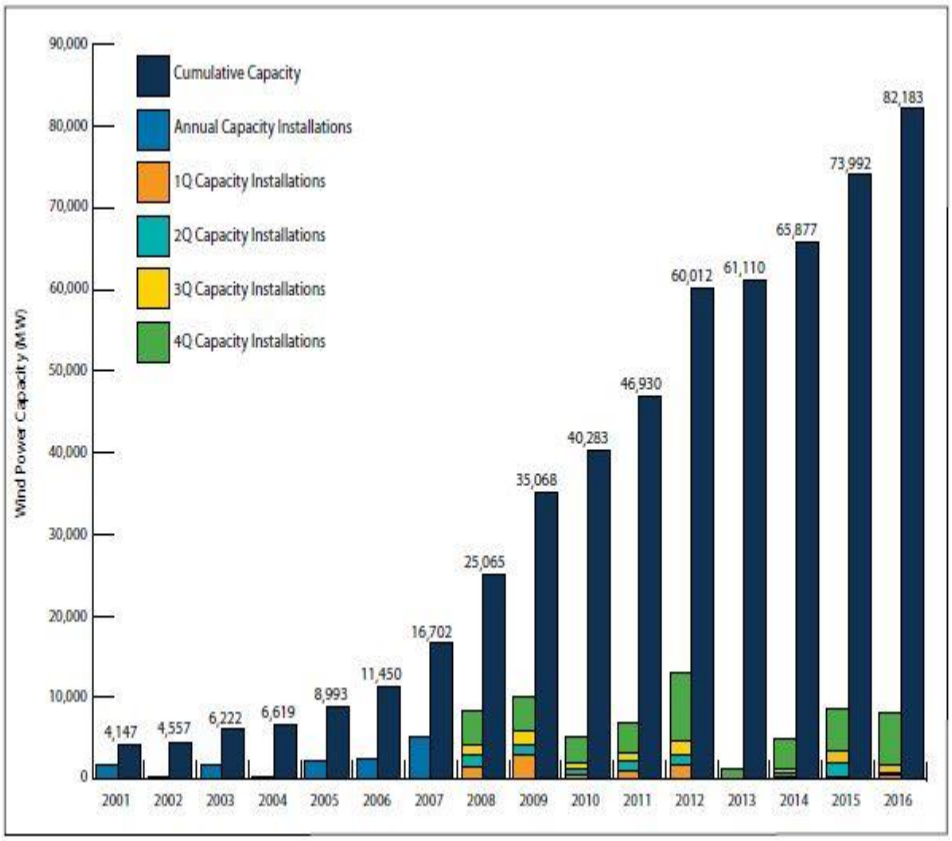

1.1 Wind Power Capacity Growth 2001-2016 (source: AWEA 4th Quarter Report 2016).

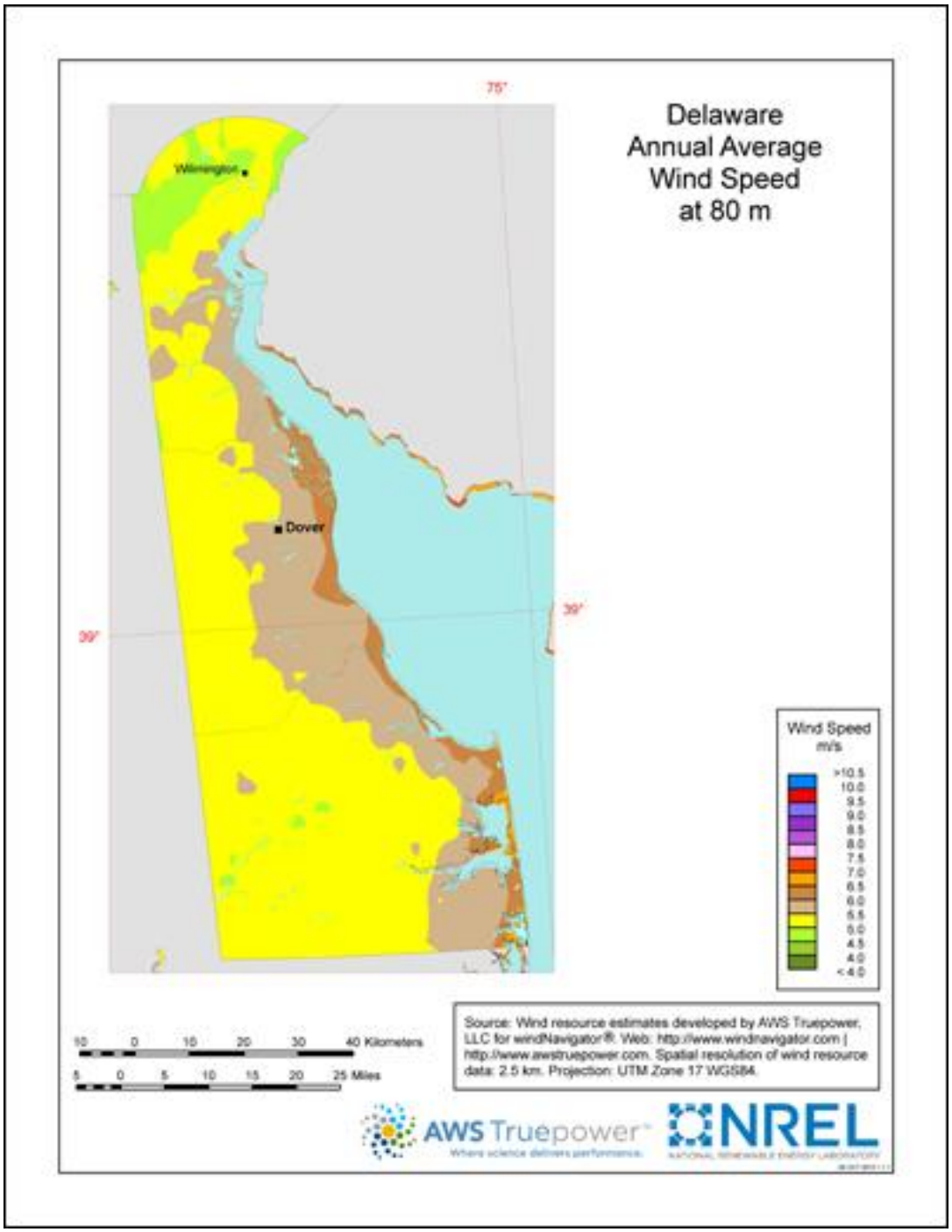

1.2 NREL 80-m wind resource for the state of Delaware (source: NREL 2017).

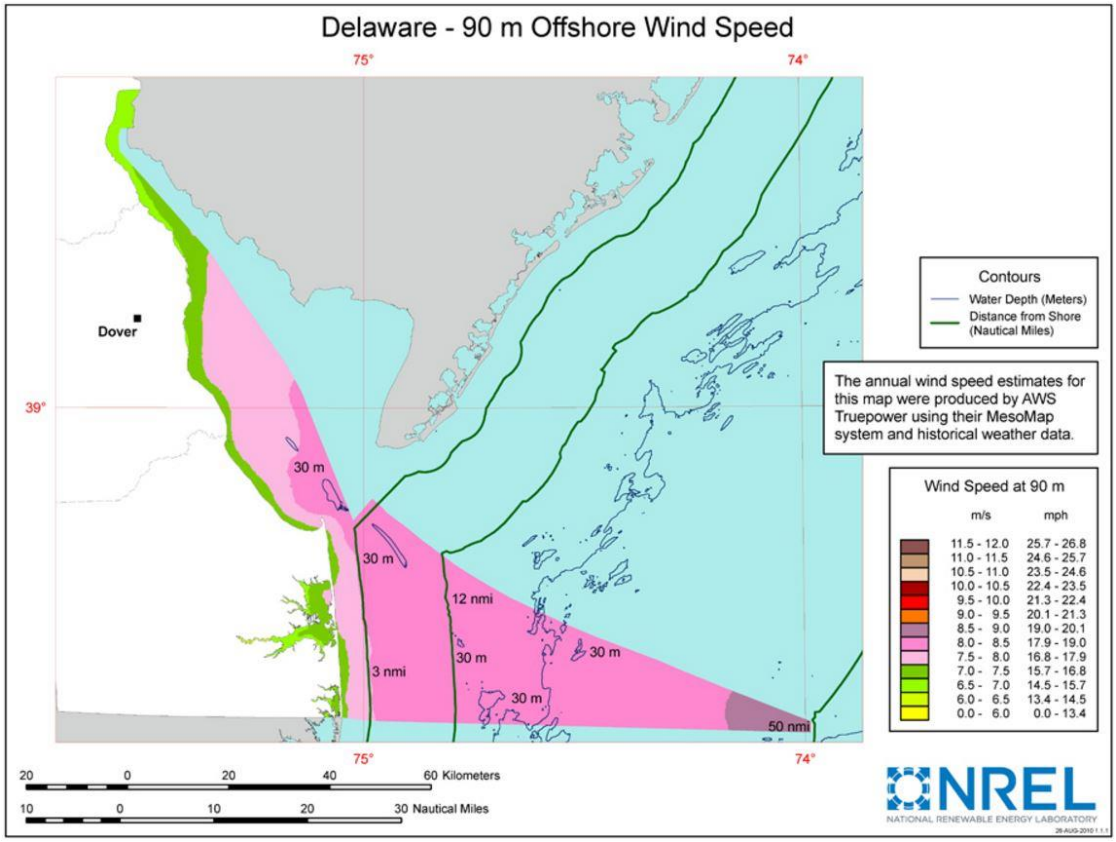

1.3 Offshore wind resource map from NREL for a hub height of 90-m (source: NREL 2017).

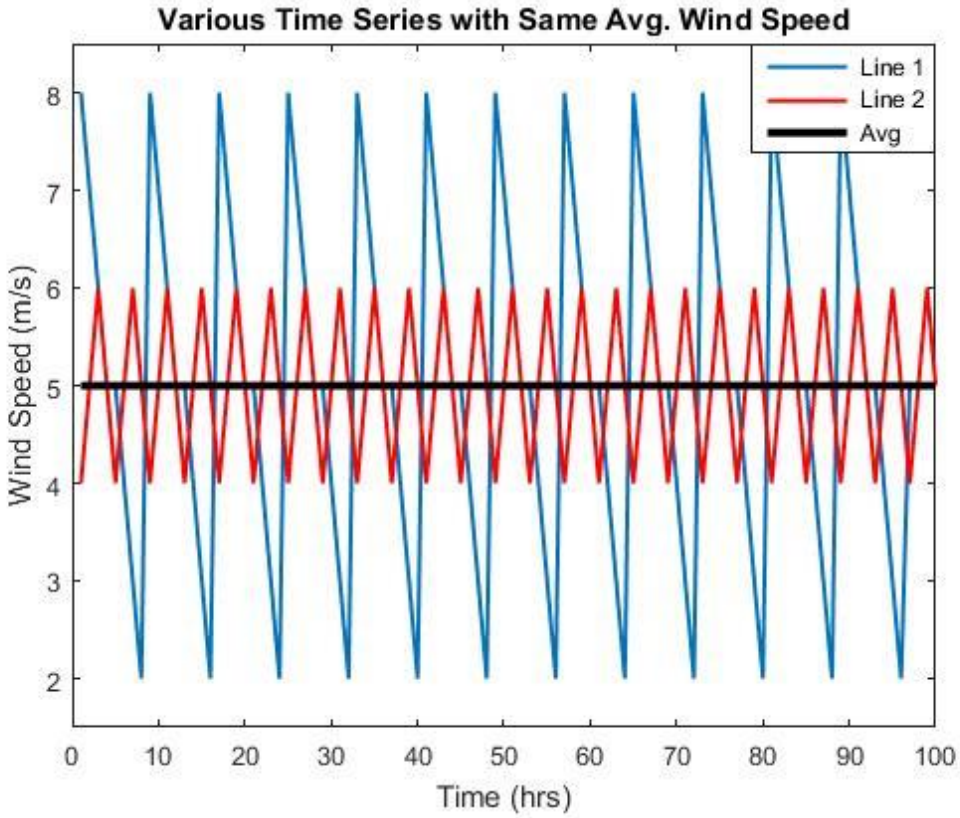

1.4 Hypothetical example of 2 different wind series with same average wind speed.

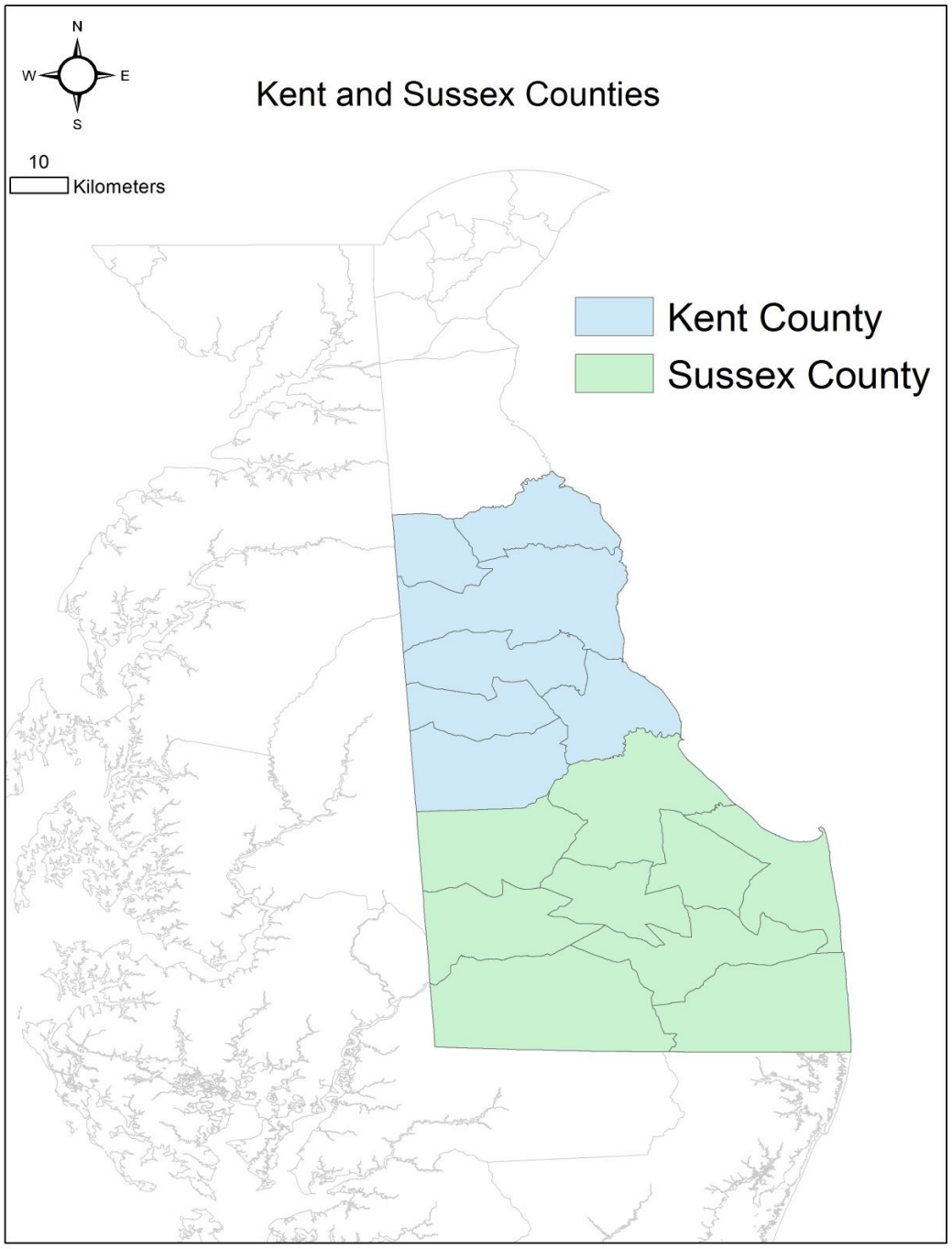

1.5 Map of the Delmarva Peninsula highlighting the location of Kent (blue) and Sussex (green) Counties.

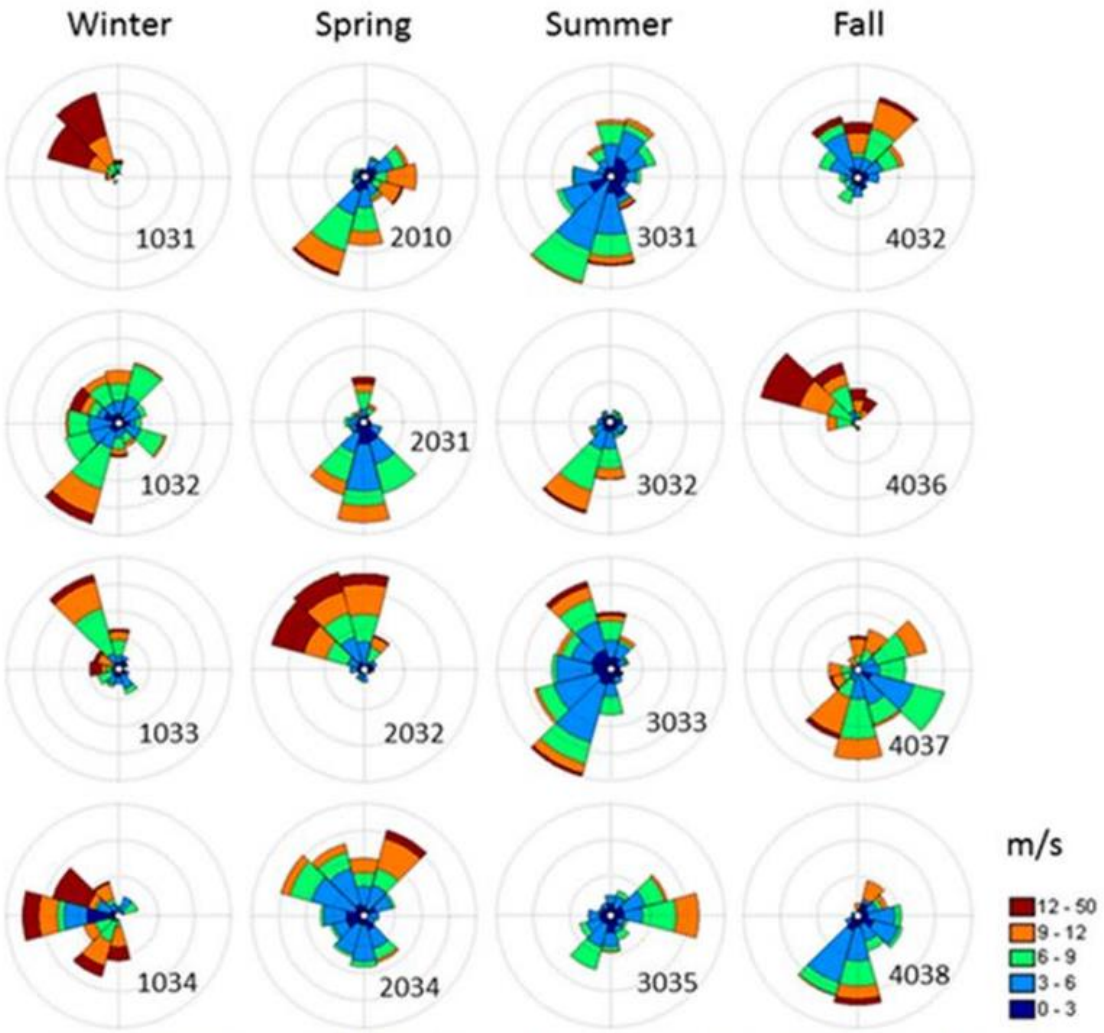

FIG. 5. Observed 10-m wind roses for B44009 for the most frequent synoptic types per season. Each wind rose is plotted on the same axes as in Fig. 1 and is composed of at least 12 days between 2006 and 2012.

1.6 Figure 5 from Hughes and Veron (2015) showing the typical distribution of wind speeds and direction at buoy 44009 by synoptic type.

Chapter 2

DATA AND METHODS

Wind speed can be observed using numerous techniques, ranging from standard 3-cup anemometer measurements to satellite remote sensing. The most frequently used method employs a 3-cup anemometer, sometimes coupled with a wind vane, which can be placed in almost any environment with relative ease at a low cost as evidenced by the Department of energies anemometer loan program (Fields et al. 2016). Despite their ease of installation and wide spread use, anemometers have been known to produce data plagued with ambiguity due to lack of quality control and regular maintenance of observation systems. In this study, all of the observations were taken by cup anemometers mounted on meteorological towers of varying height.

Several other methods of sampling in situ wind data are available, two common forms of which are using ultrasonic anemometers and GPS tracked weather balloons. Ultrasonic anemometers are stationary devices that use sound pulses between emitter and sensor that are modified by passing winds interacting with the ultrasonic anemometer to measure wind speeds and direction (NYSERDA 2010). These ultrasonic anemometers require very little maintenance, although they can be expensive.

A final method often used to measure profiles of atmospheric characteristics is in-situ sampling with radiosondes. Radiosondes are measurement devices hung under a weather balloon that report atmospheric conditions of the atmosphere as they rise through it. Radiosondes are affordable and useful for spot sampling the atmosphere, however because they are launched at specific times and can take up to 2 hours to profile the atmosphere, they are not a good tool for providing continuous sampling of

the near-surface atmosphere. In addition, they can be heavily influenced by local weather, especially winds, in terms of where they observe (Hall et al. 1984).

Meteorological towers are structures similar to scaffolding that are used to mount a series of instruments at a desired height or heights in a professionally selected setting. These towers are installed and maintained by a parent organization that is usually responsible for numerous towers. Typical quantities measured at a meteorological tower include atmospheric temperature, humidity, and pressure, along with wind speed and direction, among others. Meteorological tower observations are quality controlled and the tower is maintained by the organization that owns it, thus these towers tend to produce more reliable quality-controlled data than an aggregated group of independently owned anemometers (DEOS). Unfortunately, the installation of a meteorological tower can be expensive, especially at tower heights beyond 10-m. Any meteorological tower that has the capability of hosting instrumentation at multiple levels are more expensive than towers with a single set of instruments and are thus not as widely employed (NYSERDA 2010).

There are other ways of observing atmospheric properties, such as wind speed, through remote sensing techniques by sensors on both ground based and satellite platforms. Sonic Detection and Ranging, or SODAR, is one of these methods. SODAR technology has been around for over 50 years but has become a popular method of measuring wind speeds due to the needs presented by the wind energy industry (Fields et al. 2016). SODAR applications are ground based with a range of roughly 200 meters, and rely on interpreting the Doppler Shift of sound waves interacting with different air densities within the atmosphere, thus wind speeds can be derived from the change in Doppler shift detected (Hasager et al. 2008). An additional

ground based data gathering technique employs 915 MHz profilers. These profilers behave in a similar way to SODAR in that they rely on the Doppler shift to calculate wind speeds, although they rely on radio waves instead of sound waves (NYSERDA 2010). One detriment of 915 mhz profilers is that they can be highly influenced by precipitation as demonstrated in the work conducted by Lambert et al. (2003).

Doppler LIDAR (Light Detection and Ranging) is another surface remote sensing technique that has been recently adapted to measure wind speeds in a given volume. Doppler LIDAR has become more feasible and applicable to modern wind resource assessment as LIDAR technology has improved (Korb et al. 1997). In fact, the International Electrotechnical Commission (IEC 2017) just published a new standard, that allows LIDARs as an alternative or supplementary measurement technique to cup anemometers mounted on a meteorological tower, a sign that LIDARs are becoming accepted in the wind energy community (IEC 2017). Advantages of LIDAR are high accuracy and consistent measurement for a given area, as well as the ability to sample the atmosphere at various levels without having to construct a tower to host the meteorological instruments (Hasager et al. 2008, Korb et al. 1997). Despite the numerous advantages of LIDAR measurement techniques, this measurement system is overshadowed in large part by relatively high cost associated with installing and maintaining these systems on land and thus they are generally not the first choice to be used for wind observations.

Wind speeds can also be remotely observed though various satellite remote sensing techniques. The satellite-retrieved winds are frequently calculated by tracking the motion of features such as clouds, water vapor or surface waves and then converted to wind speed (Chang and Wilheit 1979). These methods also employed in

tracking tropical cyclones and other large scale atmospheric phenomena and have been growing in acceptance and use over the last several decades (Huffaker and Hardesty 1996). Satellite remotely sensed data were not used for this study because of the generally large coarse spatial resolution (Bourassa et al. 2009) relative to the size of the area of study. Additionally, satellite sensing is not generally capable of providing the temporal resolution necessary for this study (Pimenta et al. 2008).

Due to the large accessibility and quality of observations made by several quality observing networks at meteorological near-surface stations in and near the two Southern counties in Delaware, the data in this thesis are exclusively from cup anemometers mounted on short towers or buoys.

2.1 Station Data

In this study, wind speed measurements were obtained from 29 meteorological stations for a single year, 2015. This year was chosen because it has the most complete time-series possible for all 29 stations. Although many additional stations were considered for use, they eventually were dismissed due to missing or inconsistent data. Figure 2.1 provides a graphical representation of the stations employed in this study. Note that there are several stations outside the study area. These stations have been added to the study to evaluate the winds of the stations at the edge of the study area. Even though only one year of data was used to characterize wind variability in Southern Delaware, studies have shown that this is sufficient to explain 85-95% of the meteorological variability within a potential wind farm location (Bechrakis et al. 2004). In comparison to the buoy data shown in Hughes and Veron (2015), this year does not appear to be an outlier in terms of annual average wind speed.

The data employed in this study came from four different observational databases. These databases are the Delaware Environmental Observing System (DEOS), the National Data Buoy Center (NDBC), the National Estuarine Research Reserve System (NERRS), and the WeatherBug Monitoring System (WB). All stations used in this project are designated by their call signs (Table 2.1). DEOS weather stations begin with the letter "D", NDBC buoy stations are prefixed with "BUOY", the sole NERRS station is BUOY_SCLD1, and the WB station is LEWE_MOB. These stations and their locations are listed in Table 2.1 and are geographically represented in Figure 2.1.

2.1.1 Delaware Environmental Observing System (DEOS)

DEOS is an environmental data service provider based at the University of Delaware that has been in operation for over 10 years (DEOS 2017). The DEOS program is committed to providing environmental data to private, academic and industry professionals to better assist these groups in their varied pursuits. The State of Delaware relies heavily on DEOS to assess various environmental events and provide guidance as to steps to take in preparation (DEOS 2017). DEOS operates 50 different weather monitoring stations throughout the state of Delaware and Chester County, Pennsylvania, and archives data from over 200 additional environmental observation stations supplied by numerous partnering organizations. Figure 2.2 shows a typical DEOS weather monitoring station located at 39.6059°N, -75.7269°W that monitors temperature, pressure, humidity, wind speed and direction. The DEOS data can be found at http://www.deos.udel.edu.

The 20 DEOS stations (see Table 2.1) employed in this study are located in various settings ranging from local airports to beachfront property to waste

management plants. These settings have unique terrains and require individual characterization of the surface features for each site. Each station was assessed using the roughness scale developed by the Danish Wind Industry Association which was preferred in this study over other roughness coefficient scales due to its highly detailed classification scheme (DWIA 2003). Sensor heights for measuring wind speed were recorded and accounted for in all calculations performed s described in section 2.2.4;all DEOS wind speed instrumentation for these 20 station sampled wind speeds at 3-m above ground level with the exception of station DIRL which had sensors located at 4.6 meters. All DEOS observations consist of 5-minute average wind speeds and directions. Table 2.2 lists all DEOS stations with roughness coefficient length, and the location of the sensor.

2.1.2 National Data Buoy Center

The National Data Buoy Center (NDBC) is part of the National Weather Service's effort to monitor, educate and investigate the variability and dynamic nature of the planet's oceans and its related processes by providing continuous surface observations of meteorological and atmospheric phenomena such as wind speed and direction, tidal fluctuations, and temperature variation (NDBC 2016). Some of these stations are located on moored buoys while others are located on land, in coastal waters. NDBC has been around since the late 1960s and aids the scientific community and the public in understanding oceanographic processes. NDBC quality controls all data through a series electronic and manned approaches. All NDBC stations receive routine maintenance to ensuring all observations adhere to strict tolerance levels listed on the NDBC database found at http://www.ndbc.noaa.gov/qc.shtml. Additionally, data are cross referenced between stations to ensure similar reporting between stations

of the same area (NDBC 2016). Further proof of NDBC data quality was showcased in 1987 by Gilhousen who found that wind speed data from buoys within 5 km of one another will have only 0.6-0.8 m/s differences in standard deviation between one another with reference to mean wind speed. Wind speed and direction data from 7 buoys or stations in the NDBC network were used in this study. NDBC Buoy data can be found at http://www.ndbc.noaa.gov (NDBC 2016).

In the region of study, most of the 7 stations utilized in this project are actually located on land, as opposed to on an ocean buoy (Figure 2.3). NDBC stations tend to be located near or in open water. Roughness coefficients vary between NDBC station locations, and unlike DEOS stations, NDBC sensor heights vary considerably as well. Sampling frequency among NDBC stations are uniform with 6-minute averages. Table 2.3 lists all NDBC stations with ID number, roughness coefficient, and location.

2.1.3 National Estuarine Research Reserve System

The National Estuarine Research Reserve System (NERRS) monitoring program was implemented by the National Oceanic and Atmospheric Administration through the Coastal Zone Management Act of 1972 for monitoring water quality, biodiversity, and land-use and habitat changes within estuaries. The monitoring of these resources is accomplished by taking continuous observations of temperature, wind speed and atmospheric pressure over long periods of time. The goal of NERRS is to use these monitoring techniques to conceptualize and disseminate knowledge about best practices to be used in estuary systems. The NERRS data used in this study can be found at http://cdmo.baruch.sc.edu (NERRS 2016) and has similar quality control specifications to those found in the NDBC organization as the NERRS is a

special project of the NDBC. Additionally, as a federally funded observing system, NERSS is required to adhere to strict federal data management guidelines.

Observations of wind speed and direction from the NERRS station, BUOY_SCLD1, were utilized in this project. This particular station is located in swamp land on the east coast of Delaware. The NERRS station has a 0.1 m roughness length, a 4.5-m sensor height and a 15-min sampling frequency. Table 2.4 lists BUOY_SCLD1 with roughness coefficient length, location and a brief description of the surrounding area.

2.1.4 WeatherBug

The WB monitoring system is a widely distributed private weather reporting service that provides the public with daily weather reports and safety alerts. Most of the stations in this network are privately owned.

The single station utilized in this study is located on the marine operations building on the Lewes Campus of the University of Delaware. This station has been taking meteorological data, such as air temperature, relative humidity, pressure, wind direction and wind speed, since 2003 and provides one of the longest coastal wind records for this area. The sensor is located at 16.15-m height and is located very close to the water's edge. In 2008, station maintenance and data archiving was taken over by WeatherBug. The data obtained from the WB database can be accessed on request by contacting the General Council Director at EarthWorks at https://www.earthnetworks.com. The WB station has a 0.2-m roughness length and a 5-min sampling frequency. Table 2.4 lists the WB weather station roughness coefficient length, location and a brief description of the surrounding area.

2.2 Methods

2.2.1 Data Processing and Quality Control

All data provided by the four networks mentioned above were quality controlled to ensure consistency throughout the entire study. Both the DEOS and NDBC monitoring systems already have significant protocols in place to ensure quality of the instrumentation and quality and consistency of the data; both networks actively maintain and calibrate their instrumentation. The NERRS database, being an offshoot of the NDBC network, similarly maintains its instrumentation in accord with NDBC standards. WeatherBug quality control is maintained via the EarthWorks company quality control guidelines, which can be found at the Earthworks site mentioned above. In this project, an additional quality control was implemented upon data retrieval. This method included removing all stations with large sections of missing data, thus preventing a given station from inaccurately represent seasonal wind speeds.

2.2.2 Variations in Temporal Sampling

To address the varying time sampling resolutions among data sources, all observations were averaged into hourly intervals. In the averaging process, all missing data values were excluded from further analysis, the number of missing hourly averages are found in Table 2.5 as well as the percentage of available data samples each station had per year. Hourly averages were calculated based on the available data and no attempt was made to estimate missing data.

For the 2015 calendar year, analyses were conducted on annual, seasonal and monthly time periods. Seasonal time periods of the study were based on a single month for each season, represented by its center month, similar to Davy et al.'s (2010)

use of seasonal time steps to represent 2 individual years of data. This was done to avoid bias found at the edges of transitioning seasons; January, April, July, and October were chosen to represent winter, spring, summer and fall, respectively.

During October 2015 hurricane Joaquin was present off the coast of Delaware between October 1 and October 6. Joaquin never made landfall but significantly influenced both Bay and Coastal wind speeds as shown in Figure 2.4 for station DBNG in Bethany Beach. The presence of Hurricane Joaquin in early October made this monthly dataset less representative of a typical October. Therefore, "October" was redefined to be between October 7th and November 6th, removing the influence of the hurricane from the wind speed time series. October 7th was selected as the date at which wind speeds returned to their normal seasonal level after the hurricane passed by.

2.2.3 Variations in Land Use and Surface Roughness

The 29 stations used in this study are installed in a variety of terrains ranging from open water to highly vegetated sites inland. All measurements were taken between 3.0 and 21.1 meters above ground level (Table 2.1). Wind speed measurements at or near ground level are influenced by the land surface types, land and sea breeze effects, trees and buildings, and other downwind effects, experienced at the station location, all of which impact calculating wind speeds aloft, as discussed in the following sections. To adjust for the land surface surrounding each stations, site roughness coefficients were taken from the Danish Wind Industry Association (DWIA 2003) roughness classification system shown in Table 2.6.

2.2.4 Conversion of Surface Observations to Hub Height

To standardize the wind speed measurements, which were taken at varying heights, and to convert them to hub height for a typical onshore wind turbine, wind speeds were extrapolated from anemometer height to 114 meters above ground level using the logarithmic wind profile (Bañuelos-Ruedas et al. 2011). This elevation was chosen as it represents the height suitable for the most advanced modern turbines in use in the United States (MidAmerica 2017).

The Logarithmic Wind Profile Law (Equation 2.1) was used to adjust wind speeds to a common height (Bañuelos-Ruedas et al. 2011) and can be written as:

$$\frac{v}{v_0} = \frac{ln\left(\frac{H}{z_0}\right)}{ln\left(\frac{H_0}{z_0}\right)} \tag{2.1}$$

where v is the wind speed at the desired height H (here, H=114 m), v_0 is the wind speed at observation level H_0, and z_0 is the roughness coefficient length in meters.

There are numerous techniques for extrapolating surface wind speeds to wind speed aloft. The Log Law and Power Law techniques are the two most commonly used methods of predicting wind speeds at height based on surface measurements (Hiester and Pennell 1981). The Power law (Equation 2.2) is as follows:

$$\frac{U(z)}{U(z_r)} = \left(\frac{z}{z_r}\right)^a \tag{2.2}$$

where $U_{(z)}$ is the wind speed at height z. $U(z_r)$ is the referenced wind speed for height z_r and a is the power law exponent with a commonly used value of 1/7 for open land without obstructions (Bañuelos-Ruedas et al. 2011).

Both methods have their shortcomings in that they are affected by site measurement biases such as elevation, season, temperature and atmospheric stability (Zoukmakis 1992, Archer and Jacobson 2003). Despite these draw backs, the Log Law was chosen for use in this study because of its wide acceptance in Europe (Bañuelos-Ruedas et al. 2011), the largest wind market in the world, and because of its more comprehensive nature that allows for site specific roughness to be included in calculations more effectively than the Power Law. The Power Law has also been blended with the Log Law to provide a more in depth prediction of winds aloft, however in doing so adds complication to the Power Law such that its utility of simplicity vanishes and therefore the technique becomes obsolete (Manwell et al. 2010).

It should be noted that the Log Law is not a perfect tool and lacks the ability to account for variations in stability within the Planetary Boundary Layer (PBL) of Earth's atmosphere. The Log Law assumes that the surface layer and PBL are independent of each other even though this has been disproven for some time (Tennekes 1972). The Logarithmic Wind Profile Law is derived from the Monin-Obukhov equation (Equation. 2.3) outlined in (Johnson 2006) and can be written as:

$$V(z) = \frac{v_f}{K}\left[ln\frac{Z}{z_0} - Q\left(\frac{z}{L}\right)\right] \quad (2.3)$$

In the Monin-Obukhov equation, $V(z)$ represents the wind speed at height z, v_f is friction velocity, K is the von Karman constant, L is the Monin-Obukhov length, and z is the elevation above ground. In practice, the stability term, Q, is usually assumed to be for neutral stability when predicting winds at height with the ratio of z/L being equal to zero (Bañuelos-Ruedas et al. 2011). In these calculations, the von Karman constant is often assumed to be 0.40, but can actually vary between 0.33 and 0.40. For the purposes of this study, the von Karman constant is treated as a fixed value at 0.40 as was the case in Tennekes (1972).

In assuming neutral stability in all calculations, the complexity of the atmosphere is significantly simplified, thus allowing for consistent results within the study. However, the atmosphere is not inherently stable. As early as 1970, Paulson found that using Log Law relationships do not accurately account for the considerable variability within the range of atmospheric stability. More recently, Archer et al. (2016) found that the marine boundary layer in the Nantucket Sound is unstable up to 61% of the time, suggesting that the power law will only be appropriate for extrapolating surface winds to hub height 40% of the time for coastal locations. Moreover, stability at the land-ocean boundary can vary considerably as Barthelmie (1999) has demonstrated. Despite these shortcomings, Log Law predictions remain a constant standard within the industry (NYSERDA 2010). This remains true because if neutral stability is not assumed, substantial data requirements are needed to estimate the actual stability conditions and to calculate a revised wind extrapolation from observational height to the desired target height. The vast majority of atmospheric datasets do not have sufficient information to calculate accurately the stability throughout the atmosphere (Newman and Klein 2014). Moreover, Blanc (1987) calls

into question the utility of buoyancy corrections as the methods to account for stability are still subject to error and may not be worth the additional effort. Therefore, this study assumes neutral stability in all calculations using the Monin-Obukhov equation.

Significant wave heights from Buoy 44009 were used to calculate zero plane displacement for portions of the study area over water. Zero plane displacement is a constant used to enable Log Law calculations to be applied to various surfaces in that zero plane displacement is the height at which impacts of a given surface roughness on wind speed are null (Harmel et al. 2002).

NDBC BUOY 44009 wave heights expressed in hourly averages were used to calculate zero plane displacement. BUOY 44009 was used as a proxy for wave heights at the NDBC stations in the Delaware Bay as there were no wave height data available at these stations. This means that the wave heights are likely overestimated as the winds in the Bay tend to be lower than at 44009 and the wave heights tend to be smaller, thus for this study zero plane displacement values over water may be represented as slightly higher than they are in reality.

NDBC BUOY 44009 wave heights expressed in hourly averages were used to calculate zero plane displacement. BUOY 44009 was used as a proxy for wave heights at the NDBC stations in the Delaware Bay as there were no wave height data available at these stations. This means that the wave heights are likely overestimated as the winds in the Bay tend to be lower than at 44009 and the wave heights tend to be smaller.

Using the Monin-Obukhov equation (Equation 2.3) a relationship can be derived such that winds at various heights can be predicted relative to a maximum standard height. The addition of the zero-plane displacement, *d*, modifies the Monin-

Obukhov Equation. Without *d*, zero wind speed height is assumed to be ground level. Equation 2.4 shows this modified wind profile equation with the zero-plane displacement, *d*, indicating the height in meters at which wind speed is zero for a given ground cover;

$$V(z) = \frac{v_f}{K} ln \frac{z-d}{z_0} \quad (2.4)$$

The maximum height used in this study was 114 meters, thus wind speeds at 114 meters are assumed to be the maximum wind speeds at this location. This assumption is true for stable environments. Wind speed at other elevations can be expressed as a percentage of this maximum wind speed to provide planners with the ability to consider multiple turbine heights. Figure 2.5 illustrates this in inland areas, as well as over the bay and along the coast. Bay area winds are stronger than inland winds throughout the study, due in large part to minimal surface roughness within this region. For this reason, wind speeds in this region decrease the least with height (Figure 2.5). Coastal wind speeds are lower relative to Bay wind speeds, due to higher surface roughness, which means that winds aloft will also be lower, while inland station wind patterns exhibit a similar yet more exaggerated trend due to increased surface roughness.

The wind speeds aloft were calculated using the Log Law derived from Equation 2.3 and suggested parameters based on local vegetation from Hansen (1993) using the Danish Wind Industry Surface Roughness scale (DWIA 2003). For example, areas with marshland and small crop vegetation used overall roughness coefficients and zero plane displacement values of 0.4 meters and 5.3 m, while ocean

coastal sites had roughness lengths of 0.2 m and zero-plane displacements of 5.3 m, based upon coastal vegetation and conditions. Similarly, the bay coastal sites had roughness lengths of 0.0002 m and the zero-plane displacement was 0.7 m. To determine ocean coastal sites' zero-plane displacements, wave height measurements at the NDBC Buoy closest to the ocean coastal sites for the 2015 year were averaged and used to calculate the zero-plane displacement value of the ocean coastal sites this was done referencing relationships derived between land cover height and zero-plane displacement distances found in Rosenberg et al. (1983). Based on these coefficients, observed winds were standardized to a common height of 114 meters and averaged to produce hourly averages.

2.3 Statistical and Mapping Methods

To explore the most useful way to communicate wind variability to the wind farm industry and to assist in identifying wind farm sites, several techniques to characterize wind variability were employed. All of these techniques use hourly averaged data generated using the techniques described in the previous sections to determine annual average wind variability. In addition, the results were then assessed seasonally. The seasonal wind variability was calculated using a representative month per season, to avoid unwanted biases that may occur in transition months between seasonal peaks.

The techniques used during this study to characterize wind variability are mean and median wind speeds, the difference between the mean and median wind speed (MMD), skewness, probability distribution analysis and comparison to Weibull and normal distributions, upper quartile (UQ) and lower wind speed quartiles (LQ), wind speed quartile deviation (QD), autocorrelation between wind speeds, wind speed

Pearson correlations and wind rose diagrams. Once the methods were applied, then maps of the wind variability using ESRI ArcMap were generated.

2.3.1 Mean Wind Speeds

Hourly mean wind speeds were used in this study to reduce the influence of sub-hourly wind variation, to put all the sampled datasets on a similar time step, and due to the frequent use of average wind speed measurements in current wind farm siting (Fields et al. 2016) as evidenced by Weekes and Tomlin (2014), Rogers et al. (2005) and Mirhosseini et al. (2011). An average wind speed is a representation of the central tendency of the data (Hennessey 1977) at a given station. Averages include all time steps available in a given hour. These values were then averaged annually and for the season-representative months. Annual and seasonal averages are calculated by summing all available hourly values together for the period of interest and dividing by the number of hours. There is a significant difference between the data availability in Lewes and the rest of the stations (Table 2.5).

2.3.2 Median

Median wind speeds were employed in this study to be used in conjunction with mean wind speeds. The median will give the center point of the range of data (Wolf-Gerrit 2013) at a given station. Median wind speeds were calculated by placing wind speeds in order from least to greatest and selecting the center most measurement within the series. Differences in the mean and median wind speeds will be used to provide information about whether the distribution of wind speeds follows a normal distribution.

2.3.3 Mean-Median Difference (MMD)

Mean and median are both quantities, along with mode, that are used to calculate the central tendency of a distribution (IESS 2008). The MMD value was derived from mean and median metrics under the assumption that in a Gaussian distribution, mean and median should be identical (Trauth 2015); separation between these two metrics then represents the degree of skewness present within a dataset. Therefore, since mean wind speeds are used by the wind energy industry (Fields et al. 2016), MMD represents the amount of skew present within a dataset and consequently demonstrates how reliable the mean and the coincident assumption of a normal distribution is in representing a particular wind dataset.

2.3.4 Probability Distributions

The probability distribution of the hourly average wind speed values was compiled annually and seasonally for this study. A probability distribution is a distribution in which a variable is measured and graphically represented such that an observer will be able to determine graphical representation of the likelihood that a particular observation will occur based on previous patterns of occurrence (Everitt and Skrondal 2010). In order to create a probability distribution, wind speeds were sorted into bins of 1.0 m/s and then normalized by the bin width. Then the resulting distribution was compared to several known fits, similar to Bludszuweit et al. (2008) and Lange (2004).

Normal distributions theoretically are distributions of which given a dataset of infinite sample size, values will disperse around the mean of the distribution such that 50% of values will fall to the left and to the right of the distribution (Trauth 2015). Thus, normal distribution is a distribution that has a symmetrical partitioning of data

on each side of the maximum frequency of occurrence (Jagdish et al. 1996). However, it can easily be seen that a normal distribution is not very representative of observed wind speeds (Figure 2.6). It is for this reason that numerous other probability distributions have been explored in the field of wind resource assessment (as far back as the late 1970's (Justus et al. 1977).

Two probability distributions commonly used in describing and characterizing wind speed data are the Weibull and Rayleigh distributions (Jowder 2006). Weibull distributions are the preferred favorite probability distribution of the wind energy industry (Carta et al. 2008, Wolf-Gerrit 2013) because this distribution incorporates both shape and scale factors, whereas a Rayleigh distribution accounts for average wind speed alone as a single factor (Manwell et al. 2010). Rayleigh distributions treat the shape factor of the distribution as a constant of 2, where Weibull distributions calculate the shape factor with respect to the provided data. Thus, Weibull distributions are more reliable and accurate than Rayleigh distributions as shown in Jowder (2006).

2.3.4.1 Skewness

A probability distribution can be considered skewed if the distribution of data is asymmetrical around the peak such that one of its tails is longer than the other (Trauth 2015). Wind speeds by their nature are non-negative and generally will exhibit positively skewed distributions because larger wind speeds are much less frequent than lower wind speeds. (Wolf-Gerrit 2013). This can be seen in Figure 2.6, which shows a probably distribution for winds at the coastal station DBNG in Bethany Beach. Despite being infrequent, the presence of occasional high wind speeds, caused by frontal activity and seasonal anomalies such as hurricanes and mesoscale

metrological cycling, in an observed wind dataset will serve to adjust the mean accordingly (Kahn 1979). This high wind speed adjustment to the mean will influence the mean disproportionately in that an anomalous high wind speed will exert more influence on the mean than a standard low wind speed. The skewness, or asymmetrical deviation of a probability distribution away from a normal distribution, is one way of calculating the degree that a distribution has been shifted (Hodge et al. 2012). It can be calculated and then compared to the MMD values. Skewness can be calculated as shown in Equation 2.5 where x_i is the current measurement of the data set and $\bar{x}$ is the mean of x (Trauth 2015).

$$s_1 = \frac{\frac{1}{n}\sum_{i=1}^{n}(x_i-\bar{x})^3}{\left(\sqrt{\frac{1}{n}\sum_{i=1}^{n}(x_i-\bar{x})^2}\right)^3} \tag{2.5}$$

Skewness is a third moment statistic and provides additional insights into wind speed variability beyond mean and standard deviation of wind speeds (Hodge et al. 2012). Kahn (1979), Hodge et al. (2012) and Tagle et al. (2017) as well as many others have investigated skewness as it relates to wind variability. Findings by Hodge et al. (2012) shows that skew in wind speed distribution impacts measurements in all wind analyses across the globe. Additionally, mean wind speed does not appropriately account for skewness in its calculation. These finding provide further support for using Weibull distributions to represent the probability distribution of wind speeds, as they have been used to a satisfactory level to conceptualize skewness within a wind data set, although new methods are continuing to be pioneered (Hennessy 1977). Most recently, Tagle et al. (2017) has attempted to conceptualize skewness in wind speeds

and reports that in doing so, accuracy in prediction of wind speeds is refined and improved.

2.3.4.2 Weibull Distributions

Weibull distributions are frequently used in calculations to determine the available wind resource in a given area (Mirhosseini et al. 2011, Carta et al. 2008 and Justus et al, 1977), and are designed to be used with non-negative positively skewed data. A Normal distribution (Trauth 2015) can be written as

$$y = f(x|u,\sigma) = \frac{1}{\sigma\sqrt{2\pi}} e^{\frac{-(x-u)^2}{2\sigma^2}} \tag{2.6}$$

where μ is the mean of wind speeds *x*, and σ is the standard deviation of wind speeds. The Weibull Distribution (Equation 2.7) can be written as

$$p(U) = \left(\frac{k}{c}\right)\left(\frac{U}{c}\right)^{k^{-1}} exp\left[-\left(\frac{U}{c}\right)^{k}\right] \tag{2.7}$$

where *k* and *c* are the shape factor and scale factor of the distribution, respectively, and *U* represents the mean of the wind speeds being analyzed (Manwell et al. 2010). A comparison of the two distributions can be shown in Figure 2.6 overlaid on a probability distribution of annual wind speeds for station DBNG. The appropriateness of the Weibull Distribution to represent wind variability is explored in this work.

There are numerous wind resource studies that have compared the Weibull and Rayleigh distributions to observed wind data (Pishgar-Komleh et al. 2014, Safari and Gasore 2010, and Celik 2004). All of these studies have demonstrated the Weibull distribution outperforming the Rayleigh distribution in all scenarios. Celik (2004) found that the Weibull distribution does particularly well in fitting probability density distributions as well as better representing power performance of turbines based on wind speed distributions. Hennessey (1977) demonstrated preference of the Weibull distribution because of its limited yet satisfactory ability to estimate skewness within a wind speed distribution. The outperformance of the Weibull distribution to the Rayleigh distribution is attributed to the Weibull distributions ability to capture both scale and shape factors of a wind data set (Safari and Gasore 2010), unlike the Rayleigh distribution which relies solely on a single mean wind speed parameter (Manwell 2010). The Weibull distribution will be explored in this study due to the wind industry's broad use of this distribution (Carta et al. 2008). Skewness was investigated in this study to provide a better conceptualization of winds in a given data set.

2.3.4.3 Wind Roses

Wind roses are another way of displaying the frequency distribution of winds using a combination of wind speeds and wind directions (Mirhosseini et al. 2011). Wind roses created using meteorological standards use the ordinal directions to indicate which direction winds were blowing from. In this study, wind directions are binned by 10°; wind speeds are binned by 1 m/s and are displayed as colored areas in each directional bin. Wind roses have been used in other studies to characterize

surface winds (Hughes and Veron 2015, Hasager et al. 2008) and can be particularly useful in understanding seasonal variations in the wind

An example of a wind rose is shown in Figure 2.7, using data from station DBRG. Wind roses were used to identify the predominant wind directions within the observed data annually and by season, and thus provide context for observed patterns in the maps generated later in the study. Seasonal and annual wind roses were created for all stations, and geographical areas (coastal, over water, inland) within the study. For example, in Figure 2.7 it can be seen that the winds blow most frequently from the south and northwest, however the highest wind speeds are related to winds coming from the northwest, similar to what was seen in Hughes and Veron (2015). Seasonal and annual wind roses allow for more detailed study of the relationship between wind speed and direction throughout the year. Wind roses were created for all stations, and geographical areas (coastal, over water, inland) within the study, annually and seasonally.

2.3.5 Upper and Lower Quartiles

An upper quartile (UQ) is defined as a limit above which 25% of a given dataset will have a greater value (Crum et al. 1993). Winds being non-uniformly distributed do not naturally lend themselves to arithmetic characterizations but more so to geometric characterizations, similar to the way Wolf-Gerrit (2013) used quartiles to assess wind speeds and Krumbein (1936) used quartiles to compare sediments. The UQ in this study identifies the upper 25% wind speeds for each station, thus indicating the largest possible power generation available; this analysis does not account for turbine cut out speeds as all data were used and no distinction was made to neglect wind speeds deemed too slow for power generation. One reason for ignoring the cut in

speed is that wind turbines are constantly improving and what may be considered too slow at present may be harvestable in the near future as evidenced by Gamesa's (2015) product evolution guide . Conversely, the lower quartile (LQ) is defined as a limit below which 25% of a given dataset will have lower values. The lower quartile indicates the minimum theoretical potential power generation available within a standard time-period.

Limited work has been done using upper and lower quartiles to represent wind speeds in a given area. As stated previously, mean wind speeds and related metrics are the norm in the wind energy industry and developers seldom venture outside of these metrics. Despite the lack of excessive use, when quartiles are used, they are effective in delivering accurate conceptualizations of wind speeds in otherwise highly skewed data (To and Lam 1995). Experts use quartiles as a geometric representation of wind speeds because doing so removes large biases created by outliers when using arithmetic representations of wind speeds, such as mean wind speed. Similar to how Wolf-Gerrit (2013) used quartiles to represent ranges of wind speeds in his study, quartiles will be used in a similar way in this study

2.3.6 Quartile Deviation

The Quartile Deviation (QD) is defined as the average distance between the mean and the upper and lower quartiles, and provides a representation of the dispersion, or spread, of the dataset and thus indicates the range in wind speeds at a given location (Holden 1993). Larger QD values indicate large wind speed ranges and may indicate that the winds in locations with high QD will be inherently less predictable (EWEA 2009). This study will use QD to represent wind speed

distributions similar to how other studies have used QD in representing data, such as Buller and McManus (1973) and there use of QD in comparing glacial deposits.

2.3.7 Standard Deviation

Another measure of the dispersion in a dataset is the standard deviation (Trauth 2015). The standard deviation is the square root of the variance and can be written as:

$$S = \sqrt{\frac{1}{N-1}\sum_{i=1}^{N}|A_i - u|^2} \tag{2.8}$$

where *S* is the standard deviation of *A* with *u* being the mean of *A* and *N* being the number of samples in the dataset (Trauth 2015).

There are numerous studies that have explored standard deviation as a means for characterizing winds at specific sites such as, Fisher's 1987 work where it was fond that standard deviation and assumptions made using it can often be misleading and inaccurate. The ability of the standard deviation to accurately represent wind variability in the Southern Delaware region is explored in this work.

2.4 Interpolation

This analysis of wind variability relies entirely on station data. However, it is useful when trying to understand a wind resource, to look at the spatial variation in wind characteristics spatially using a map. Cartographic representations of mean, median, MMD, UQ, LQ, QD, and station-to-station correlations were generated. The geographic maps created in this study to illustrate wind fields were mapped using ArcGIS employing geographical data such as state and county and census tract

boundaries from the online Geographic Information Systems (GIS) databases iMap for Maryland and the United States Census Bureau for Delaware.

For all of the analyses described in section 2.3, annual and seasonal maps were developed to further investigate the spatial patterns in wind variability.

Maps resulting from all of the statistical techniques described above (e.g. mean, median, MMD) were spatially interpolated using the Inverse Distance Weighting tool (IDW) available through ESRI ArcMap to smooth the data field. Ozelkan et al. (2016) has demonstrated the successful use of IDW application available through ArcGIS and its superiority to interpolating wind speeds over other methods; however, this is a recent finding and literature up until this point has generally been in poor favor of using IDW to interpolate wind speeds (Lou et al. 2008). The IDW formula (Equation 2.9) used by the ArcGIS program is as follows:

$$\hat{Z}(u_0) = \frac{\sum_{i=1}^{N} Z(u_i) w_i}{\Sigma_{i=1}^{w} w_i} \tag{2.9}$$

where u_0 represents an estimated point, u_i represents known points, and w_i is the weight of the current value at increment N (Ozelkan et al. 2016). The IDW tool is set up so that the influence of a given point is inversely proportional to its distance from a given location. However, ArcMap also permits manipulation of key aspects of the IDW tool by allowing the power of the weighting function to be modified to better suit various problems. ESRI notes that there is no objective weighting function power that can be applied generally. Instead, the choice of the power of the weighting function is a subjective assessment that the user makes according to their specific data and application (ESRI 2016).

The weighting function power varies in a known way and so can be used to develop smoothed fields that are appropriate to an individual application. Specifically, the higher the power, the more influence a single point has over longer distances, whereas the lower the power, the less influence a point will have far away from it. In other studies, (e.g. Albani et al. 2011) the IDW has been applied to station data and has been found to effectively model wind speed over a given area. The weighted function power used in this study for all interpolations was 0.1. This low power value limits the influence of one meteorological station on areas surrounding it; interpolations are smooth and the wind speed transitions gradually among stations. An interpolation with higher power values creates a clustering, or bull's eye, effect of wind speeds surrounding stations. Figure 2.8 shows an example of the bull's eye effect where a power of 2 was used to create the interpolation of average annual wind speeds at 114 meters. The 0.1 power value produces a smoother field overall in wind patterns across a large study area such as the state of Delaware.

The weighted power of the interpolation used in this study for all interpolations was 0.1. This low power value limits the influence of one meteorological station on areas surrounding it; interpolations are smooth and the wind speed transitions among stations gradually. Whereas an interpolation with higher power values creates a clustering, or bull's eye, of wind speeds surrounding stations. Figure 2.9 shows an example of the bull's eye effect where a power of 2 was used to create the interpolation of average annual wind speeds at 114 meters. The 0.1 power value produces a smoother field overall in wind patterns across a large study area such as the state of Delaware.

IDW representations were chosen over Kriging or spline techniques. Historically IDW has not been the preferred method used for interpolating wind speeds at ground level. However, Ozelkan et al. (2016) found that when winds are projected to a desired height, IDW becomes the most accurate interpolation method available because of the unique ability of the IDW projection method to account for surface roughness and local topography. The geographic coordinate system used was the GCS_WGS_1984, Datum D_WGS_1984 with a spatial resolution of 4.73 km per grid cell. Neighbor influence was set to 5 meaning that the 5 closest data points impact a single point of interpolation.

While mapping mean, median, MMD, UQ, LQ and QD representations, all values were in the units of meters per second. Mean, median, UQ and LQ were graphically represented in 0.5 m/s intervals while MMD and UQ were represented in 0.1 m/s intervals. All maps produced were standardized with the same key relative to the map type to aid in comparison of the metric across different time periods. Inverse distance weighting was performed on all fields listed above except for station-to-station correlations of which were represented via the line tool in ArcMap.

2.5 Correlations

Correlation techniques can be used to identify how similar the wind speeds are between two or more stations (Apt 2007, Loui 2014 and Kahn 1979), and how similar a single station's own measurements to itself over time (Brokish et al. 2009 and Brown et al. 1984).These two techniques, called the Pearson's Correlation and autocorrelation, are of particular interest to this study because of what they can tell us about the spatial variability of the wind field. Loui (2014) and Kahn (1979) both have researched the ability to correlate wind farms and turbines with each other so as to

develop a large grid of interconnected wind power generation robust enough and dispersed enough to provide consistent power generation through wind energy. Brown et al. (1984) identify the importance of accounting for temporal autocorrelation, yet as Brokish et al. (2009) demonstrate, attempts to do this do not produce significant results. This is understandable when power swings of up to 70% can be generated in the wind resource within a single 12 hour period (Oswald et al. 2008).

2.5.1 Pearson's Correlation

The Pearson's correlation is a method which is used to determine the covariance between stations (Feijóoa et al. 2011). In the study of a wind resource, this gives an estimate of how similar the wind field is in time between two stations. This information is particularly interesting to the wind power industry because spatially and temporally correlating stations may provide opportunities for developing wind farms such that grid power generation will not be subject to shortages, thus providing consistent power supply as proposed by Apt (2007).

Kempton et al. (2010) were able to identify correlations between stations decreases with distance between stations, particularly in this study of United States East Coast stations, correlations of 0.6 or higher were not attainable beyond station separation distances of 350 km. However, within 350 km range with attainable of 0.6 correlations, wind farms via transmission sharing would be able to produce sustainable and consistent power generation. Pearson correlations were performed between all stations in all time periods (annually and seasonally). The correlation among stations is calculated using Equation 2.10 (Apt 2007):

$$p(A,B) = \frac{1}{N-1}\sum_{i=1}^{N}\left(\frac{\overline{A_i - u_A}}{O_A}\right)\left(\frac{B_i - u_B}{O_B}\right) \quad (2.10)$$

where u_A and u_B are the mean of *A* and *B*, O_A and O_B are the standard deviation of *A* and *B*. *A* and *B* represent two given independent stations. *N* is the number of samples in the dataset and must be identical between station pairs. Correlation of the wind speed was employed to calculate covariance between stations and was then used determine similar zones of influence caused by prevailing wind patterns. The majority of spatially correlated wind studies focus on correlations between wind farms of distances between 350-3000 km (Loui 2014 and Kempton et al. 2010)

2.5.2 Temporal Autocorrelations

Temporal autocorrelations were computed for representative stations within each corridor. A temporal correlation allows characterization of the persistence of the wind (Alexiadis et al. 1999). In other words, how representative is the current wind speed of what will come later on, and for how long? The time series for each station was lagged hourly from 1 up to 64 hours to investigate both short-term and daily autocorrelation. The autocorrelation function (Brokish and Kirtley 2009) is described in Equation 2.11.

$$r_k = \frac{C_k}{C_0}. \quad (2.11)$$

The autocorrelation is based on the calculations of the covariance C_k over variance C_0. Covariance is a measure of the similarity between two time-series, and

variance is a measure of dispersion in the observed wind speed values relative to their mean. Covariance is defined in Equation 2.12),

$$C_k = \frac{1}{T-1}\sum_{t=1}^{T-K}(y_t - \bar{y})(y_{t+K} - \bar{y}) \quad (2.12)$$

while variance is defined in Equation 2.13 (Trauth 2015),

$$C_0 = \frac{1}{T-1}\sum_{i=1}^{T}|y_i - \bar{y}|^2. \quad (2.13)$$

In these two equations, T is the length of a given time series, t is the index within T, k is the lag number being used and y is the given value at index t. Autocorrelations with a time lag were used to provide a measure of wind speed persistence. Previous studies have shown that it is typical for autocorrelations of wind speeds to underperform in comparison to other persistence measures such as artificial neural networks (Alexiadis et al. 1999). Damousis et al. (2004) further demonstrates the superiority of model forecasting over persistence measures to represent wind speeds even at short time scales of 20 minutes or less.

Station	Latitude	Longitude	Sampling Frequency (min)	Sensor Height (m)
DBLK	39°14'30"	-75°44'27"	5	3
DGES	38°38'10"	-75°27'18"	5	3
DWDS	39°3'38"	-75°38'23"	5	3
DADV	38°49'53"	-75°40'33"	5	3
DBBB	38°32'20"	-75°03'15"	5	3
DDFS	39°10'10"	-75°35'34"	5	3
DGUM	38°27'54"	-75°27'02"	5	3
DHAR	38°54'40"	-75°34'36"	5	3
DIRL	38°37'59"	-75°03'59"	5	4.6
DLAU	38°32'29"	-75°35'33"	5	3
DRHB	38°43'15"	-75°04'36"	5	3
DSEA	38°39'09"	-75°42'13"	5	3
DSMY	39°16'38"	-75°34'50"	5	3
DSTK	38°37'46"	-75°19'19"	5	3
DWAR	38°40'43"	-75°14'47"	5	3
DBNG	38°32'47"	-75°03'45"	5	3
DBRG	38°43'14"	-75°35'19"	5	3
DELN	38°48'30"	-75°25'38"	5	3
DJCR	38°35'41"	-75°26'12"	5	3
DSBY	38°28'17"	-75°12'52"	5	3
BUOY_BRND1	38°59'13"	-75°06'46"	6	21.1
BUOY_LWSD1	38°46'58"	-75°07'8.4"	6	9.5
BUOY_CHCM2	39°31'37"	--75°48'36"	6	6.8
BUOY_OCIM2	38°19'40"	-75°05'27"	6	8.5
BUOY_CMAN4	38°58'04"	-74°57'36"	6	9.7
BUOY_CAMM2	38°34'26.4"	-76°4'8.4"	6	6.4
BUOY_BISM2	38°13'12"	-76°2'20.4"	6	7.1
BUOY_SCLD1	39°5'20.1"	-75°26'12.8"	15	4.5
LEWE_MOB	38°47'3"	-75°9'25.9"	5	16.15

Table 2.1 Station Locations, sampling frequencies and sensor height.

DEOS Station	Coefficient (m)	Surrounding Area	Surrounding Terrain
DBLK	0.1	Farm Land	Farm fields
DGES	0.1	Farm Land Adjacent to Highway	Grassy
DWDS	0.1	Farm land	Farm Fields
DADV	0.2	Farm Land with Neighboring Hedgerows	Fields with surrounding trees
DBBB	0.2	Boardwalk with Large Structure to East	Beach and buildings
DDFS	0.1	Delaware State Fire School	Grassy
DGUM	0.2	Gordo Farms	Farm fields
DHAR	0.2	Adjacent to Raceway Casino	Grassy
DIRL	0.2	Beach Front	Beach
DLAU	0.2	Laurel Airport	Grassy
DRHB	0.2	Boardwalk with Hedgerow to East	Beach and buildings
DSEA	0.2	Willin Farms Main Road	Grassy with buildings
DSMY	0.2	Swamp Adjacent to Mount Joy Observatory	Grassy w/tall pond plants
DSTK	0.2	Residential Yard	Grassy
DWAR	0.2	Farm Land (High Crops)	Planted/harvested fields
DBNG	0.4	Delaware National Guard Academy Grounds	Field surrounded by trees and buildings
DBRG	0.4	Delaware State Police Lawn	Buildings surrounding field
DELN	0.4	Residential Lawn	Grassy surrounded by trees and buildings
DJCR	0.4	Landfill	Trees around field
DSBY	0.4	Selbyville Waste Water Plant	Trees around field

Table 2.2 Meteorological station description for the 20 DEOS stations including, surface roughness coefficient, location and a description of the surroundings.

NDBC Station	Coefficient (m)	Surrounding Area	Surrounding Terrain
BUOY_BRND1	0.0002	New Jersey Bay (NJ)	Open water
BUOY_LWSD1	0.0024	Cape Henlopen Ferry (DE)	Water and developed shore
BUOY_OCIM2	0.1	Ocean City Inlet (MD)	Water and developed shore
BUOY_CMAN4	0.055	Cape May Canal (NJ)	Water with adjacent Shoreline
BUOY_CAMM2	0.0002	Cambridge Creek Inlet (MD)	Open water
BUOY_BISM2	0.0002	Hooper Strait Sanctuary (MD)	Open water
BUOY_CHCM2	0.03	Back Creek (MD)	Water with adjacent Shoreline

Table 2.3 NDBC stations employed in this study, with ID, roughness coefficient, location, and a description of the surroundings.

NERRS and WB Stations	Coefficient (m)	Surrounding Area	Surrounding Terrain
BUOY_SCLD1	0.1	Swamp Land (DE)	Swamp land
LEWE_MOB	0.2	Residential (DE)	Grass with surrounding trees

Table 2.4 NERRS and WB station identification, along with roughness coefficient, location, and a description of the surroundings.

Call Sign	Missing Hourly Values	Percent Hourly Representation
DBLK	0	100%
DGES	0	100%
DWDS	4	100%
DADV	0	100%
DBBB	12	100%
DDFS	3	100%
DGUM	124	99%
DHAR	4	100%
DIRL	1	100%
DLAU	0	100%
DRHB	1	100%
DSEA	0	100%
DSMY	0	100%
DSTK	7	100%
DWAR	178	98%
DBNG	0	100%
DBRG	0	100%
DELN	0	100%
DJCR	390	96%
DSBY	0	100%
BUOY_BRND1	659	92%
BUOY_LWSD1	21	100%
BUOY_SCLD1	72	99%
BUOY_OCIM2	76	99%
BUOY_CMAN4	21	100%
BUOY_CAMM2	88	99%
BUOY_BISM2	96	99%
BUOY_CHCM2	41	100%
LEWE_MOB	3810	57%

Table 2.5 Number of missing hourly averages and percentage representation per station.

Roughness Class	Roughness Coefficient (m)	Landscape
0	0.0002	Water surface
0.5	0.0024	Completely open terrain with a smooth surface, e.g. concrete runways in airports, mowed grass, etc.
1	0.03	Open agricultural area without fences and hedgerows and very scattered buildings. Only softly rounded hills
1.5	0.055	Agricultural land with some houses and 8 meter tall sheltering hedgerows with a distance of approx. 1250 meters
2	0.1	Agricultural land with some houses and 8 meter tall sheltering hedgerows with a distance of approx. 500 meters
2.5	0.2	Agricultural land with many houses, shrubs and plants, or 8 meter tall sheltering hedgerows with a distance of approx. 250 meters
3	0.4	Villages, small towns, agricultural land with many or tall sheltering hedgerows, forests and very rough and uneven terrain
3.5	0.8	Larger cities with tall buildings
4	1.6	Very large cities with tall buildings and skyscrapers

Table 2.6 Surface roughness criteria as described by the Danish Wind Industry Association (DWIA 2003).

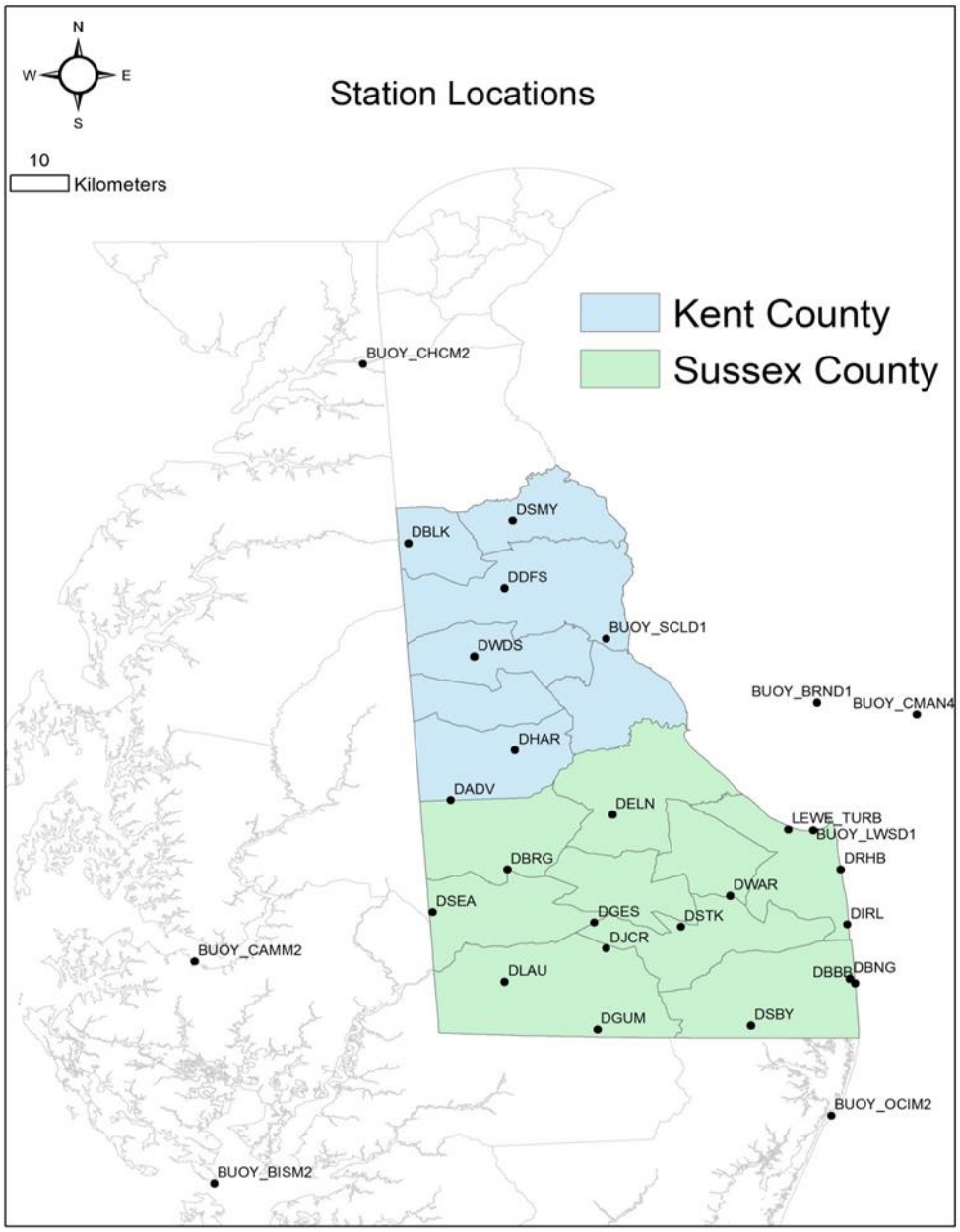

2.1 Map of the DelMarVa peninsula highlighting the Location and station ID for all stations used in this study generated using ESRI ArcMap and GIS databases from iMap and United States Census Bureau (2010).

2.2 DEOS Sensor located at Delaware State Police Troop 2, photo provided by DEOS Network

2.3 Ocean Buoy Sensor Buoy 44009 located at (38°27'40" N 74°42'9" W). (Photo credit: NDBC)

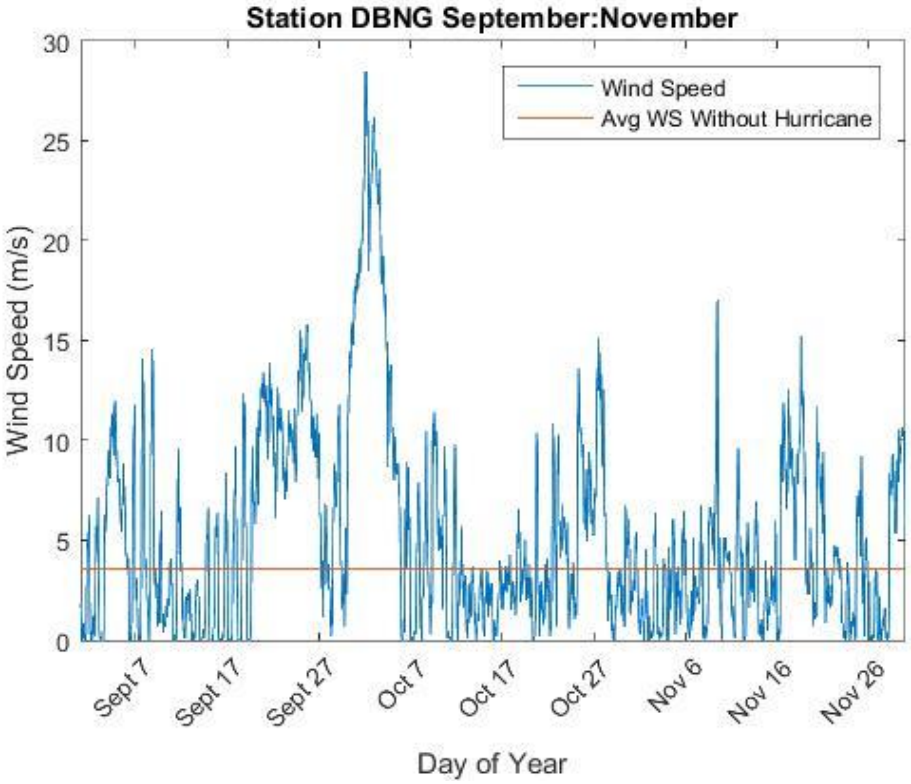

2.4 Hourly average wind speed from Bethany Beach station DBNG for September-November 2015. The presence of Hurricane Joaquin is clearly seen between September 27th and October 7th. The red line indicates the October monthly average wind speed with the hurricane removed.

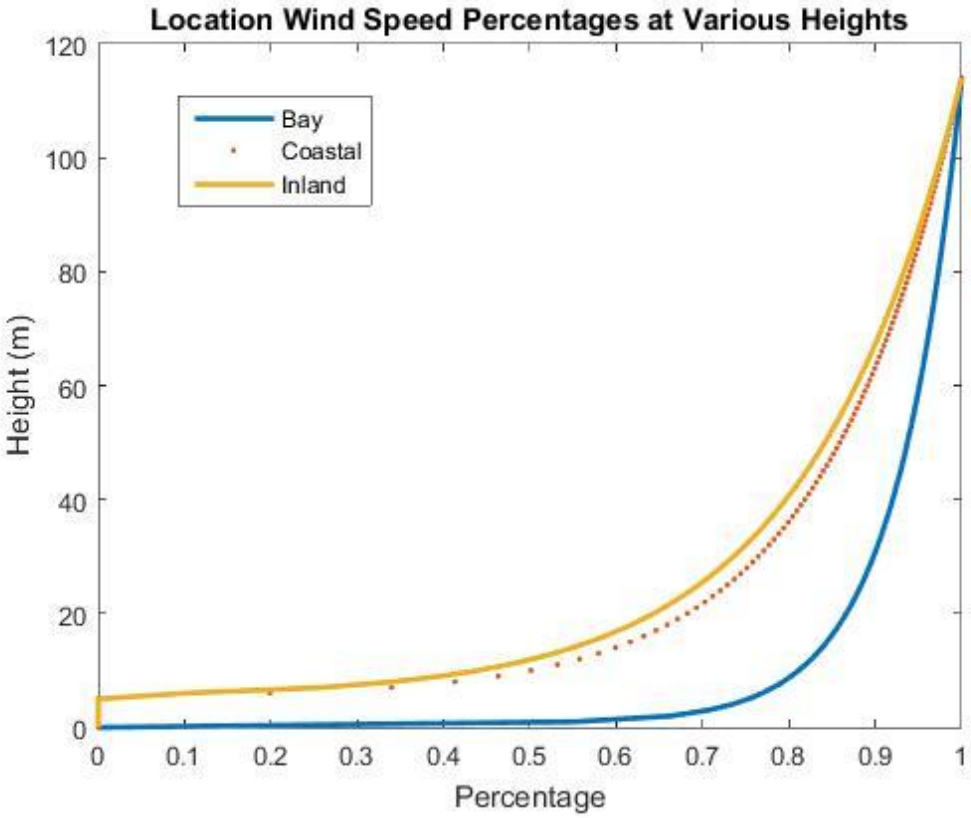

2.5 Idealized wind profiles created using the Log Law (Equation 2.4) and observed characteristics for surface roughness and zero plane displacement for three generalized areas in this study: inland, over the bay and along the coast.

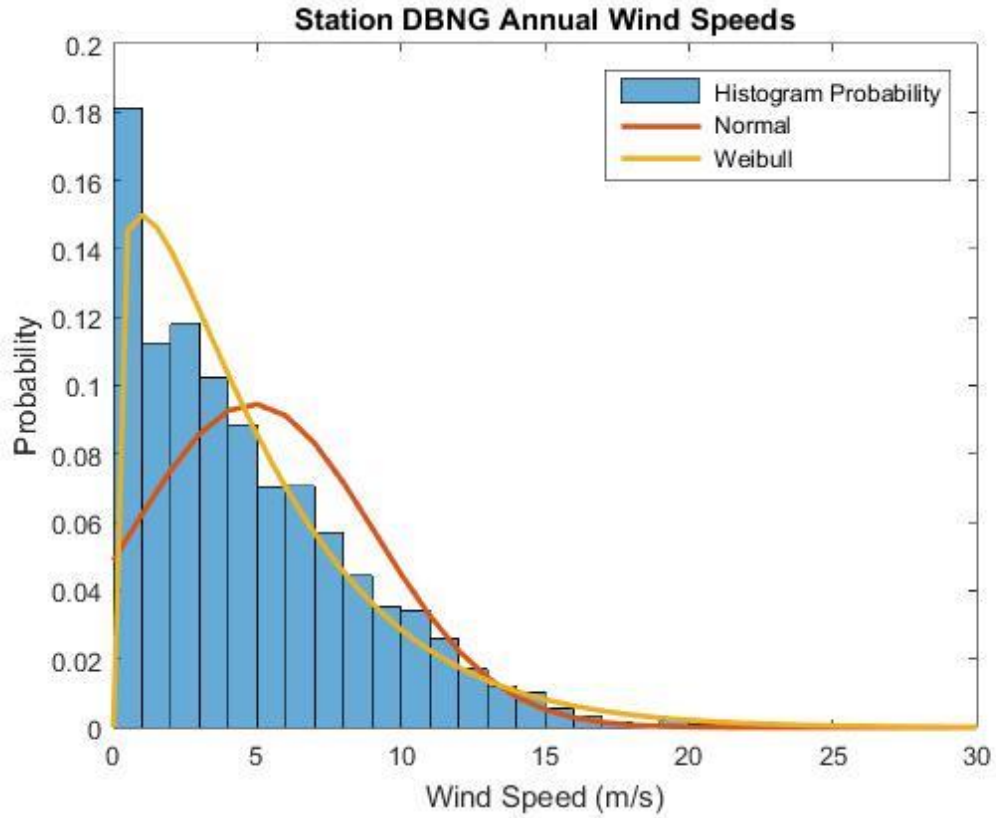

2.6 Probability distribution of the hourly average wind speed from DBNG with a Normal distribution and Weibull distribution superposed over the data.

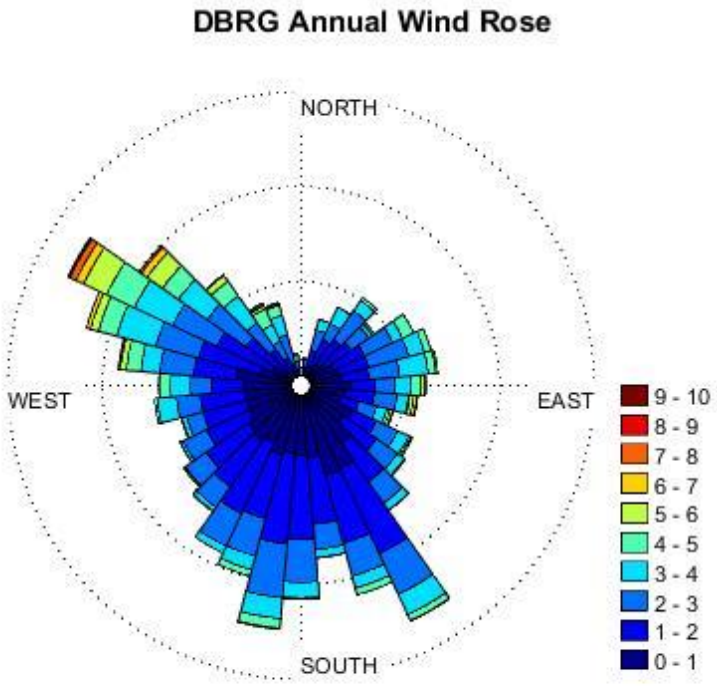

2.7 Wind rose for hourly averaged winds as observed at station DBRG in 2015.

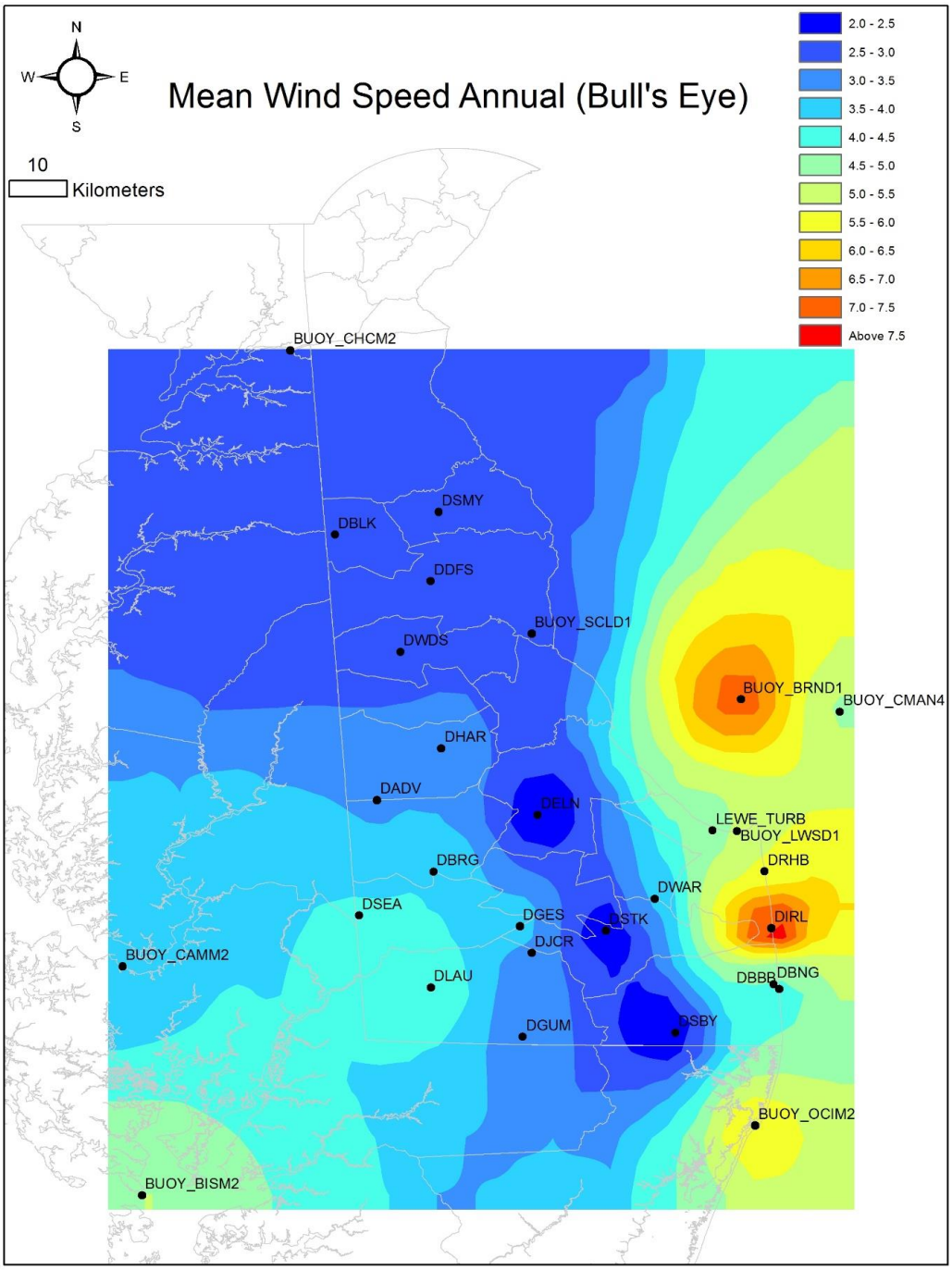

2.8 Annual mean wind speed at 114 meters shown with an inverse weighting function power of 2. Note how there are hot spots, or bull's eyes, around many of the stations.

Chapter 3

RESULTS

3.1 Results Review

In this section, results of all metrics and analysis performed will be described. Maps generated through ArcMap will be shown for numerous metrics such as mean, median and MMD as will skewness statistics, wind roses, and correlation metrics. Several key aspects of this study are noteworthy and will be further discussed. This discussion will include the utility of the Weibull distribution in representing wind data, the MMD metric's ability to gauge the effectiveness of the mean wind speed metric as a representation of a wind data set, the QD metric's ability to best represent wind data in variable data sets, and the emergence of the southwest corner of the state of Delaware as a viable location for wind farm development in the state of Delaware.

All results were calculated and interpreted using hourly-average, near-surface wind speeds interpolated to those aloft at 114 meters as described above. This is the case for all wind speeds discussed throughout this chapter. Annual and seasonal maps were generated for most analyses and will be used to describe the spatial variation in the derived quantity.

3.1.1 Mean Wind Speed

Annual and seasonal mean wind speeds, which are defined by a single month, were calculated for all the data from the 29 stations in this study and are shown in Figure 3.1 and in Table 3.1.

Annual

The annual average (2015) wind speed aloft for the entire study area is 5.0 m/s, as calculated by averaging the station data. As seen in Figure 3.1, the wind speeds

along the Bay are higher than anywhere else in the region. Wind speeds decrease inland the further away the station is from the coast. This corresponds well with what prior studies have shown (Rosenberg et al. 1983, Hughes and Veron 2015). Annual wind speeds are highest out over open water (6.1 m/s) and are relatively consistent. Near the coastline, the wind speeds decrease to 5.4 m/s, in comparison to the winds over the Bay. The projected lowest average annual mean wind speed is 4.1 m/s, in an inland area that runs roughly north-south through the middle of Kent and Sussex Counties. This area expands to encompasses the entire northern part of the State. In looking at Figure 3.1, it is clear that there is an increase in annual mean wind speed in the southwest portion of the state, with this area having a mean annual wind speed of 5.2 m/s.

Indeed, in looking at the map of the annual mean wind speeds, several interesting geographic features are observed. Four regions or "corridors" appear that have distinct characteristics. As these geographical features are present in most of the maps generated from the data analysis, these corridors were defined and named in Figure 3.2, as the Coastal, Inland, Southwest and Bay corridors. The Inland area is further divided into North and South regions to help in description of certain seasonal features.

The Bay corridor (rose color in Fig. 3.2) includes stations BUOY_BRND1 and BUOY_CMAN4. The Bay corridor represents the study area between the coast of Delaware and the NDBC buoy BUOY_CMAN4 and is supposed to represent stations that experience limited coastal influence on the winds aloft. Note that this corridor includes both Delaware Bay and Atlantic Ocean waters.

The Coastal corridor (green area in Fig. 3.2) includes stations BUOY_SCLD1, LEWE_MOB, BUOY_LWSD1, DRHB, DIRL, DBBB and DBNG; this corridor covers the area between the Bay and Inland corridors and is exclusively located on the Delaware coast including both Delaware Bay Coast and Atlantic Ocean Coast. Previous studies have shown that the winds on these two coasts have distinct differences in both average wind speeds and dominant wind directions (Hughes and Veron, 2015). However, for the purposes of this study, the characteristics of the wind along Bay and Ocean Coasts are more similar to each other than to the other corridors defined and so the Bay corridor will not be subdivided.

The Inland corridor (blue colors in Figure 3.2) exhibits uniformly low wind speeds. However, in certain seasons, there is a notable north-south variation that appears. For this reason, the Inland corridor is subdivided into two adjacent areas, the Inland-North and Inland-South corridors. When there is a significant difference within the Inland corridor, the North and South designations will be used, although generally this corridor will be referred to just as the Inland corridor. The Inland-North corridor contains stations DBLK, DSMY, DDFS, DWDS, DHAR and DADV and geographically represents Kent County Delaware. The Inland-South corridor contains stations DELN, DGES, DJCR, DSTK, DWAR, DGUM and DSBY and covers the inland extent of Sussex County Delaware, with the exception of the Southwest corridor, described below.

The Southwest corridor contains stations DBRG, DSEA and DLAU and geographically is located in the Southwest corner of the state of Delaware with its boundaries being the Delaware-Maryland state boundary to the south and west. The northern boundary of the Southwest corridor extends from a perpendicular line

between the Delaware-Maryland state boundary to the west of Station DBRG. The eastern boundary of the Southwest corridor is a diagonal line between station DBRG and the southern Delaware-Maryland state boundary line anchored midway between Stations DLAU and DGUM horizontally. The four stations used to bound this corridor are BUOY_CHCM2, BUOY_CAMM2, BUOY_BISM2 and BUOY_OCIM2. These additional stations allow for smoother mapping of the wind field, and avoids spurious features in the map that appear by having station data at the boundary of the study area. The Southwest corridor is delineated separately from the Coastal and Inland corridors because it consistently has higher wind speeds than the Inland corridor, suggesting a need for additional analysis of this area.

Seasonal

Seasonal average wind speeds are represented by a monthly mean in the middle of each season, as described in Chapter 2. Winter (January) mean wind speeds (Figure 3.3a) are the highest in the Bay corridor with a seasonal average of 6.6 m/s. The difference between Bay and Southwest corridor wind speeds is only 0.2 m/s with Southwest wind speeds averaging 6.4 m/s. Inland-North and Inland South wind speeds are 4.6 m/s and 5.1 m/s respectively, significantly lower than in the corridors proximate to or over the water.

Overall, spring wind speeds were 6.0 m/s and are the highest wind speeds throughout year (Figure 3.3b). The highest spring (April) average wind speeds (Figure 3.3b) are located in the Southwest corridor. The Coastal corridor spring mean wind speed is similar to the mean winter wind speed, with average Bay wind speeds of 6.8

m/s and Coastal wind speeds of 6.1 m/s. Inland-North mean wind speeds are 5.2 m/s and Inland-South wind speeds are 5.5 m/s. The Southwest corner has the second highest wind speeds observed in the region for the spring at 6.7 m/s. Moderately high wind speeds between 5.5-6.5m/s are found along the Maryland-Delaware border within the central portion of the study area.

In the spring, the wind patterns show highest wind speeds localized in the central Bay corridor and wind speeds drop along the coast. Wind speeds are even lower in the inland corridor which has a distinguishable north and south divide; Inland-North wind speeds are lower than Inland-South wind speeds.

The summer (July, Figure 3.3c) has the lowest observed mean wind speeds for the year for all corridors as well as the lowest overall wind speed for the entire study area with a value of 3.5 m/s. The highest wind speeds in this season are 4.0 m/s, present in the Bay corridor with Southwest corridor wind speeds only 0.1 m/s slower. Coastal corridor wind speeds were lower than Southwest corridor wind speeds at 3.7 m/s. Inland wind speeds were the lowest recorded wind speeds for the duration of the study at 2.9 m/s and 3.0 m/s for Inland-North and Inland-South sections respectively.

The low wind speed area present in all time periods in the Inland corridor has grown in the size in the summer season compared to spring projections and now covers the northern portion of the Delaware Bay.

Fall (October; October 6 to November 5) mean wind speeds (Figure 3.3d) are shown to be a transition between the summer and winter. Bay and Coastal corridor mean wind speeds are 5.5 m/s and 4.9 m/s, respectively. Inland-North and Inland-South Wind speeds are 2.9 m/s and 3.4 m/s, respectively. Southwest corridor wind

speeds are higher than surrounding areas at 3.9 m/s although they are a full meter per second slower than Coastal corridor mean wind speeds within this season.
The area of low wind speeds is present throughout the Inland corridor during the fall and mimics patterns observed in the summer, although overall wind speeds are at a higher magnitude, especially in the Bay corridor.

Overall, mean summer (August) wind speeds (Figure 3.3c) are the lowest wind speeds found throughout the entire year at 3.5 m/s, and spring (April) wind speeds (Figure 3.3b, 6.0 m/s) and not winter wind speeds (5.6 m/s) are the highest observed throughout the study. In comparison to the longer time-series analyzed by Hughes and Veron (2015), this seasonal variability is typical of what is found in the region. In looking at Figure 3.3a-d, the spatial variation in seasonal wind speed is similar to those seen in annual wind patterns (Figure 3.2) with high wind speeds offshore, slightly lower winds speeds at the coast followed by a channel of low wind speeds inland and a moderate increase in wind speeds in the Southwest corner of Delaware. The northeastern portion of the study area exhibits the lowest wind speeds during the winter season.

3.1.2 Median Wind Speed

The median wind speed is the wind speed at the midpoint between the lowest and highest wind speed observed. Median wind speeds were analyzed in this study to avoid the biases associated with mean wind speeds (Hennessey 1977). Median wind speeds are helpful in analyzing wind data because they are not subject to outlier influences the same way as mean wind speeds (Wolf-Gerrit 2013).

Annual

Similar to the annual mean wind speeds, annual median wind speeds are highest in the Bay corridor, however the median wind speed in general is lower than the mean wind speeds with an overall annual median wind speed of 5.4 m/s; annual average median wind speeds were produced by taking the median of each station and then averaging this value per corridor (Table 3.2 and Figure 3.4). Coastal and Southwest corridors have identical median wind speeds of 4.5 m/s (Table 3.2) and Inland-North and Inland-South have similar median wind speeds of 3.4 and 3.6 m/s. Median wind speed patterns mimic the geographical distribution of mean wind speeds with few exceptions. The general trend of annual median wind speeds across the study area (Figure 3.4) is for winds to be highest in the Bay corridor with lower median wind speeds in the Coastal corridor. Inland annual median wind speeds are roughly 1.0 m/s lower than annual Coastal corridor median wind speeds. Median wind speeds are higher in the Southwest corridor than Inland corridor median wind speeds, and most importantly, mimic intensity levels previously reached at the coast. The entire Inland corridor demonstrates a very low annual median wind speed.

Seasonal

Overall, winter (January) median wind speeds (Figure 3.5a) are higher than annual median wind speeds by 0.7 m/s with a value of 5.0 m/s. Bay corridor median winter wind speeds are the highest median of all the corridors and have an average median wind speed of 6.0 m/s. Southwest corridor median wind speeds are the second highest median wind speeds in winter with a median wind speed of 5.6 m/s. Coastal winter median wind speeds are 0.7 m/s less than Southwest corridor median wind

speeds. Inland corridor winter median wind speeds are 4.1 m/s and 4.4 m/s for the Norther and Southern sections, respectively.

The Inland region of low wind speed discussed in the annual and seasonal mean wind speed maps (Figures 3.2, 3.3) is similar in geographical extent to the region of low median wind speeds present within the winter season. However, this feature is not as pronounced in winter as it is present annually. It should be noted that the Coastal corridor has median wind speeds significantly lower than the median wind speeds in the Southwest corridor for the winter season.

Spring (April) median wind speeds (Figure 3.5b) are the highest seasonal median wind speeds for the entire study with an average value of 5.5 m/s. Bay corridor and Southwest corridor median wind speeds are nearly identical at 6.3 m/s and 6.2 m/s, respectively. Coastal corridor spring median wind speeds of 5.4m/s are significantly lower in magnitude than either Bay or Southwest corridor median wind. Inland corridor North and South median wind speeds are 4.8 m/s and 5.0 m/s, respectively.

The same spatial patterns observed in the maps of the annual and winter median wind speeds are present throughout the spring season (Figure 3.5b). However, the Inland area of low median wind speeds is smallest in extent during this season. A notable exception present in the spring median values when compared to winter and annual median wind speeds is that the lowest median wind speeds are concentrated in the central portion of the northern most boundaries of the study area.

Summer (August) median wind speeds (Figure 3.5c) are the lowest median wind speeds observed throughout the entire study period with a value of 3.2 m/s. Bay and Southwest corridor summer median wind speeds are nearly identical at 3.7 m/s

and 3.6 m/s. Coastal summer median wind speeds are 3.3 m/s and Inland-North and Inland-South summer median wind speeds are 2.7 m/s and 2.6 m/s respectively. The Inland region of low median wind speeds is present throughout the entire Inland corridor and borders the Southwest and Bay corridors in the summer, extending also into the Northern section of the Coastal corridor. Inland-South summer median wind speeds are the lowest in the study area.

Fall (October) median wind speeds (Figure 3.5d) are slightly larger in magnitude than summer median wind speeds by 0.2 m/s at a value of 3.4 m/s. Bay corridor fall median wind speeds are the highest out of all the spatial corridors for the fall at 5.0 m/s, followed by Coastal corridor fall median wind speeds with a value of 3.9 m/s. Southwest corridor fall median wind speeds are 3.1 m/s and Inland corridor fall median wind speeds are 2.4 m/s in both Northern and Southern sections. It is important to note that the relationship between the Southwest corridor and Coastal corridor median wind speeds has inverted such that in the fall season the median wind speeds are greater within the Coastal corridor than in the Southwest corridor, while the opposite is true for all other seasons.

The Inland region of low median wind speeds is largest in area during the fall season and extends into the Inland corridor and into the Southwest corridor. Relative to the summer, this area of low median wind speeds has receded from northern portions of the Coastal corridor. This region of low median wind speeds covers most of the northern portion of the study area, although is mostly not present in the Bay corridor.

3.1.3 Mean-Median Difference

The mean median difference (MMD) maps graphically display the degree of difference between mean and median wind speeds and represents the divergence between the midpoint of the data range and the average (Rosa et al. 1993). This metric allows for comparison with mean wind speeds to determine how the dispersion and skewness of a distribution causes the mean and median wind speeds to diverge. The larger the MMD value, the greater the likelihood that the increased presence of very high winds speeds, even if still a small portion of the dataset, has shifted the mean away from the midpoint of the data. Thus, areas of high MMD values may indicate areas that experience a larger variation in wind speeds, or a higher occurrence of high winds speeds, and may be less optimal for wind farm development. It is possible that the winds at these sites will require more study than those with small MMD because of the larger dispersion in the data.

Annual

Annually, the MMD (Table 3.3, Figure 3.6) varies between 0.4 m/s at its lowest in the Inland-North corridor and 0.9 m/s at its highest in the Coastal corridor. Inland-South, Bay and Southwest corridors all have MMDs of 0.7 m/s. Within the annual MMD map, areas of low MMD are restricted to the Northern portion of the study area. Higher MMDs are present along the Coastal corridor. The northern portion of the Bay corridor shares the lowest MMD with the Inland-North corridor, yet the southern half of the Bay corridor has some of the highest MMD present annually. High MMDs present within the Coastal corridor indicate that the mean is farther away from the midpoint of the data range. The Northern portion of the study area have the

smallest data dispersion, however this is also an area of relatively low mean wind speeds overall.

There is low winter (January) MMD (Figure 3.7a) in the Northern half of the study area with the lowest values of 0.4 m/s along the west central portion of Delaware and adjacent areas of Maryland. There is a gradual increase in winter MMD within the Inland corridor transitioning from north to south where MMD reaches 0.6 m/s. Winter MMD is highest in the Southwest corridor with values of 0.8 m/s followed, and slightly lower in the Coastal (0.7 m/s) and Bay corridors (0.6 m/s). There is a large area of low MMD in the northern portion of the study area, present from North-Central Maryland through the Inland-North corridor continuing to the Coastal corridor. At the Coastal corridor, the winter MMD increases to 0.4 m/s. Inland-South corridor low MMDs are bordered to the east and west by higher MMD in the Coastal and Southwest corridors.

Spring has the second lowest MMD (Figure 3.7b) among the four seasons analyzed with an overall value of 0.5 m/s. The spring MMD over the entire Inland corridor is 0.3 m/s in the North and 0.4 m/s in the South. The highest spring MMD lies in the Coastal corridor (0.7 m/s), and a moderate spring MMD of 0.5 m/s is found in both the Bay and Southwest corridors.

Summer (August) MMDs (Figure 3.7c) for the entire study area are the lowest of all seasonal MMDs throughout the entire study at 0.3 m/s. This is true in all corridors. The lowest summer MMD are present in the Northern portion of the Inland corridor at 0.2 m/s. Summer MMD increases slightly to 0.3 m/s in the Southwest and Bay corridors, and is largest in the Inland South (0.4 m/s) and Coastal corridors (0.5 m/s).

Low values in summer for MMD indicate that mean wind speed is very close to the center of the data range, and so the data distribution is not very skewed with few outliers, similar to a normal distribution. Therefore, the mean wind speed is a very good representation of the general characteristics of the wind and can be used effectively when siting and planning a wind farm.

By contrast with summer, fall (October) MMD is the largest seasonal MMD for the entire study with a mean value of 0.8 m/s over the entire area (Figure 3.7d). The lowest fall MMD is found in the Bay and Inland-North corridors at 0.5 m/s. The Coastal corridor has the highest fall MMD of 1.0 m/s followed by the Inland-South and Southwest corridors with MMD of 0.9 m/s and 0.8 m/s.

Fall MMD in the Inland-South and southern portions of the Inland-North corridor is higher than the Fall MMD in the Southwest corridor, which is opposite to the other seasons when MMD is higher in the Southwest corridor than the Inland corridor, possibly due to influences along the coast where MMD values are the largest in the fall season. The fall presents itself as the most difficult season to characterize wind speeds using only the mean wind speed metric as evidenced by the high seasonal MMD, indicating that the data is likely skewed by the presence of higher wind speeds. This means that wind farm planners will need more detailed studies in siting potential wind farm locations in the area.

3.1.4 Probability Distribution

3.1.4.1 Skewness

Distributions of wind speeds often demonstrate positive skewness because there is an uneven distribution of wind speeds, with an abundance of very low wind speeds, and a significant tail of high wind speeds (Brown et al. 1984, see Figure 2.6). Assessing the degree of skewness provides a measure of dispersion, which is a measure of the spread in the data. Skewness was calculated annually and for each individual season as described in section 2.3.4.1 and these values were compared to MMD (Table 3.4). Skewness is a measure of symmetry of the probability distribution and illustrates how much the dataset diverges from a normal distribution (Trauth 2015). Large skewness indicates a longer tail in the distribution on one side of the distribution versus the other and thus a more dispersed data set. Thus, skewness may help explain the distance between mean wind speeds and the median wind speeds, and therefore can be used to gauge the representativeness of MMD in characterizing the variability in the wind speeds for an area.

The annual skewness is 0.7. Skewness for the winter (0.7), spring (0.6), summer (0.7) and fall (0.9) are shown in Table 3.4., along with corresponding MMD values. The variation in the MMD seasonal values, followed a similar trend to the skewness values, except for in the summer. Summer skewness deviates from this pattern when compared to the MMD for the other seasons, as the summer skewness is comparable to winter skewness instead of continuing to decrease like the MMD. One possible reason for this difference between MMD and skewness in the summer season is the very low wind speeds present within the summer months.

3.1.4.2 Weibull Distribution

Normal distributions assume equal dispersion around the mean of a given dataset with 50% of samples falling on either side of the curve (Trauth 2015). However, numerous studies (e.g. Bludszuweit 2008, Safari and Gasore 2010) have demonstrated that the normal distribution is not as applicable to wind observations as the Weibull distribution. The Normal distribution assumes that the mean, median and mode will all be the same; as the MMD metric developed above has demonstrated, this assumption is frequently inappropriate for wind data and means that the normal distribution will be a limited method for accurately representing wind observations (IESS 2008). The benefits of the Weibull distribution to represent wind data relative to the Rayleigh distribution can be found in section 2.3.4.

Weibull distributions (Figures 3.8, 3.9) were calculated as a fit to the wind speed data in each of the corridors and overlaid on top of the probability distributions of the annual and seasonal wind speeds. It should be noted that in the annual dataset, and in the summer and fall seasons, Inland wind speeds 1.0 m/s bins extend beyond the vertical access shown; these bins make up 21%, 24% and 34% of wind speeds respectively even though this is not accurately represented within the figures provided. The probability distributions show that Bay corridor had the largest range of wind speeds followed by Southwest, Coastal, and Inland corridors.

Annual

Annual wind speed distributions show that the Coastal corridor has the largest dispersion of wind speeds followed closely by Southwest corridor while the Bay corridor has the smallest dispersion of wind speeds annually. The difference between

the normal distribution and the Weibull distribution in the annual data is largest within the Coastal and Southwest corridors; this is most likely due to the lack of asymmetry in these distributions and the long tails of both datasets. The Weibull and normal distributions are in closest agreement in the Bay corridor where the tail of the distribution is the smallest observed.

Seasonal

The winter season has the most widely dispersed wind speed data within the study. The probability distributions show the largest tails in the distributions (Figure 3.9a). This feature is most notable in the Southwest corridor, followed by Coastal, Bay and Inland corridors respectively. The Weibull distribution peak accurately portrays the distribution peak while the normal distribution peak consistently appears significantly to the right of the probability distribution of the observed data.

The spring probability distribution shows less widely disperse data with a notable decrease in the frequency of high wind speeds (Figure 3.9b). Spring probability distribution tail lengths are largest in the Southwest corridor. The normal distribution peak again is located to the right (at a higher wind speed) of the peak of the probability distribution.

In the summer, the Weibull distribution is very similar to the normal distribution, and both do a reasonable job in representing the probability distribution of the observed wind data. Summer probability distributions show the least distributed winds in the study with the smallest dispersion in the hourly wind data (Figure 3.9c). As in the spring, the Weibull and the normal distribution exhibit similar patterns to

each other although the Weibull distribution clearly providing a better fit to the hourly data.

Fall Season probability distributions are the second most dispersed after the winter showing the greatest range in wind speeds (Figure 3.9d). The Coastal corridor probability distribution has the longest tail followed by Southwest, Inland and Bay corridors probability distributions respectively. Like in all previous seasons, Normal distributions placed the peak at higher winds speeds than the peak of the probability distribution of the observed wind speeds, while the Weibull distribution more accurately represents the data. It should be noted that in the Bay corridor, normal and Weibull distributions are the most similar in all seasons.

This characterization of the probability distributions matches well with comparisons to other studies in that almost uniformly the Weibull distribution is the preferred favorite probability density function to use in representing wind speeds (Früh 2013 and Carta et al. 2008). Safari & Gasore (2010) recognize that the normal distribution may be useful for representing wind data sets when the shape factor of the probability density function, often referred to as *k*, has a value of greater than 2. Weibull distributions calculate *k* with respect to the given data where higher k values represent steeper and more normally distributed data (Manwell 2010). Thus, in comparison to this study, Weibull distributions remain the gold standard in wind speed distribution representation, although the Normal distribution may be somewhat useful in certain locations and time periods, such as the Bay corridor and summer season, with small variation and high *k* values.

3.1.4.3 Wind Roses

Wind Roses are probability distributions that show the probability distribution of wind speeds as a function of direction (Mirhosseini et al. 2011). For this study, wind roses were produced for each corridor on an annual and seasonal basis (Figures 3.10-3.11). Bay corridor wind roses indicate that annually (Figure 3.10) wind speeds are highest coming from the Northwest but are most abundant coming from the Southwest. Seasonally, Bay corridor winds almost exclusively blow from the Northwest in the winter and spring, and switch to blowing from the Southwest during the summer and fall with a significant contribution of winds from the Northwest in the fall (Figure 3.11). Coastal corridor winds annually blow predominantly from the West. While most Coastal winds seasonally blow from the West, spring and summer winds blow from the South and Southwest. For small portions of the fall season winds blow from the East (Figure 3.11d).

Annually, Inland corridor winds blow from the Southwest (Figure 3.10). Winter Inland winds blow from the Northwest while spring, summer and fall winds blow form the Southwest (3.11). Annually Southwest corridor winds blow form the Southwest . Winds primarily blow form the Northwest during the winter Season while spring, summer and fall winds predominantly blow from the Southwest.

When comparing the wind roses to mean and median wind speeds, some interesting observations can be made. Winds generally blow from the West and Southwest. Because winds from these directions travel across the Chesapeake Bay, an area of lowered surface roughness; this may explain in part why mean wind speeds in the Southwest corridor are unexpectedly high. This pattern is seasonally observable and overlaps with median wind speeds as well in that higher median wind speeds are experienced in the Southwest corridor than was expected. These westerly and

southwesterly winds clearly influence the intensity of winds in the study area, predominantly in the Southwest corridor, although not as significantly in the Northern portion of the Inland corridor as winds must travel significant distances over land before reaching this region. The reason for this is that winds adjacent to the Southwest corridor are much less impeded by surface roughness as they travel across the larger part of the Chesapeake Bay, unlike the northern portion of the Inland corridor.

3.1.4.4 Standard Deviation

The standard deviation of wind speeds was calculated for all corridors annually and seasonally as shown in Table 3.4. Annually, standard deviation is largest in the Southwest corridor at a value of 4.0 m/s followed closely by the Coastal corridor at 3.8 m/s. The Bay corridor has a 3.4 m/s standard deviation while the Inland North and South corridors have 2.9 m/s and 3.1 m/s standard deviations respectively. Annually, standard deviation is largest in both corridors that are directly exposed to land and sea breezes; the standard deviations of the Bay, Inland-North and Inland-South corridors are notably less. This is understood as Bay corridor wind speeds although, annually higher than all other wind speeds, are the most consistent winds in the study area thus having lower standard division, and Inland-North and Inland-South both exhibit low wind speeds, thus influencing these corridors to have lower standard deviations.

Seasonally, the average winter standard deviations are the largest with an average of 3.8 m/s which is similar to the spring average standard deviation of 3.6 m/s. Fall average standard deviation is 3.0 m/s while summer average standard deviation is 2.3 m/s. The Southwest corridor has the highest standard deviations annually and in all

seasons with the exception of the fall season where Coastal corridor standard deviation is 0.1 m/s higher than Southwest corridor standard deviations.

Standard deviations relative to mean wind speeds are very high, for example the Southwest corridor has a standard deviation of 4.0 m/s and a mean wind speed of only 5.2 m/s. These findings relate to how Chang and Bai (2001) display the inadequacy of using standard deviation for characterizing wind data due to its positively skewed nature. The results of the standard deviation analysis confirm the assertions made by Leys et al. (2012) in that when analyzing data prone to high outliers, standard deviation is a poor choice of technique used to quantify the distribution of a given dataset.

3.1.5 Upper and Lower Quartiles

Upper and lower quartiles demonstrate the limit at which 25% of wind speeds will be greater or less than respectively (To and Lam 1995). These value limits are used to represent relative ideal and sub-par wind patterns.

3.1.5.1 Upper Quartile Winds

Annual

When mapped, the Upper Quartile of the annual wind speeds (Figure 3.12) present spatial patterns similar to those of the annual mean wind speeds (Figure 3.1). Overall, annual UQ wind speeds for the study area are 6.9 m/s meaning that 75% of wind speeds will be below this value. Bay corridor UQ wind speeds annually are the highest in the study area at 8.0 m/s. Southwest corridor and Coastal UQ wind speeds

are the next highest UQ wind speeds at 7.4 m/s and 7.3 m/s respectively. Inland-North and Inland-South wind speeds have UQ wind speeds of 5.6 m/s and 6.2 m/s.

The general trend in UQ wind speeds is for UQ values to be highest in the central portion of the Bay corridor, then to subside within the Inland corridor. The UQ wind speeds are higher in the Southwest corridor than in the Inland corridor. Inland-North UQ wind speeds extend from northeastern Maryland and northern Delaware with lowest UQ wind speeds present in Northern Delaware.

Seasonal

The threshold for winter (January) Upper Quartile wind speeds (Figure 3.13a) for the entire study area is 8.1 m/s, which is above the annual average UQ threshold, indicating the enhanced wind speeds in this season. Southwest corridor UQ wind speeds are the highest of all the corridors during the winter with a threshold at 9.3 m/s; the Bay corridor UQ is similar at 9.0 m/s. Coastal and Inland-South corridor UQ wind speeds are the next highest with the UQ wind speed thresholds at 7.8 m/s and 7.4m/s respectively. Inland-North UQ wind speeds have values above 6.8 m/s during the winter season.

Spring (April) UQ wind speeds (Figure 3.13b) are the highest UQ values present throughout the entire study with an average total area UQ threshold value of 8.4 m/s. This is similar to the median wind speeds which showed a maximum in the spring. The Southwest corridor has substantially higher spring UQ threshold than any other corridor with a value of 9.6 m/s; this corresponds with wind rose representations in that southwesterly winds predominated this time period within this corridor. The

next highest UQ threshold present through the spring is in the Bay corridor followed by the Coastal corridor with UQ wind speed thresholds of 8.8 m/s and 8.3 m/s.

In looking at the map of the Spring UQ wind speeds, there is a clear distinction between the Inland-South corridor UQ and Inland-North corridor UQ which appears to be caused by the southwesterly winds influencing the Southwest corridor as demonstrated Inland Spring wind rose. Bay corridor UQ is similar to the UQ values in the southern portion of the study area while, as expected, the Coastal corridor UQ is similar to the UQ of the Inland-South corridor.

Summer (July) UQ wind thresholds are overall the lowest for all seasons at 4.9 m/s (Figure 3.13c). Similar UQ threshold patterns exhibited in previous seasons are present throughout the summer, but to a lesser degree. For example, Southwest corridor UQ threshold is the highest of all of the corridors at 5.8 m/s. The Coastal and Bay corridors UQ threshold values are lower than in the Bay corridor at 5.2 m/s and 5.1 m/s, respectively. Inland-North and Inland-South UQ thresholds are 4.2 m/s and 4.5 m/s, lower than in any array that is influenced by coastal winds such as sea breezes.

Summer UQ threshold patterns exhibit the lowest UQ threshold present in the northern portion of the study area. This area of low UQ values is present throughout the Inland corridor These low wind speed thresholds are concomitant with the higher UQ values in the Southwest corridor and in southern portions of the Coastal corridor.

Fall (October) UQ wind speeds for the various corridors do not follow a similar pattern to the other seasons (Figure 3.13d). However, the Bay corridor, instead of the Coastal corridor, has the highest UQ threshold during the fall at 7.4 m/s. The next highest UQ wind speeds are found in the Coastal corridor at 6.6 m/s, and then the

Southwest corridor at 6.0 m/s. Inland-North and Inland-South UQ limits are 4.5 m/s and 5.1 m/s.

Fall UQ patterns also exhibit the lowest UQ wind speeds in the northern half of the study area. Similar to the summer, these lower UQ values extended into the Inland corridor. Southwest UQ wind speeds covers an area to the southwest that extends beyond Delaware just to the edge of the study area. Similarly, the area of relatively high Coastal corridor UQ values spreads across the southern portion of the Bay corridor continuing to the edge of the study area

3.1.5.2 Lower Quartile Winds

Annual

Overall Annual LQ wind speeds (Figure 3.14) for the study area are 2.2 m/s, meaning that 75% of wind speeds will be greater than this value. Annually, Bay corridor LQ wind speeds, similar to UQ wind speeds, are the highest in the study area with a threshold at 3.5 m/s. Coastal and Southwest corridor LQ wind speeds are the next highest LQ wind speeds at a limit of 2.5 m/s and 2.1 m/s respectively. Inland corridor LQ wind speeds are 1.6 m/s for both northern and southern regions.

Lower Quartile Annual wind speeds present annual patterns similar to Upper Quartile and annual mean wind speeds as shown in Figures 3.1 and 3.12. The general trend in LQ wind speeds is for LQ values to be highest in the Bay corridor, then to subside within the Inland corridor. The Southwest corridor LQ values are higher than those found in the Inland corridor. Annual UQ and LQ patterns mimic each other except for Lowest UQ values dominating in northern Delaware and then extending into the Inland corridor, whereas the lowest annual LQ values occur in northeastern Maryland, outside the study area.

Seasonal

Winter (January) LQ (Figure 3.15a) is higher than the average LQ value by 0.4 m/s with a threshold of 2.6 m/s, again indicating the presence of higher wind speeds overall in the winter. The highest winter LQ wind speeds were present in the Bay corridor at 3.7 m/s. The next highest LQ threshold is in the Coastal corridor with a LQ limit of 2.7 m/s. Southwest corridor LQ is similar to Coastal values at a threshold of 2.6 m/s; Inland-North and Inland-South are 1.9 m/s and 2.0 m/s respectively. Low Winter LQ values are present in the northern half of the study area and persist throughout the Inland corridor. Winter LQ are highest within the central portion of the Bay corridor, while the rest of the winter Bay corridor LQ are similar to Coastal LQ.

Spring (April) LQ wind speeds (Figure 3.15b) are the highest seasonal LQ values recorded throughout the study which is similar to the pattern observed in the median wind speeds at a threshold of 3.0 m/s. Spring LQ are the highest in the Bay corridor at 4.4 m/s. These elevated LQ values extend into the Northeast portion of the study area. Coastal and Southwest corridor spring LQ limits are 3.2 m/s and 2.9 m/s respectively. Inland corridor LQ wind speeds are the lowest at 2.4 m/s for both north and south portions.

Summer (July) LQ wind speeds (Figure 3.15c) are the second lowest seasonal threshold observed at 1.8 m/s. Summer Bay corridor LQ has a threshold of 2.5 m/s which is the highest of all the corridors. The next highest LQ thresholds were found in the Coastal and Southwest corridors with values of 1.9 m/s and 1.8 m/s, respectively. Summer Inland-North and Inland-South LQ limits were 1.4 m/s and 1.2 m/s. Patterns

of Summer LQ wind speeds in the summer are similar to Summer UQ patterns in that the area of lowest threshold spreads from the northern portion of the study area to the Inland corridor and transitions across the Coastal corridor to border the Bay corridor.

Fall (October) LQ values were the lowest of the seasonal LQ limits observed throughout the study at 1.7 m/s (Figure 3.15d). The highest LQ threshold still occurs in the Bay corridor at 3.1 m/s followed by a Coastal corridor LQ of 2.3 m/s. The Southwest corridor LQ wind speed was 1.2 m/s and Inland-North and Inland-South LQ thresholds were 0.8 m/s and 0.9 m/s respectively. The distribution of LQ spatially exhibited the same patterns as the distribution of UQ values during the fall season for the study area.

3.1.6 Quartile Deviation

Quartile Deviation (QD) is a measure of dispersion Krumbein (1936). Generally, standard deviation is the preferred metric for dispersion within a dataset. However, standard deviation metrics assume that the data in question is normally distributed in a Gaussian fashion without outliers (Leys et al. 2012). Wind speeds, by their nature, are unevenly distributed around the peak in the distribution and therefore standard deviation may not be the best representation for quantifying dispersion within a wind speed dataset. QD, therefore, was explored as a method to quantify wind speed dispersion within annual and seasonal datasets.

Annual

Annual QD within the study area range between 2.0 m/s to 2.6 m/s with an overall average of 2.3 m/s (Figure 3.16). The highest quartile deviation lies in the

Southwest corridor with a value of 2.6 m/s. The Coastal corridor Annual QD is 2.4 m/s, with both Bay and Inland-North corridors QDs at a slightly lower value of 2.3 m/s. The Northern portion of the Inland corridor has a QD of 2.0 m/s.

The quartile deviations indicate that annually the wind speeds will be most dispersed in the Southwest corridor and least dispersed in the Inland-North corridor. Mid-range levels of dispersion will be present annually within all other corridors. In general, the northern portion of the study area exhibits lower dispersion than the southern portion.

Seasonal

Winter (January) QD over the entire study area have an average value of 2.8 m/s between all corridors (Figure 3.17a). The highest quartile deviation is present in the Southwest corridor at a value of 3.4 m/s. The Southwest corridor is surrounded by regions of lower QD, such as a in the Inland-North and Inland-South corridors, with values of QD of 2.5 m/s and 2.7 m/s, respectively. The Coastal corridor QD is 2.5 m/s and the Bay corridor QD is 2.7 m/s.

Quartile deviations throughout the study area are largest in the Southwest corridor, and decrease in regions away from the Southwest corridor, especially in the Inland-South corridor. The QD is higher in the southern portion of the Coastal corridor.

Spring (April) QD patterns are similar to winter QD patterns, although as a whole, spring QD is 0.1 m/s less than winter values at 2.7 m/s (Figure 3.17b). The Spring QD is the highest in the Southwest corridor at 3.3 m/s. The Inland-North and

Inland-South QDs are 2.5 m/s and 2.7 m/s, respectively. The Coastal corridor QD is 2.6 m/s, and in the Bay corridor the QD is 2.2 m/s. To a lesser extent, the patterns exhibited in the winter persist through to the spring season.

Summer (July) QDs are the lowest of all the seasons with a QD of 1.6 m/s (Figure 3.17c). The highest summer QD of 2.0 m/s is present in the Southwest corridor. Lower QDs of 1.4 m/s and 1.7 m/s are present in the Inland-North and Inland-South corridor. The Coastal and Bay corridor QDs are 1.6 m/s and 1.3 m/s, respectfully. The summer QD values are homogenous throughout the entire northern portion of the study area as well as a significant portion of the southern half of the study area. QD values are higher only in the Southwest and the southern most parts of the Coastal corridor. Summer thus presents itself as the most uniformly distributed season with respect to wind speed.

Fall (October) QD is the second lowest observed within the study area with a value of 2.1 m/s (Figure 3.17d). The Southwest corridor possesses the highest fall QD of any corridor with a value of 2.4 m/s. Coastal corridor QD is 2.2 m/s while Bay and Inland-South QD are 2.1 m/s. Inland-North QD is 1.8 m/s. Fall QD patterns exhibit the lowest QD in the northern half of the study area except for the Bay corridor. These low QDs occur in the northwestern portions of Maryland and condition down through the Inland corridor to the bottom of the study area. Southwest corridor QD is similar to the southeastern portion of Maryland.

3.1.7 Correlation of Winds

3.1.7.1 Autocorrelation

Autocorrelations (AC) were performed seasonally for each corridor by correlating a station's hourly wind speeds with itself to determine the length of signal persistence within the winds of a particular corridor (Table 3.9). Each corridor's autocorrelation was performed on a single representative station; these stations were stations BUOY_CMAN4, DBNG, DELN, and DSEA for the Bay, Coastal, Inland and Southwest corridors respectively. Autocorrelation can be interpreted by the level of statistical significance or by the acceptable amount of correlation depending on the application (Trauth 2015, Alexiadis 1999). Alexiadis (1999) used 2 hour time lengths to compare persistence based forecasting models to Neural Network forecasting models and experienced correlation values as low as 70%. This is in contrast to (Brokish and Kirtley (2009) who used 12 hour lags often exhibiting autocorrelation values around 20%, as reference points to use in their analysis of Markov Chain utility in wind power estimation. Especially in forecasting, there is a limit below which the autocorrelation no longer makes sense even if the autocorrelation is statistically significant (Brokish and Kirtley 2009); the level chosen for this study was 50%, thus exhibiting an R^2 value and representation level of 25%.

Winter AC were the highest seasonal values recorded throughout the entire study with values of 6.75 hours. Within the fall season, persistence was highest in the Coastal and Southwest corridors at 6 hours, followed by Bay and Inland corridors with ACs of 5 hours. Fall had the second highest seasonal AC value of 5.5 hours. Within the fall season, Coastal and Southwest corridors had identical persistence levels with ACs of 6 hours. Bay and Inland corridors had the lowest AC in the fall at ACs of 5

hours. Spring had the second lowest AC values at 5 hours. The spring Bay corridor AC was the lowest corridor AC value of 4 hours followed by the Coastal and Inland corridors with 5 hours AC values. Southwest corridor spring AC was 6 hours. Summer AC values were the lowest throughout the entire study with an overall AC between corridors of 4.5 hours. Within the summer, AC for the Bay and Southwest corridors was 5 hours while Coastal and Inland corridors had ACs of 4 hours.

3.1.7.2 Pearson Correlation

Correlations (Figures 3.24-3.28) were performed between all stations annually and seasonally using the Pearson Correlation method outlined in (Equation 2.9). Correlation maps of 70%, 80% and 90% (R) were created for all time steps annually and seasonally. These maps illustrate the correlation between station measurements, or how temporally and spatially similar stations measurements are to one another in terms of wind speed. Thus, variance explained (R2) for each map respectively was 49%, 64% and 81%. The 80% and 90% maps proved useful in analysis although 70% maps were too densely correlated to be of any use in discerning correlations between stations within the study area and have not been included in this work. Pearson Correlations (PC) were used to discern zones of similarity within the study area in which wind speeds would uniformly fluctuate.

Annual

Annual patterns were present through all seasons and varied in concert with wind speed intensity. Higher wind speeds generated more correlations between stations within the study area while lower wind speeds generated fewer correlations between stations. In both 90% and 80% annual correlation maps clearly defined zones were discernable. These zones were also present in seasonal analysis, and will be

discussed further below. One key point of interest in the annual correlation representations was that within the 80% correlation map, 2 zones were readily apparent and distinguishable from one another.

Seasonal

Two predominant zones emerged within the annual PC analysis that were refined through seasonal PC analysis. Zone A, the most prevalent zone in the study is a polygon between stations DBLK, DDFS, DGES, DGUM, DLAU, and DSEA. This zone appeared in all 90% maps. Although Zone A was present in all seasons, it was much smaller during the summer season due to low wind speeds. These low wind speeds produced fewer 90% correlations because they did not have the strength to influence station wind speeds over large distances. Zone A is also present in all 80% maps and expands to include all Inland stations within this correlation class level. Zone B is the second correlation zone that is consistently present in the PC analysis. Zone B exists exclusively within Coastal corridor Stations. Correlations among these stations are weaker than Zone A correlations and appear in only 80% maps. Zone B consists of stations BUOY_LWSD1, LEWE_MOB DRHB, DIRL, DBNG, and DBBB. Zone A and Zone B are graphically represented in Figure 3.23.

In both 90% and 80% maps, there are significant seasonal differences in correlation intensities. Mean wind speeds in the summer, as indicated in section 3.1.1, were slower than any other seasons. This directly corresponds with correlation results in that during the summer, correlation densities are the lowest observed throughout the entire study. Conversely, correlations are most extensive throughout the study area in

the fall. This corresponds with wind rose analysis in that during this season, winds are most consistently blowing in the same direction, thus allowing for stronger correlations present in this time period. Winter and spring correlation patterns exhibit similar patterns of correlation, although to lesser extents than the fall

Within the 70% maps, Correlations between stations are so prevalent that there is no discernable pattern within this correlation class. Despite not exhibiting discernable patterns within the correlations, the overwhelming number of correlations in the 70% class show that winds in Delaware have a general pattern within the entire study area, possibly due to the small size of the state. Thus, 70% correlations show the presence of mesoscale features within the winds in Delaware.

Mean	Offshore	Coastal	Inland North	Inland South	South West	AVG
Annual	6.1	5.4	3.9	4.3	5.2	5.0
Winter	6.6	5.6	4.6	5.1	6.4	5.6
Spring	6.8	6.1	5.2	5.5	6.7	6.0
Summer	4.0	3.7	2.9	3.0	3.9	3.5
Fall	5.5	4.9	2.9	3.3	3.9	4.1

Table 3.1 Annual and seasonal mean wind speeds in m/s as calculated in each of the geographic corridors defined in Figure 3.2.

Median	Offshore	Coastal	Inland North	Inland South	South West	AVG
Annual	5.4	4.5	3.4	3.6	4.5	4.3
Winter	6.0	4.9	4.1	4.4	5.6	5.0
Spring	6.3	5.4	4.8	5.0	6.2	5.5
Summer	3.7	3.3	2.7	2.6	3.6	3.2
Fall	5.0	3.9	2.4	2.4	3.1	3.4

Table 3.2 Annual and seasonal median wind speed in m/s calculated by averaging median wind speeds per corridor (per station interpolation) for the corridors shown in Figure 3.2

MMD	Offshore	Coastal	Inland North	Inland South	South West	AVG
Annual	0.7	0.9	0.4	0.7	0.7	0.7
Winter	0.6	0.7	0.4	0.6	0.8	0.6
Spring	0.5	0.7	0.3	0.4	0.5	0.5
Summer	0.3	0.5	0.2	0.4	0.3	0.3
Fall	0.5	1.0	0.5	0.9	0.8	0.8

Table 3.3 Annual and seasonal mean-median difference in wind speed in m/s

Time Period	MMD (m/s)	Skewness
Winter	0.6	0.7
Spring	0.5	0.6
Summer	0.3	0.7
Fall	0.8	0.9

Table 3.4 Comparison between seasonal mean-median difference in m/s and skewness (unitless) as calculated from equation 2.5

Standard Deviation (m/s)	Annual	Winter	Spring	Summer	Fall	corridor Seasonal Average
Offshore	3.4	3.8	3.1	2.6	3.0	3.1
Coastal	3.8	3.6	3.4	2.6	3.3	3.2
Inland North	2.9	3.1	3.4	1.9	2.5	2.7
Inland South	3.1	3.5	3.6	2.0	2.8	3.0
South West	4.0	4.8	4.7	2.6	3.2	3.8

Table 3.5 Standard deviation of annual and seasonal mean wind speed in m/s calculated from hourly data.

UQ	Offshore	Coastal	Inland North	Inland South	South West	AVG
Annual	8.0	7.3	5.6	6.2	7.4	6.9
Winter	9.0	7.8	6.8	7.4	9.3	8.1
Spring	8.8	8.3	7.4	7.8	9.6	8.4
Summer	5.1	5.2	4.2	4.5	5.8	4.9
Fall	7.4	6.6	4.5	5.1	6.0	5.9

Table 3.6 Upper Quartile wind speed threshold for annual and seasonal data sets in m/s.

LQ	Offshore	Coastal	Inland North	Inland South	South West	AVG
Annual	3.5	2.5	1.6	1.6	2.1	2.2
Winter	3.7	2.7	1.9	2.0	2.6	2.6
Spring	4.4	3.2	2.4	2.4	2.9	3.0
Summer	2.5	1.9	1.4	1.2	1.8	1.8
Fall	3.1	2.3	0.8	0.9	1.2	1.7

Table 3.7 Annual and seasonal thresholds for the lower quartile of wind speeds (m/s).

QD	Offshore	Coastal	Inland North	Inland South	South West	AVG
Annual	2.3	2.4	2.0	2.3	2.6	2.3
Winter	2.7	2.5	2.5	2.7	3.4	2.8
Spring	2.2	2.6	2.5	2.7	3.3	2.7
Summer	1.3	1.6	1.4	1.7	2.0	1.6
Fall	2.1	2.2	1.8	2.1	2.4	2.1

Table 3.8 Annual and seasonal wind speed quartile deviation (difference in upper and lower quartile thresholds) in m/s.

Autocorrelation (hrs.)	Bay	Coastal	Inland	Southwest	Period Avg.
Annual	6	7	7	7	6.75
Winter	9	6	9	5	7.25
Spring	4	5	5	6	5
Summer	5	4	4	5	4.5
Fall	5	6	5	6	5.5

Table 3.9 Autocorrelations of all four corridors in all time steps with 25% persistence.

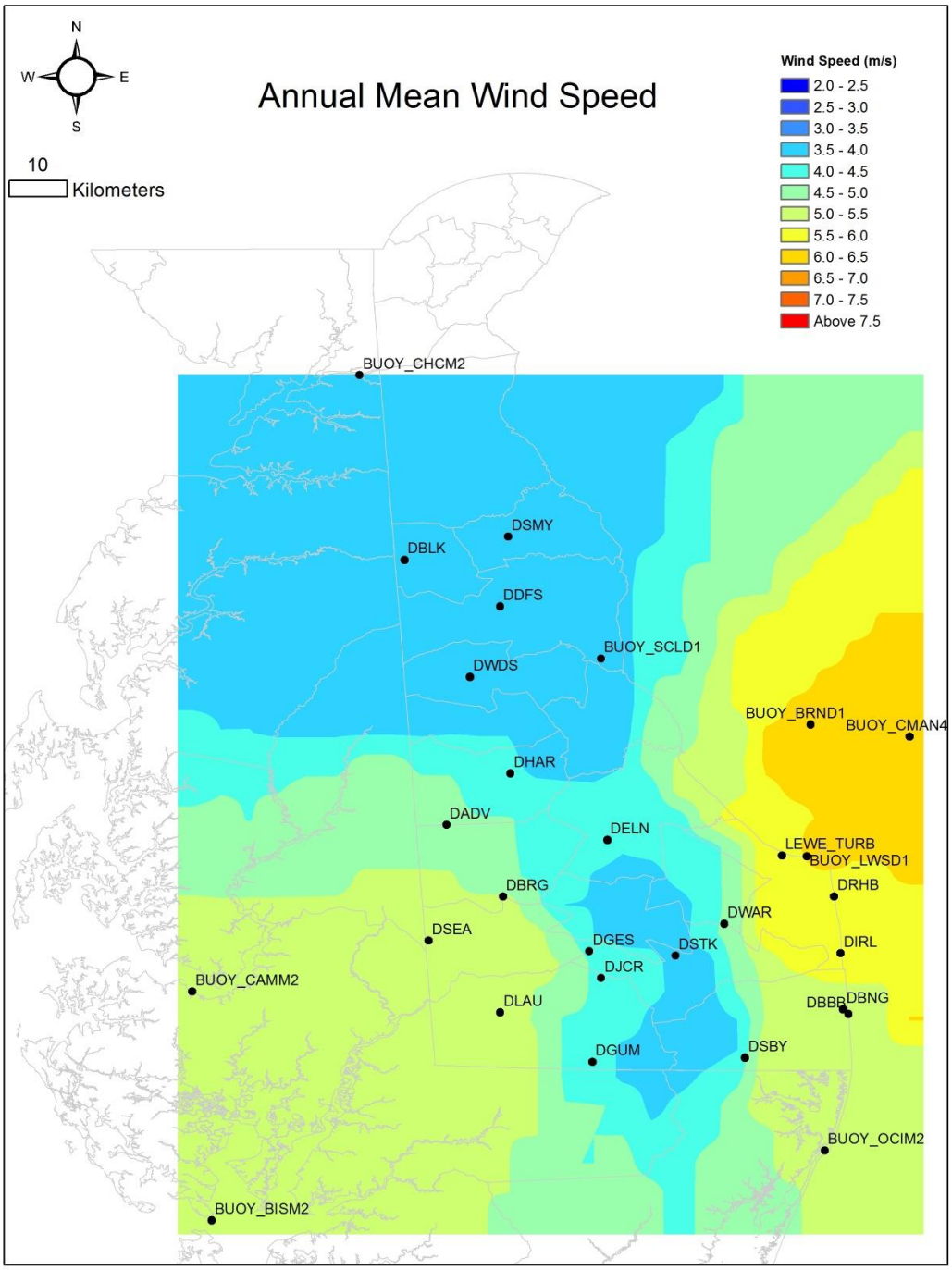

3.1 Annual mean wind speed map in m/s developed from station data of observed annual mean wind speeds for 2015.

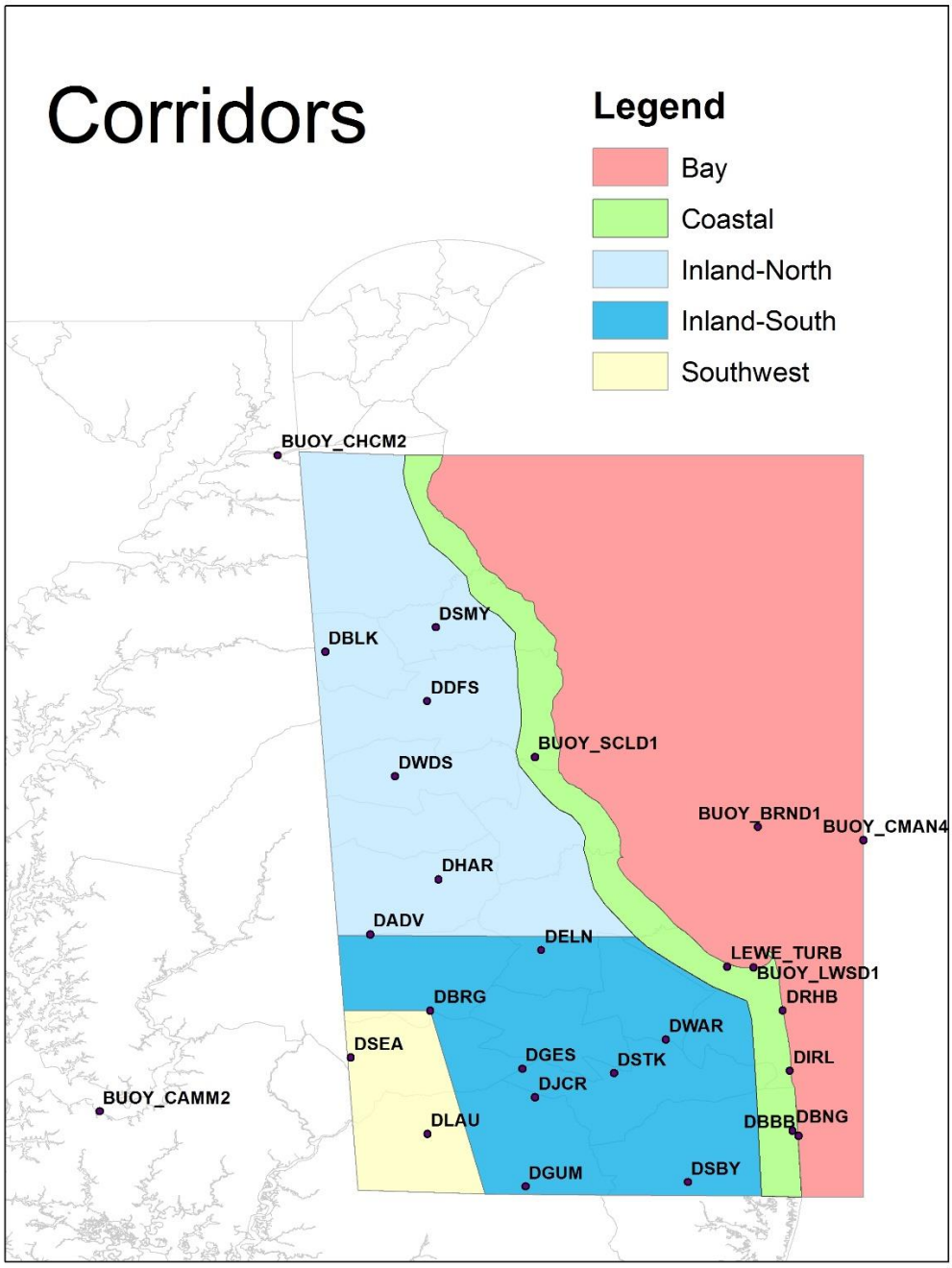

3.2 Geographical areas defined for this study based on analysis of interpolated wind data. Note that the Inland area in blue has been divided into North and South areas.

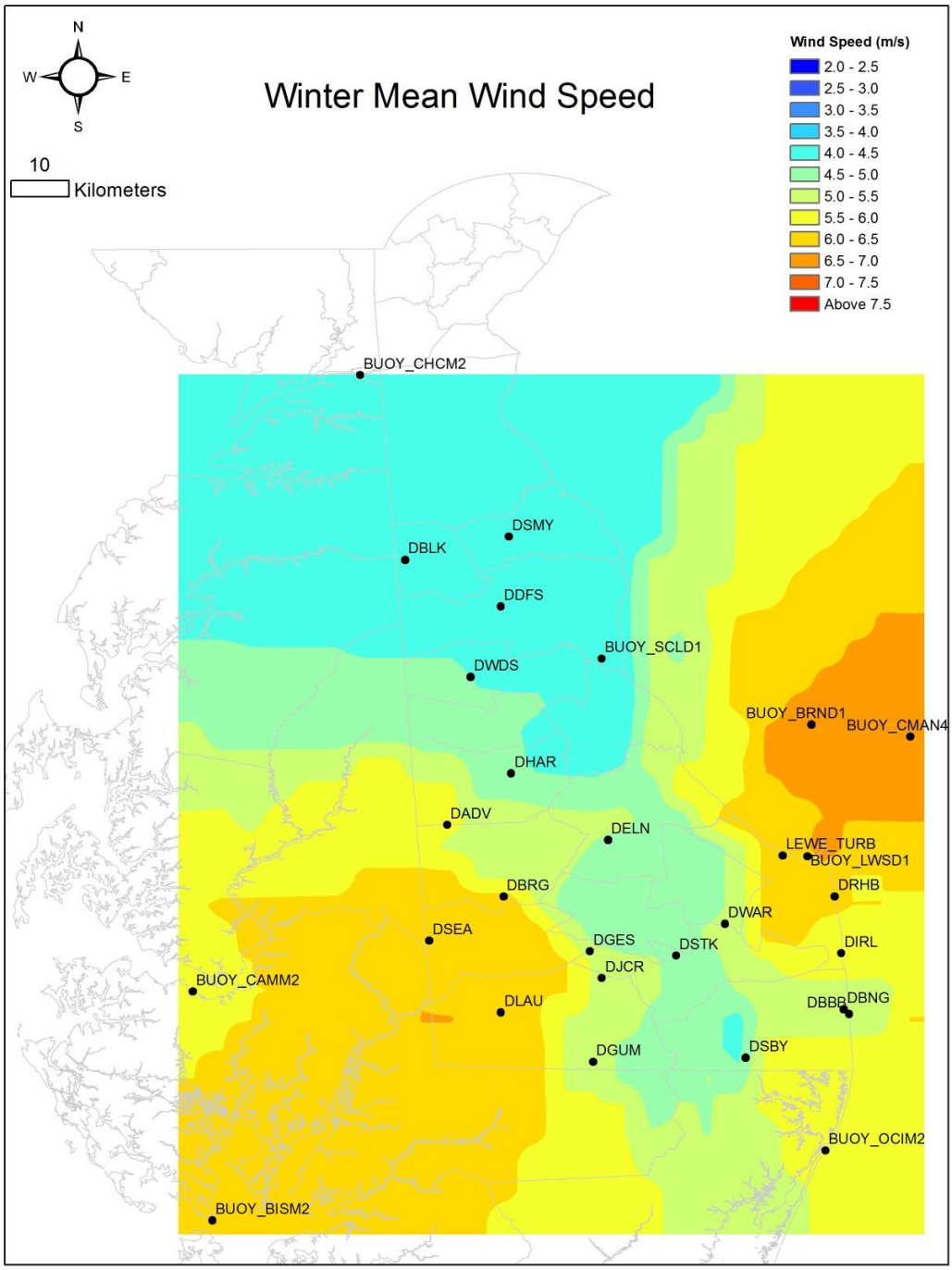

3.3a Winter (January) mean wind speed in m/s.

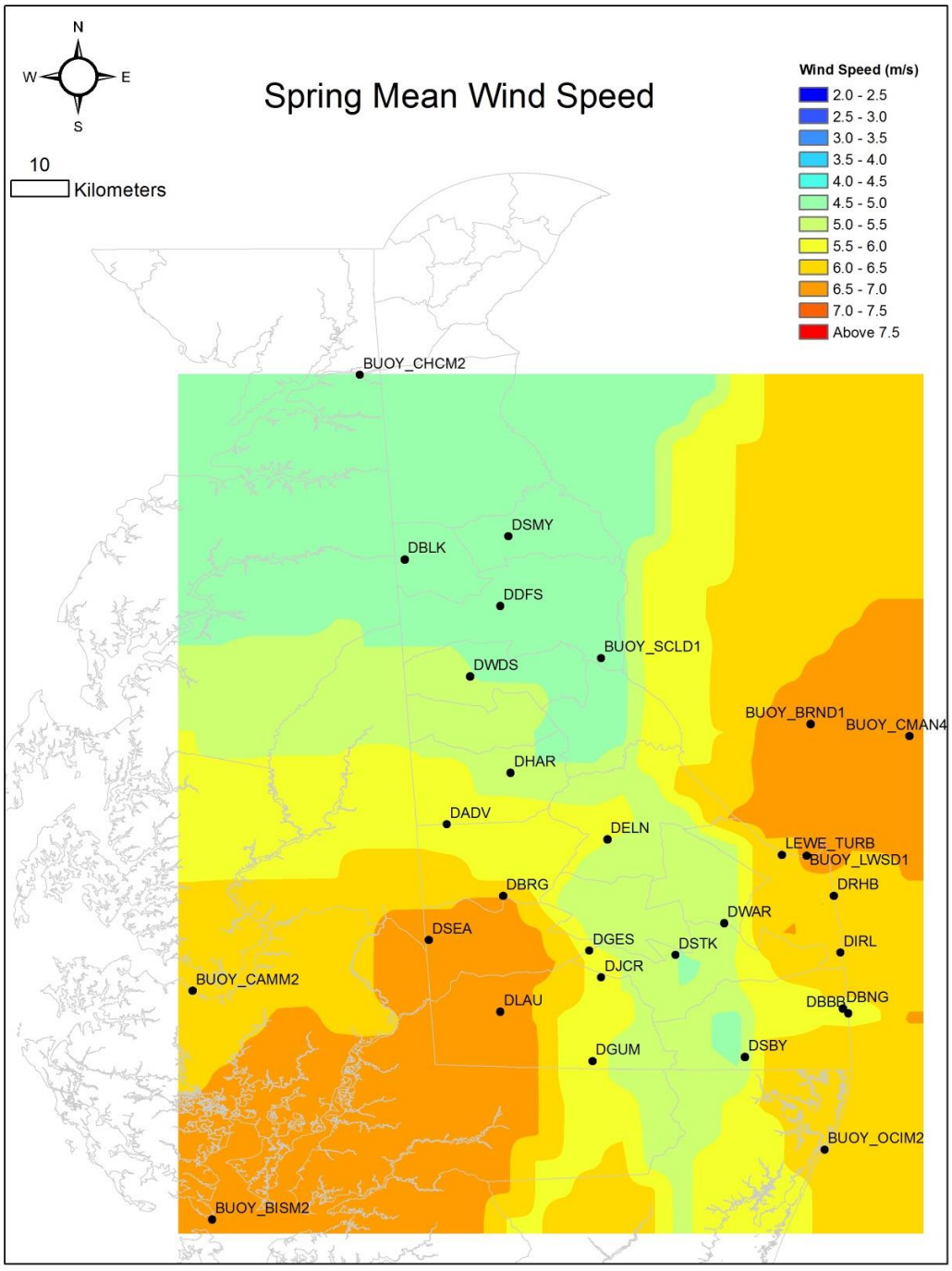

3.3b Spring (April) mean wind speed in m/s.

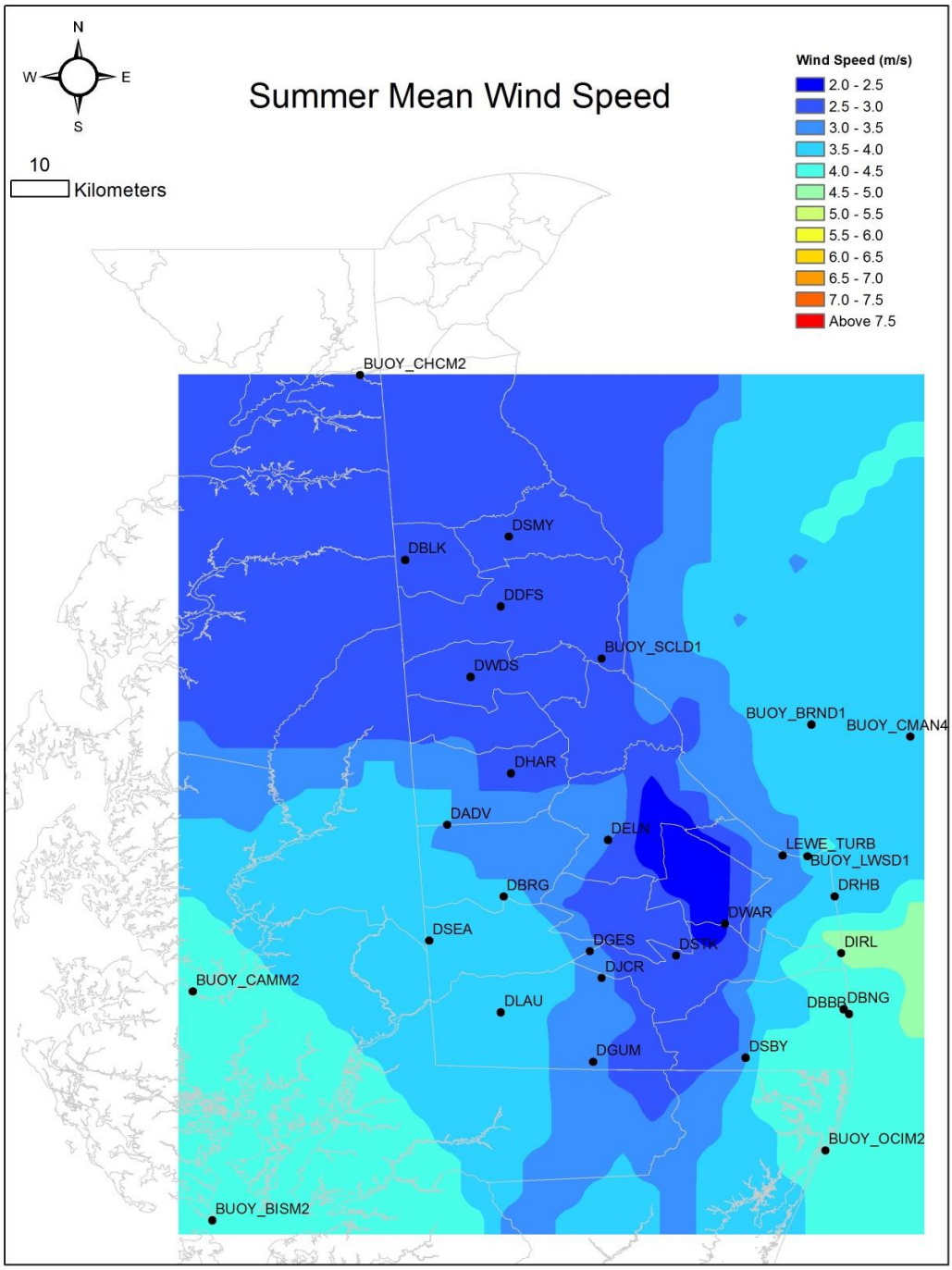

3.3c Summer (July) mean wind speed in m/s.

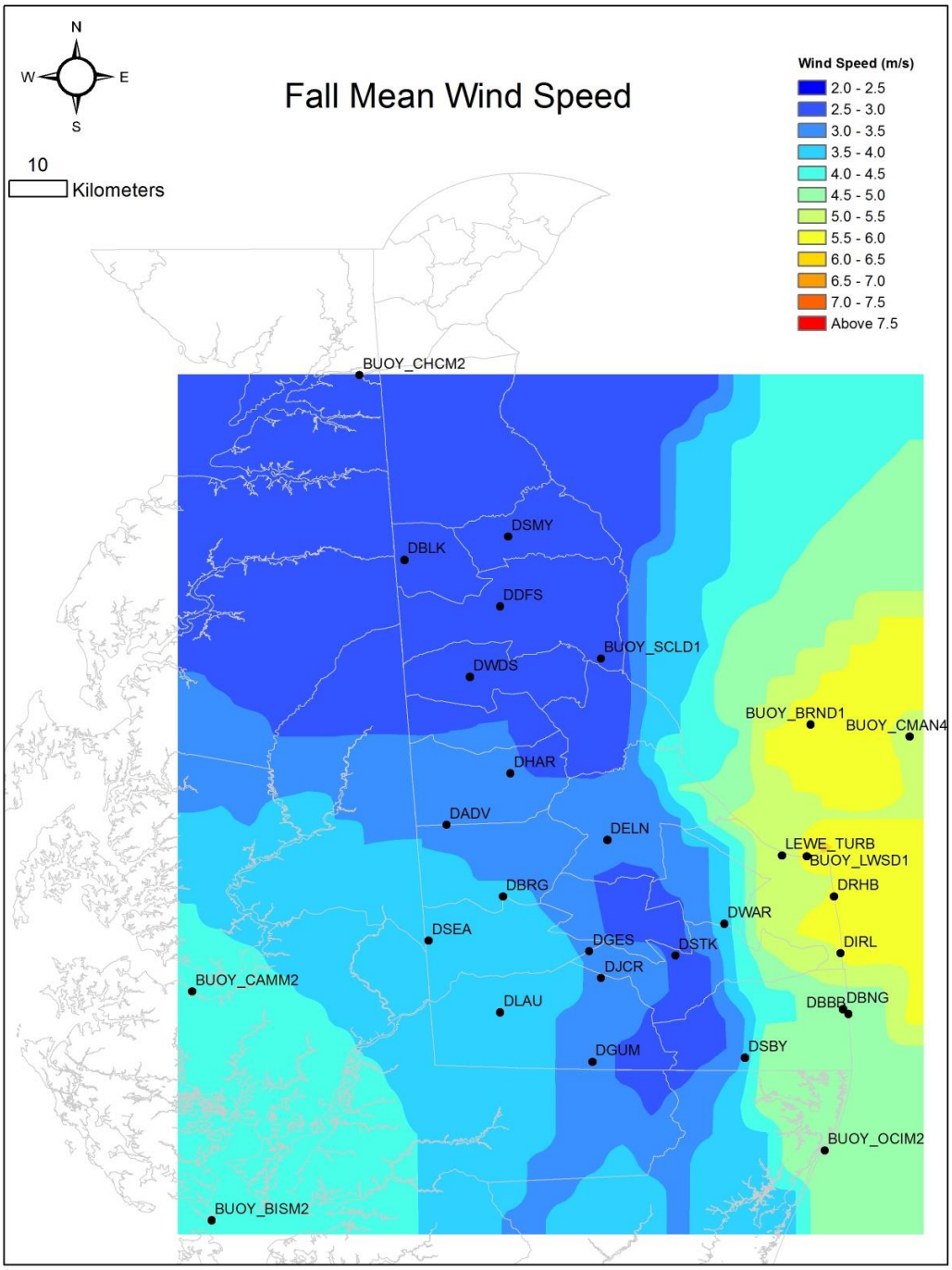

3.3d Autumn (October) mean wind speed in m/s. October defined as October 7-November.

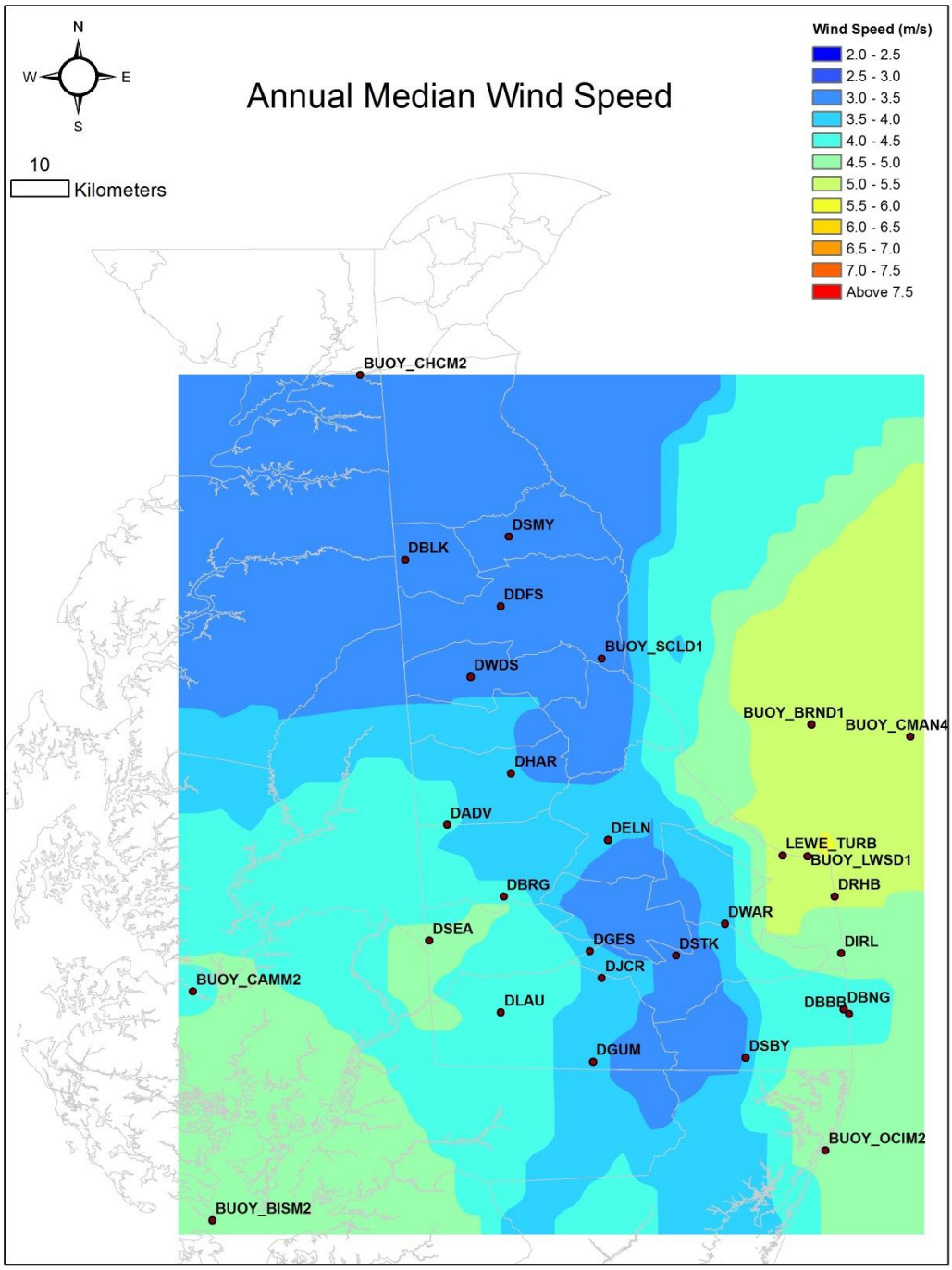

3.4 Annual median wind map developed from station data of observed wind speeds for 2015.

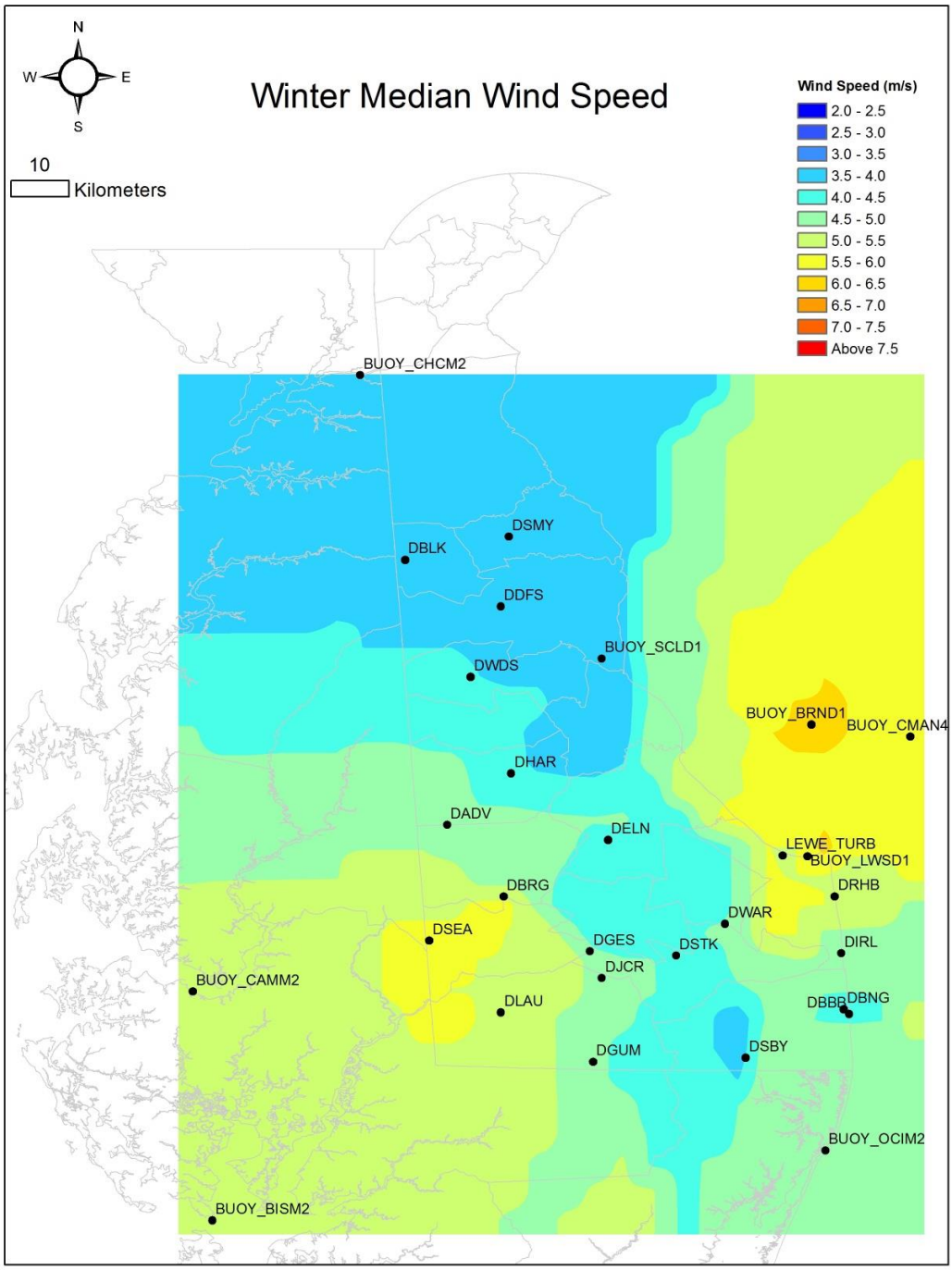

3.5a Winter (January) median wind speed in m/s.

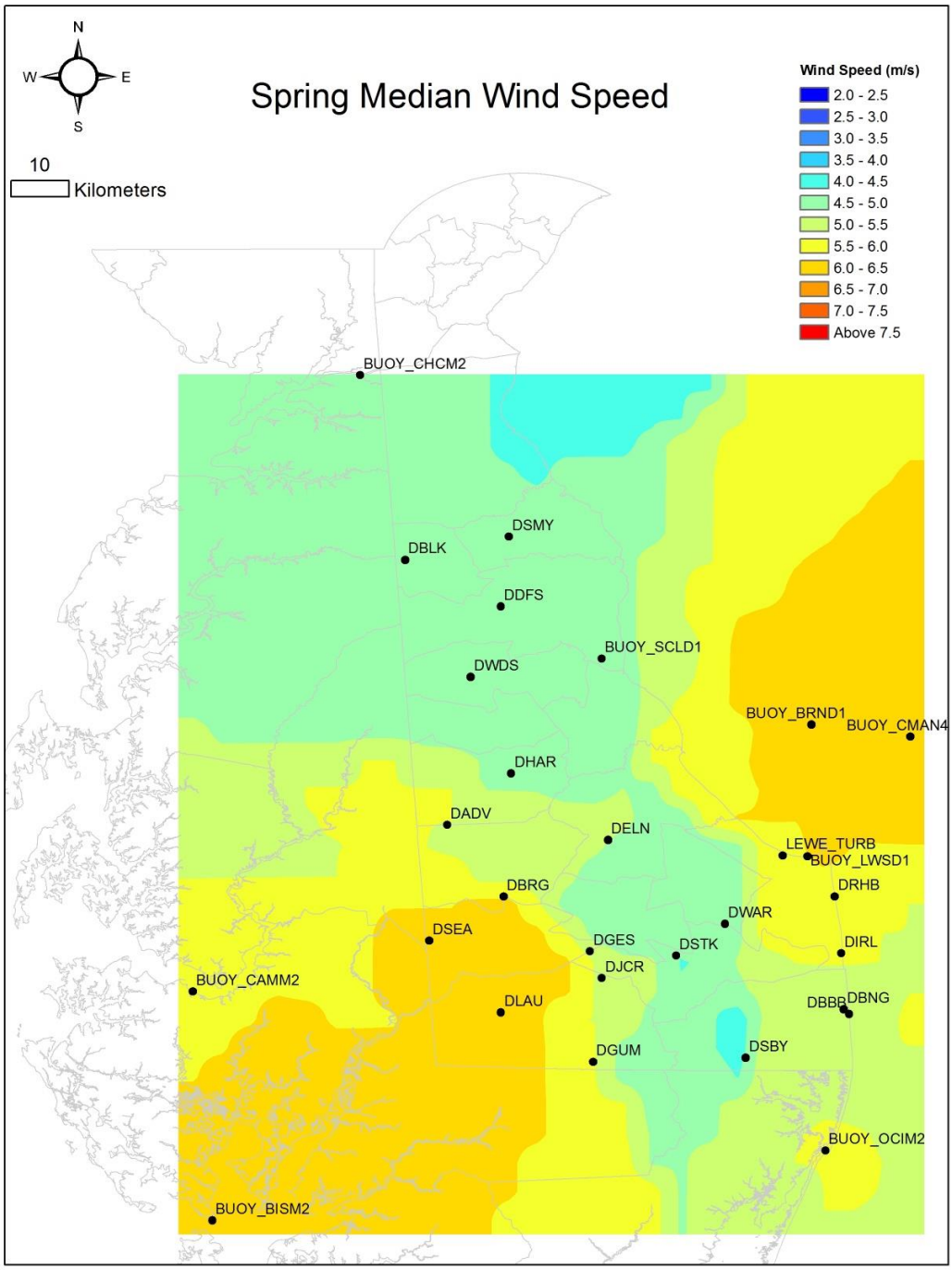

3.5b Spring (April) median wind speed in m/s.

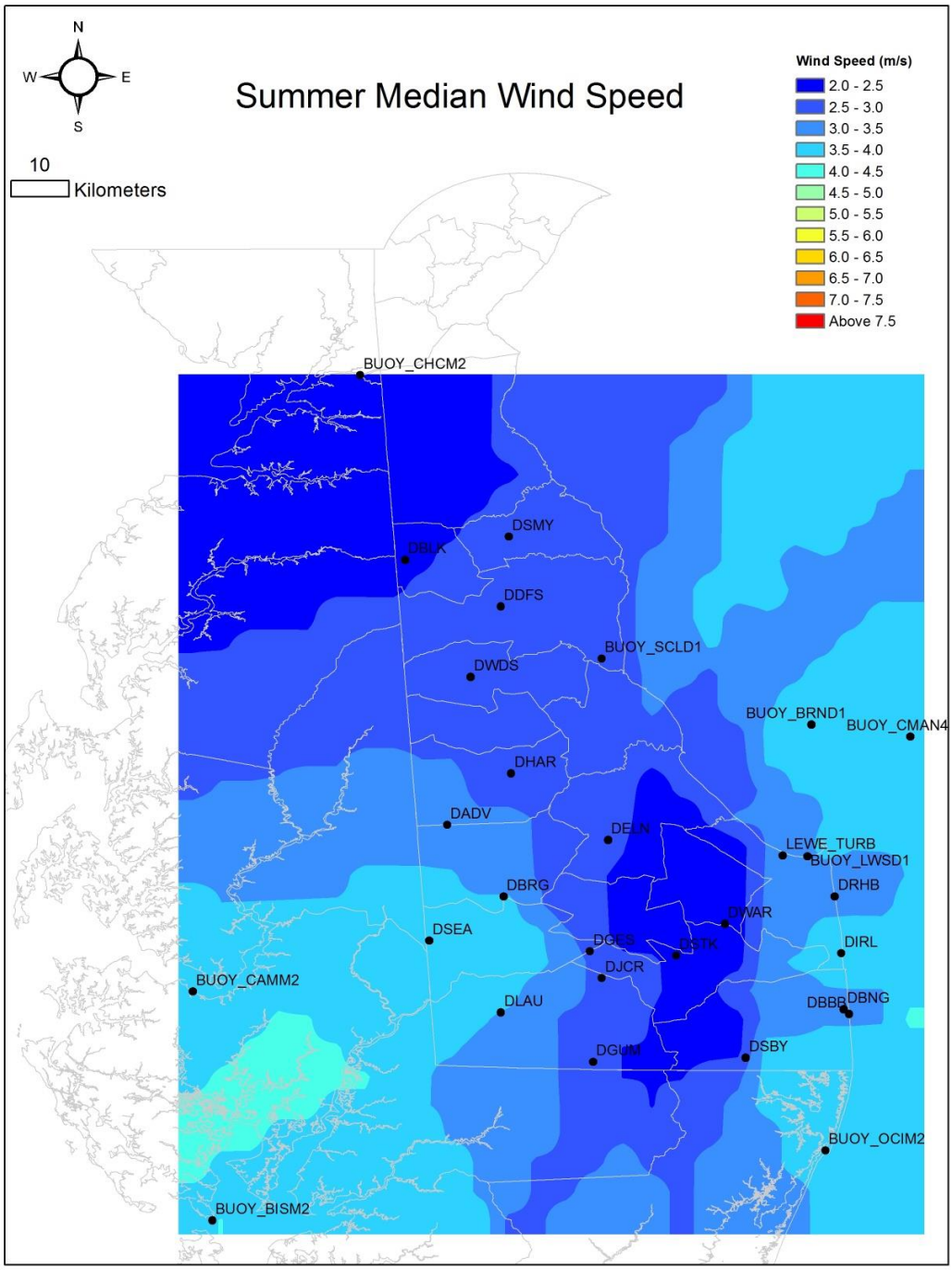

3.5c Summer (July) median wind speed in m/s.

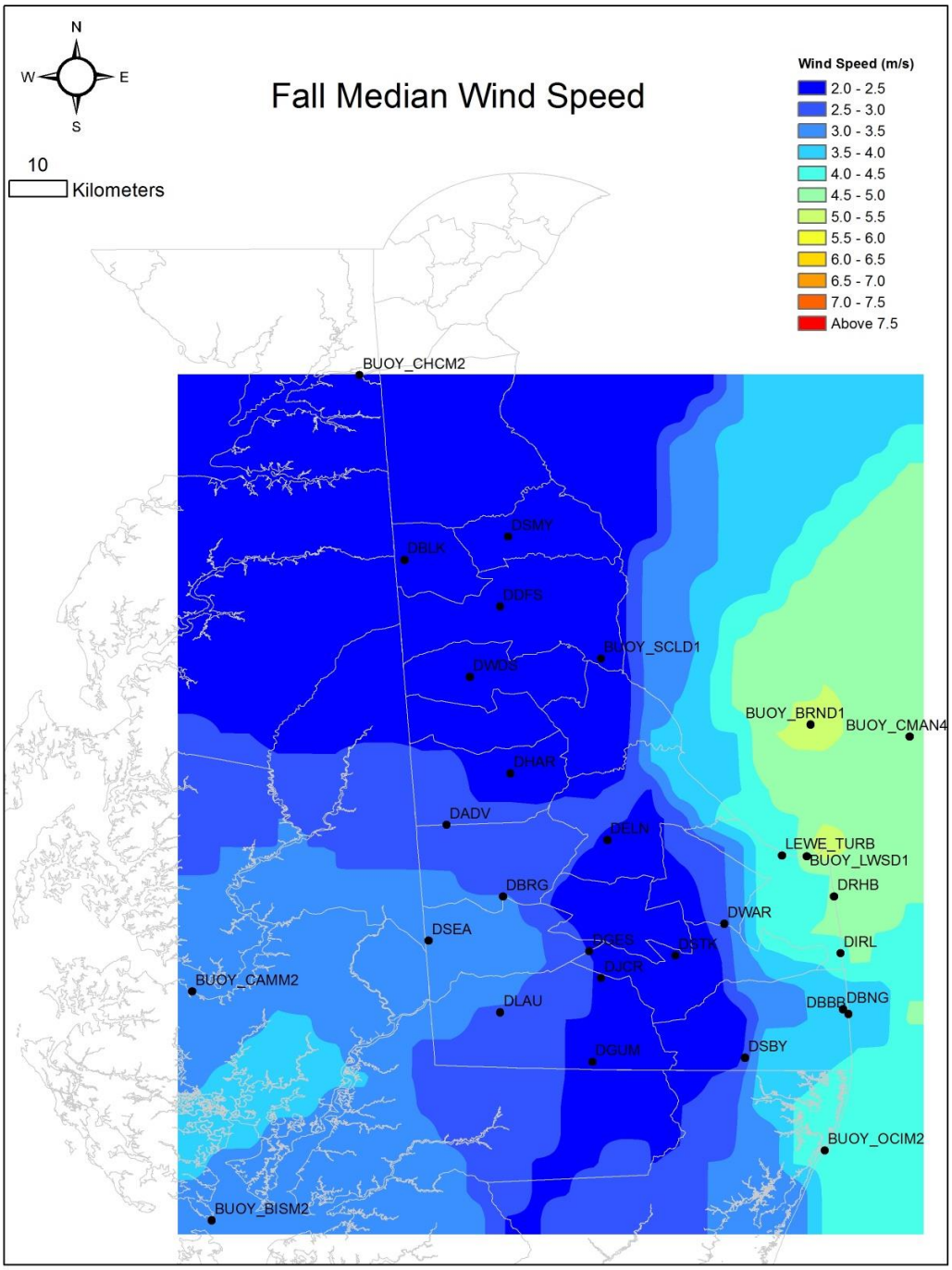

3.5d Fall (October) median wind speed in m/s.

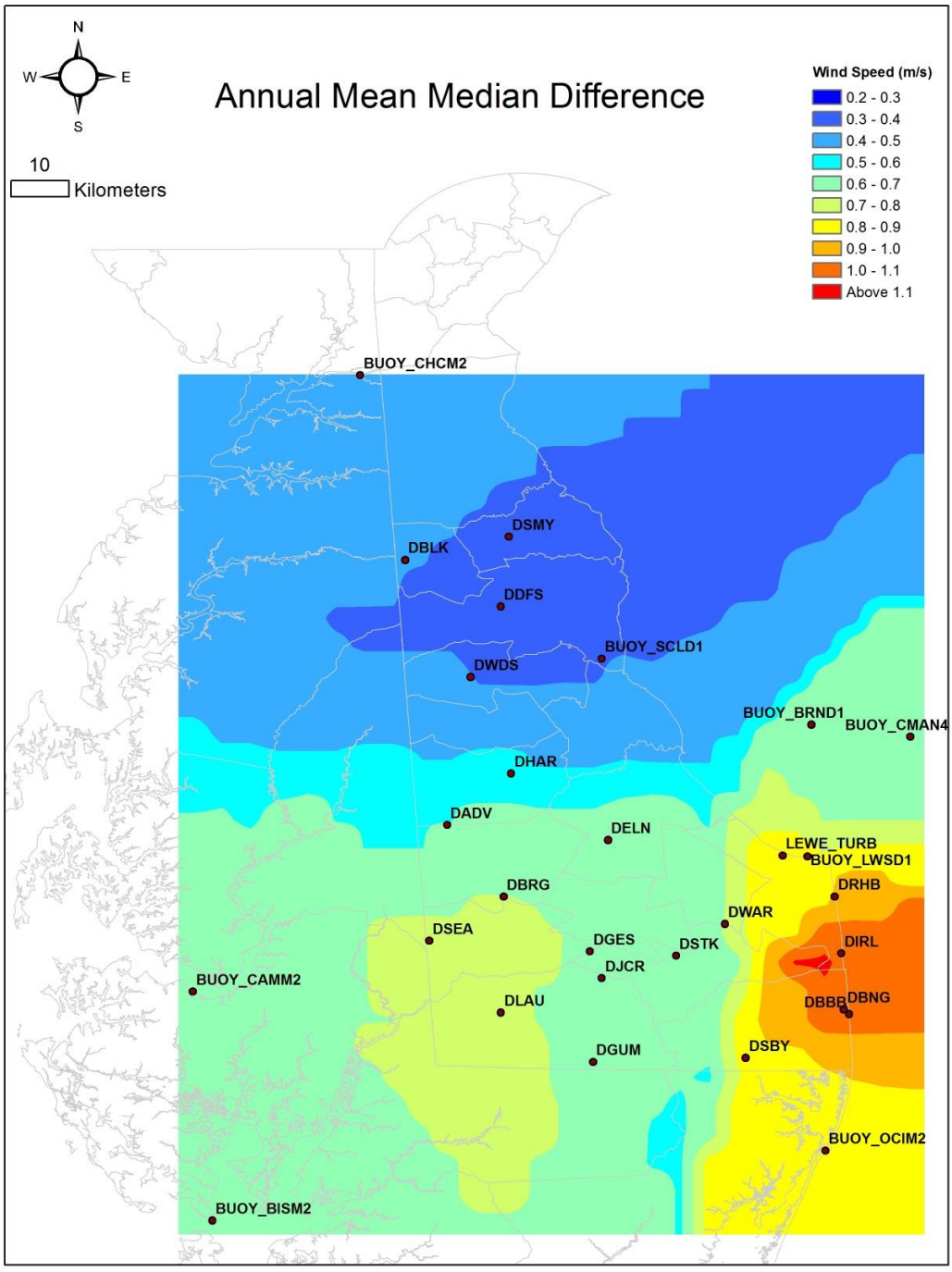

3.6 Annual Mean-Median Difference (MMD) map created from hourly mean observed wind speeds from 2015.

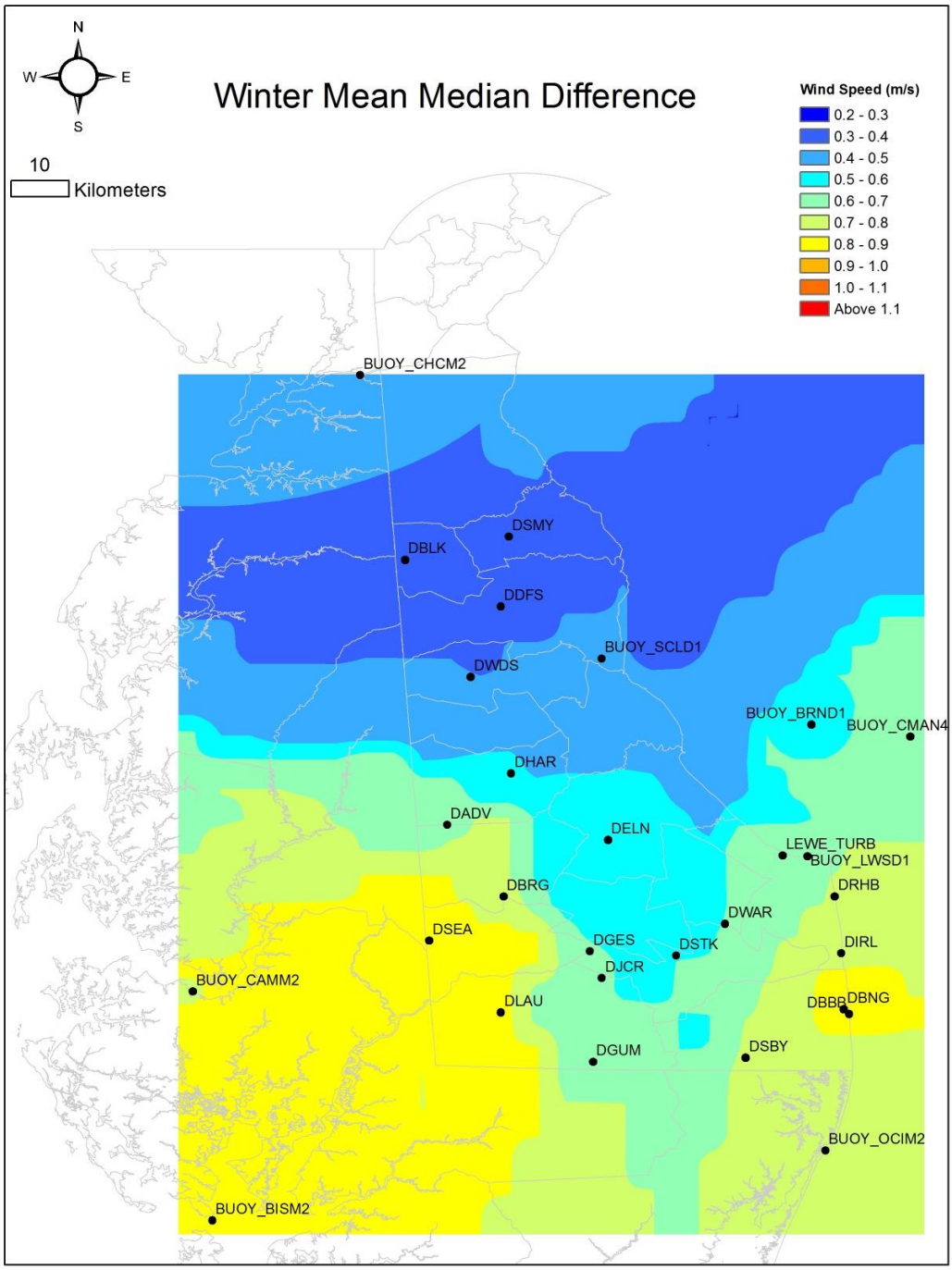

3.7a Winter (January) Mean-Median Difference (MMD) in m/s.

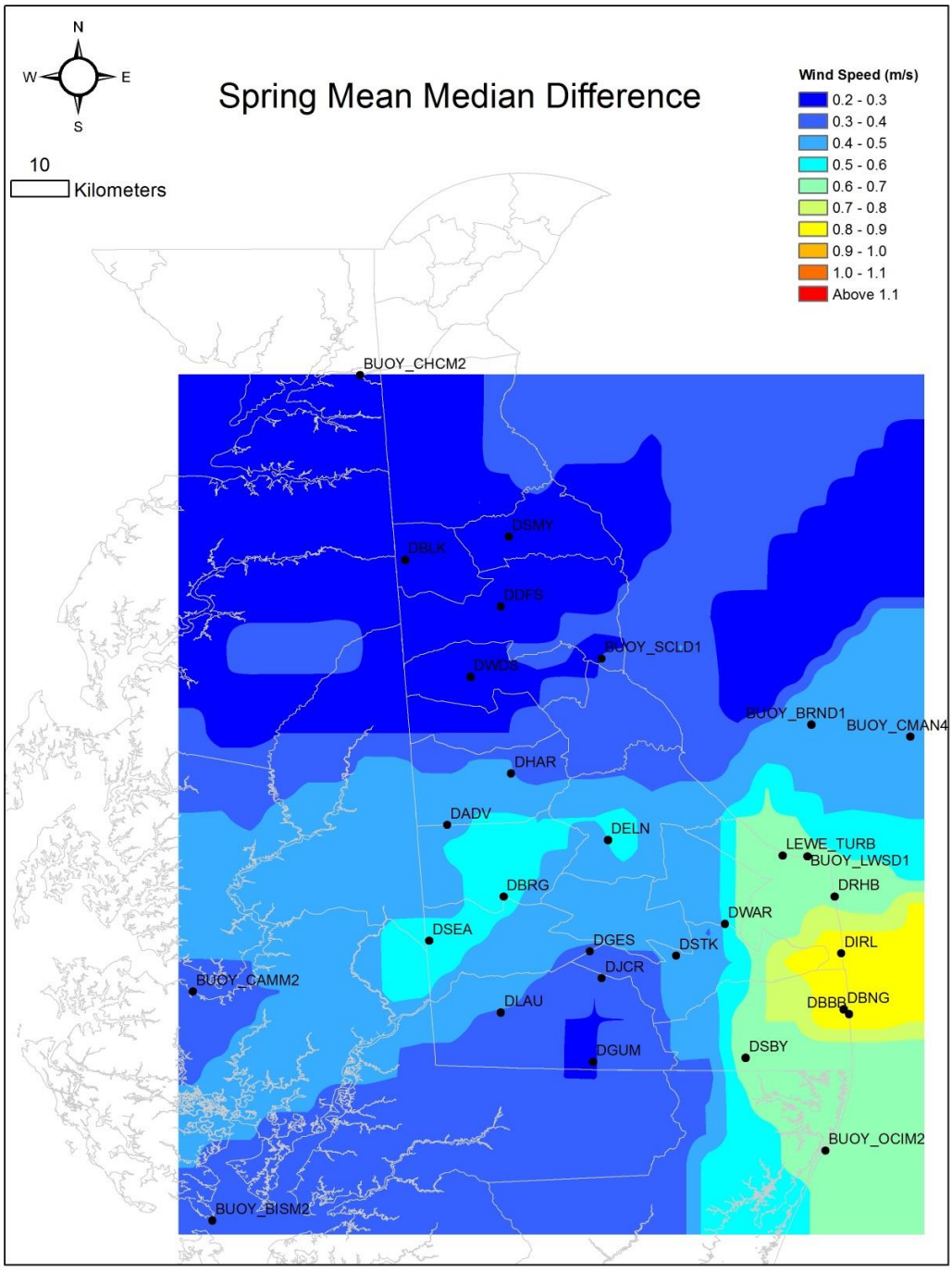

3.7b Spring (April) Mean-Median Difference (MMD) in m/s.

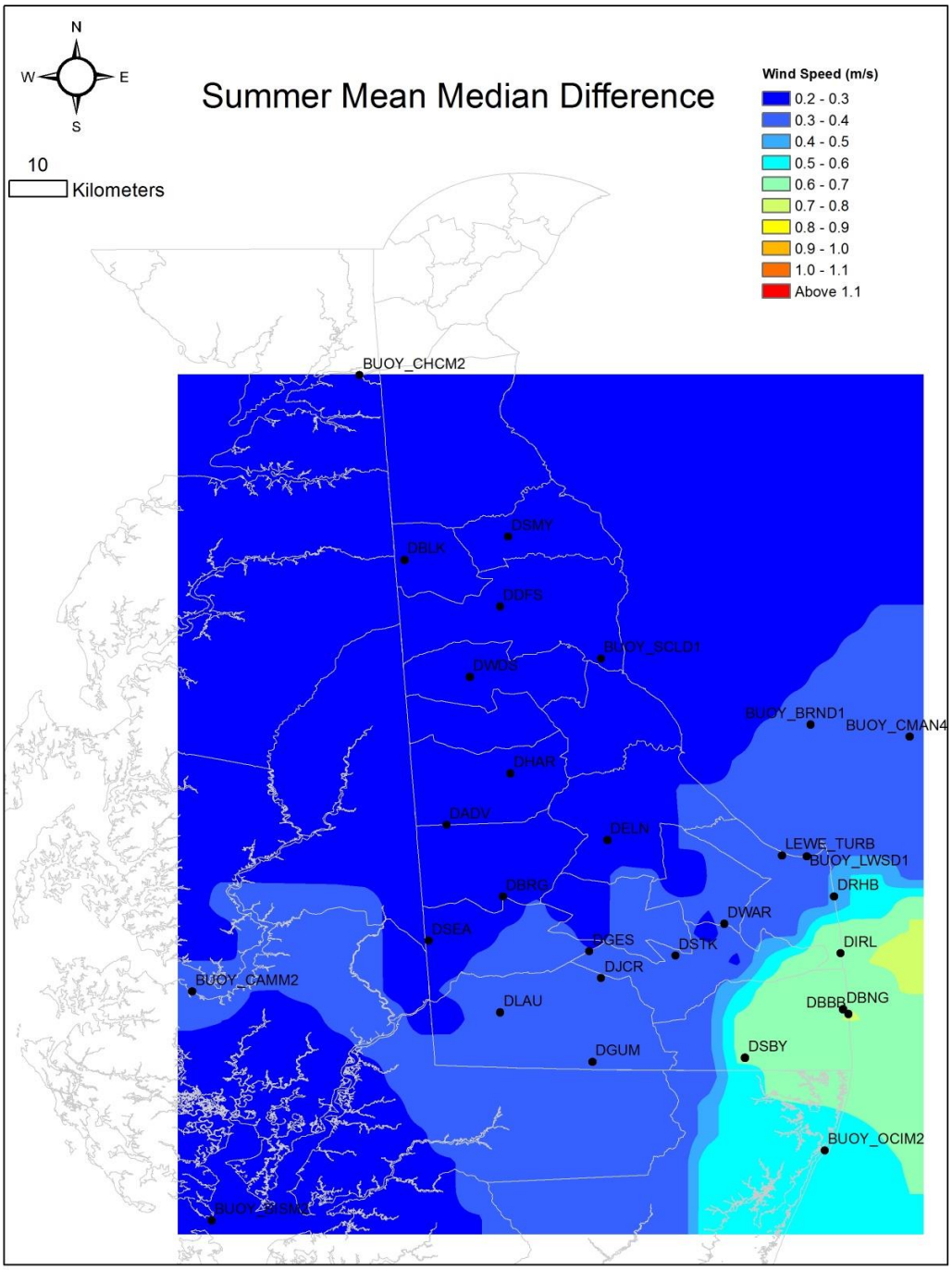

3.7c Summer (July) Mean-Median Difference (MMD) in m/s.

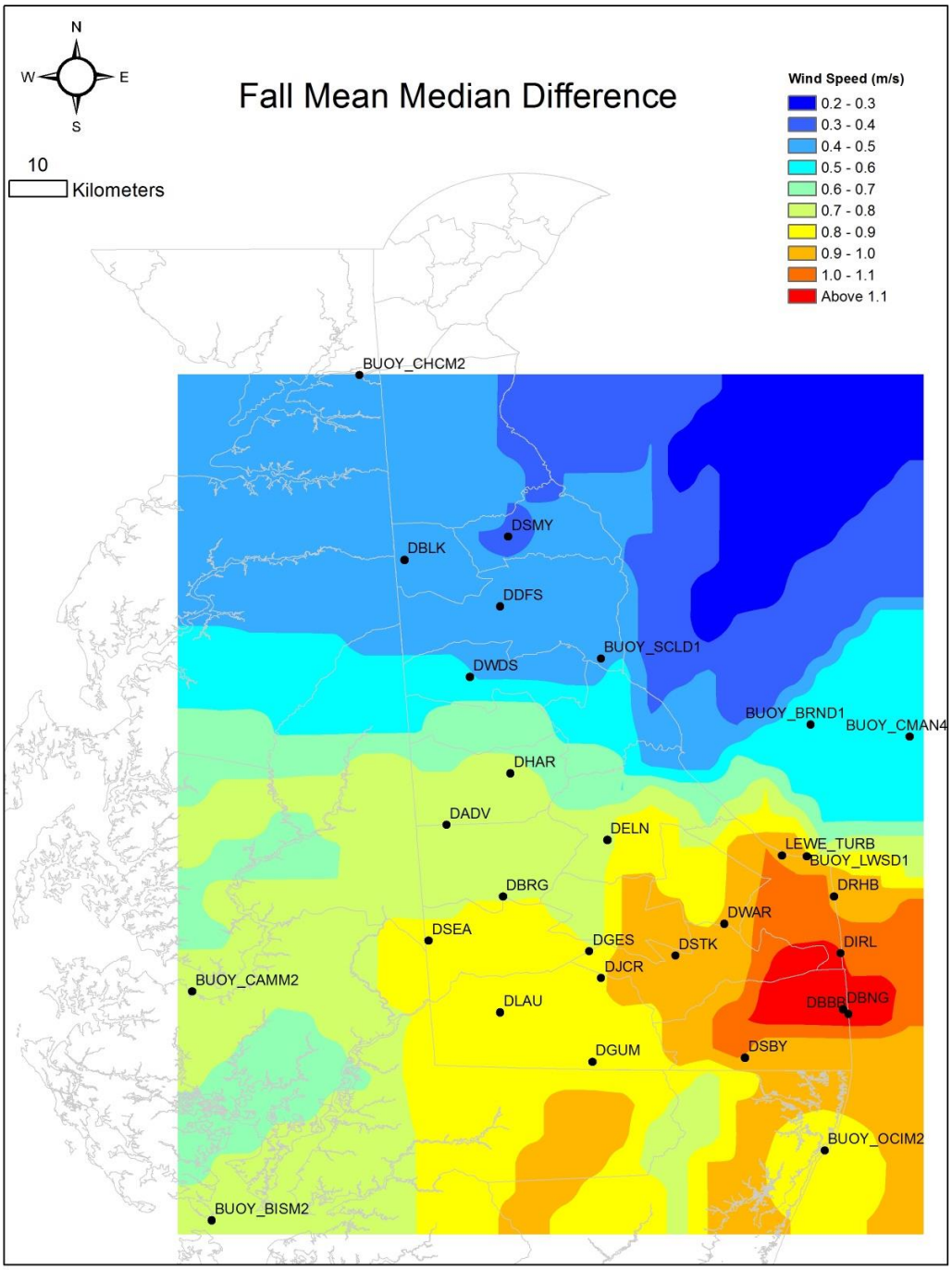

3.7d Fall (October) Mean-Median Difference (MMD) in m/s.

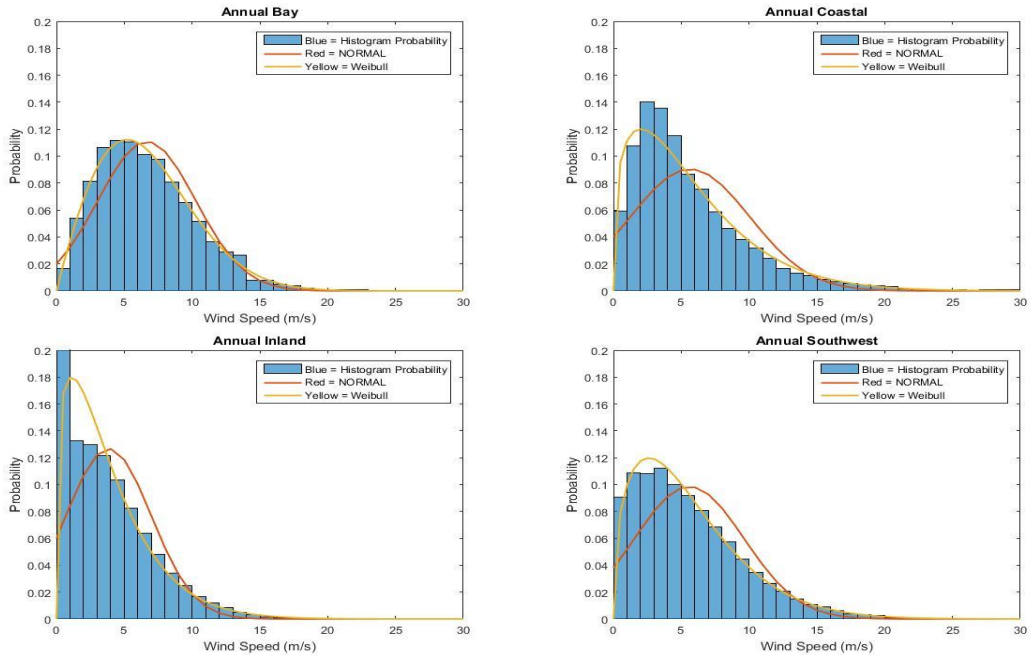

3.8 Probability distribution of hourly mean wind speeds (blue bars) for all of 2015 for the 4 main geographic corridors, overlaid with normal (red) and Weibull (yellow) probability distribution functions. Annual Inland 1.0 m/s bin size is 21%.

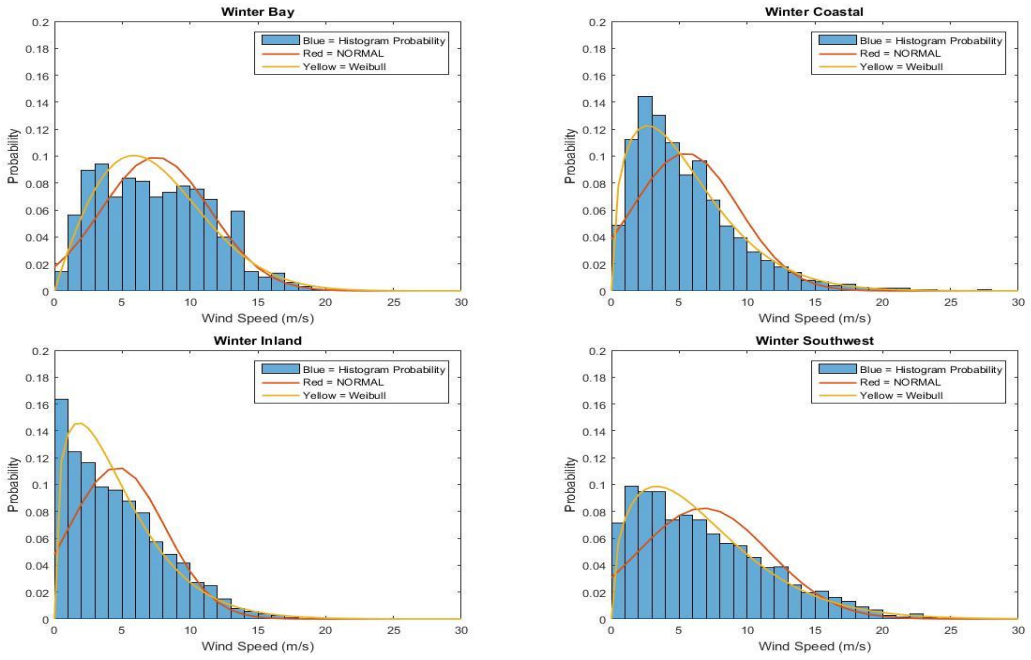

3.9a Probability distribution of hourly mean wind speeds (blue bars) for Winter (January) 2015 for the 4 geographic corridors, overlaid with normal (red) and Weibull (yellow) probability distribution functions.

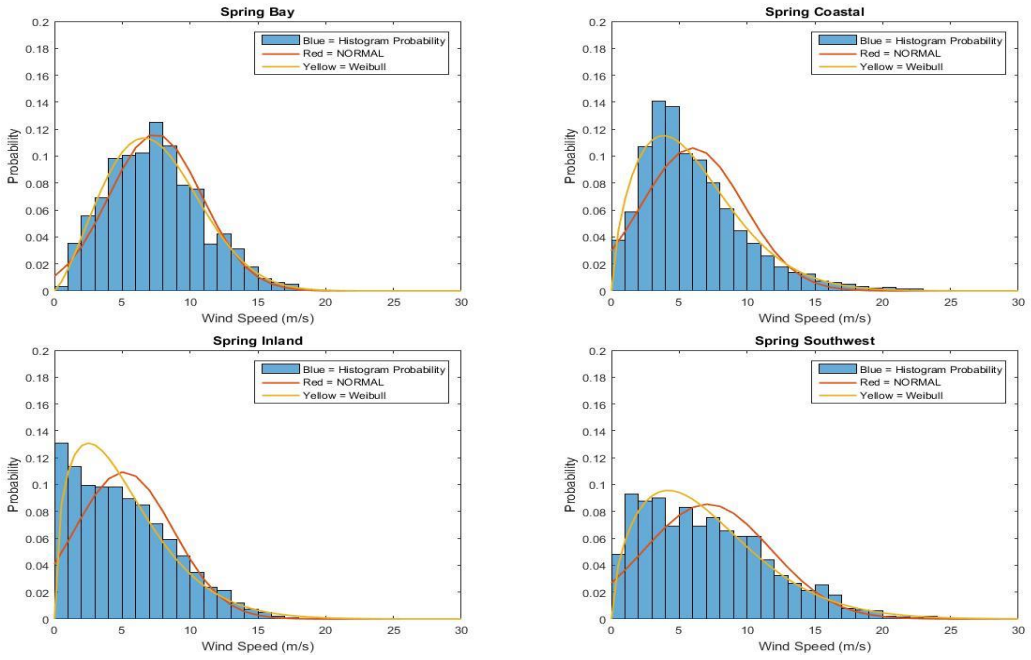

3.9b Probability distribution of hourly mean wind speeds (blue bars) for Spring (April) 2015 for the 4 geographic corridors, overlaid with normal (red) and Weibull (yellow) probability distribution functions.

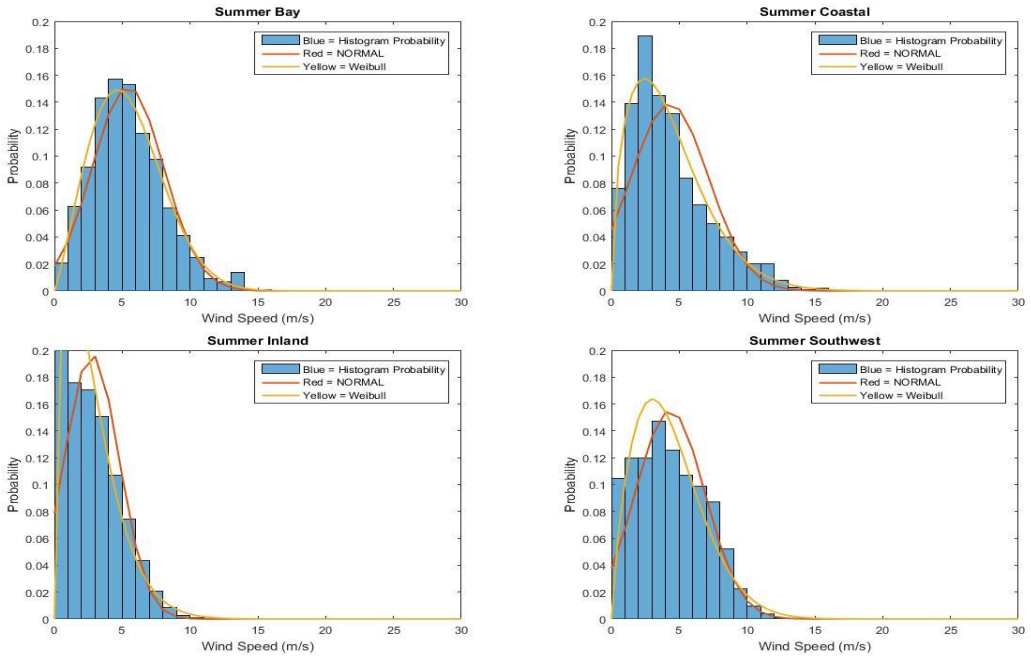

3.9c Probability distribution of hourly mean wind speeds (blue bars) for Summer (July) 2015 for the 4 geographic corridors, overlaid with normal (red) and Weibull (yellow) probability distribution functions. Summer Inland 1.0 m/s bin size is 24%.

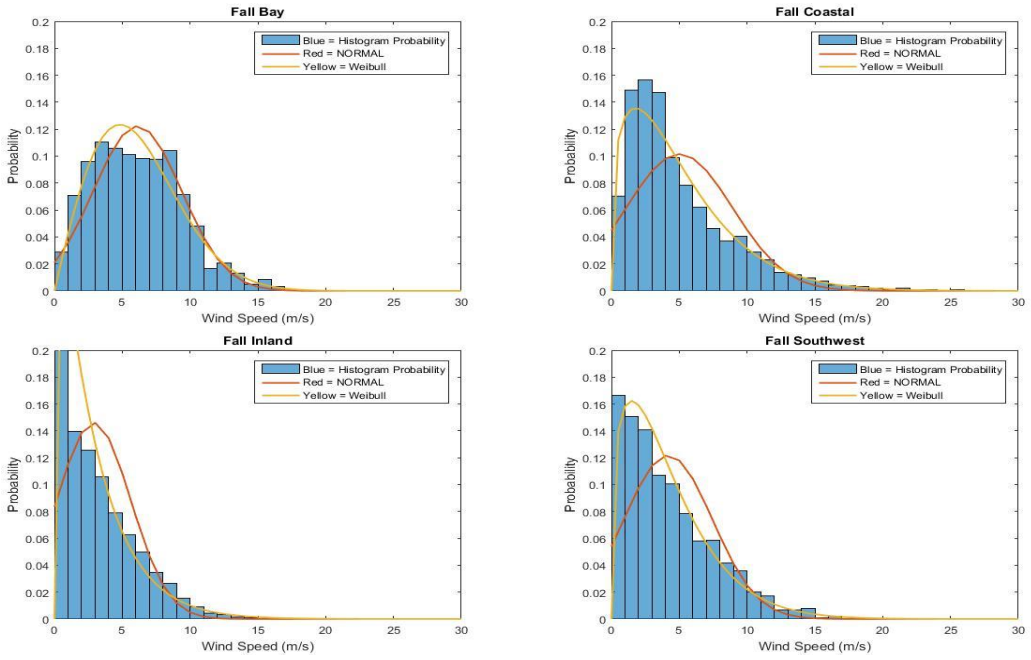

3.9d Probability distribution of hourly mean wind speeds (blue bars) for Fall (October) 2015 for the 4 geographic corridors, overlaid with normal (red) and Weibull (yellow) probability distribution functions. Fall Inland 1.0 m/s bin is 34%.

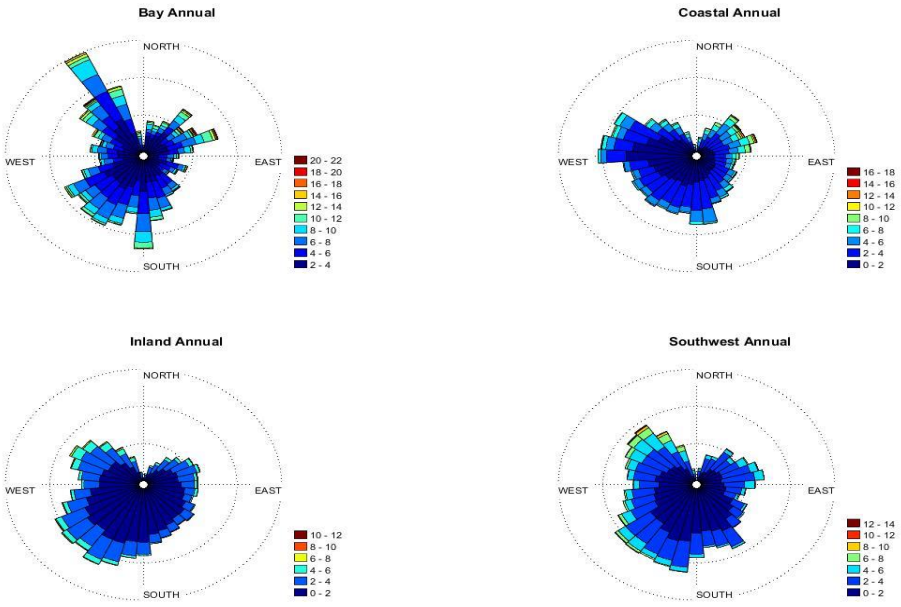

3.10 Annual wind roses composed of hourly mean wind speeds calculated for all corridors for all of 2015.

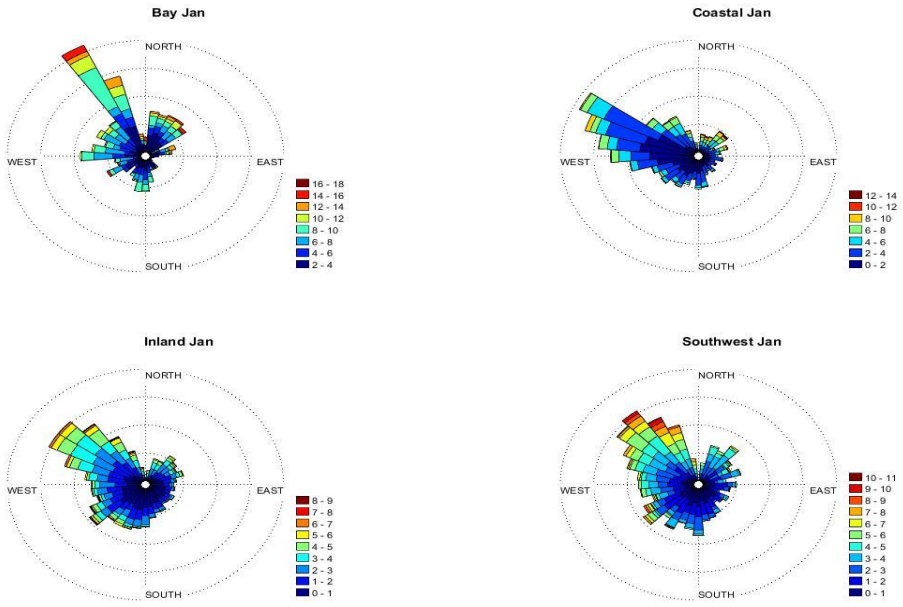

3.11a Winter (January) wind rose hourly mean wind speeds calculated for all corridors.

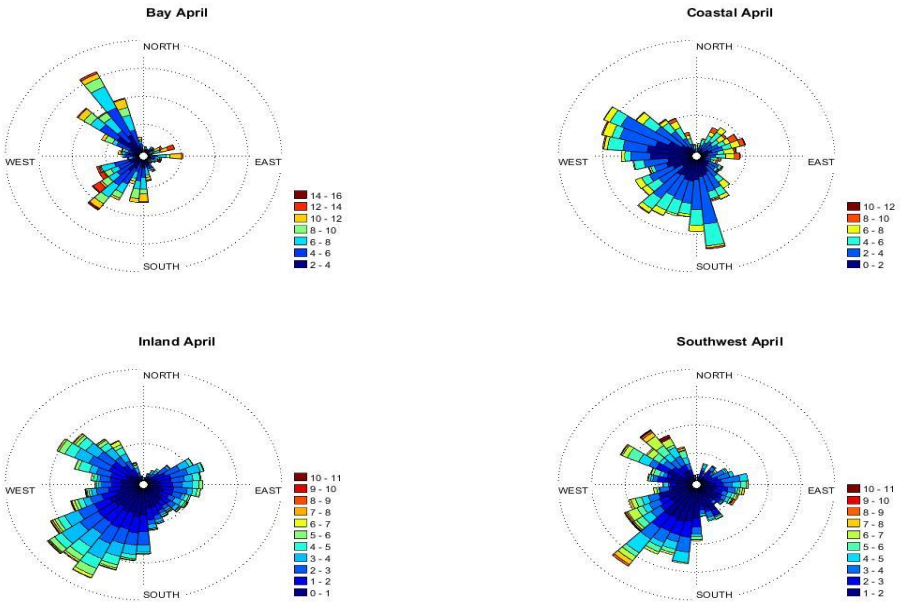

3.11b Spring (April) wind rose hourly mean wind speeds calculated for all corridors.

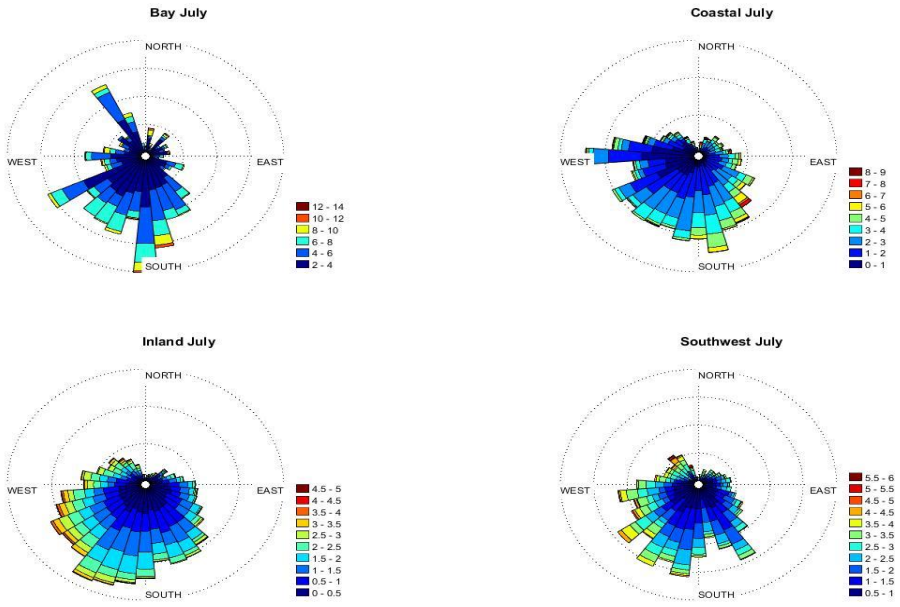

3.11c Summer (July) wind rose hourly mean wind speeds calculated for all corridors.

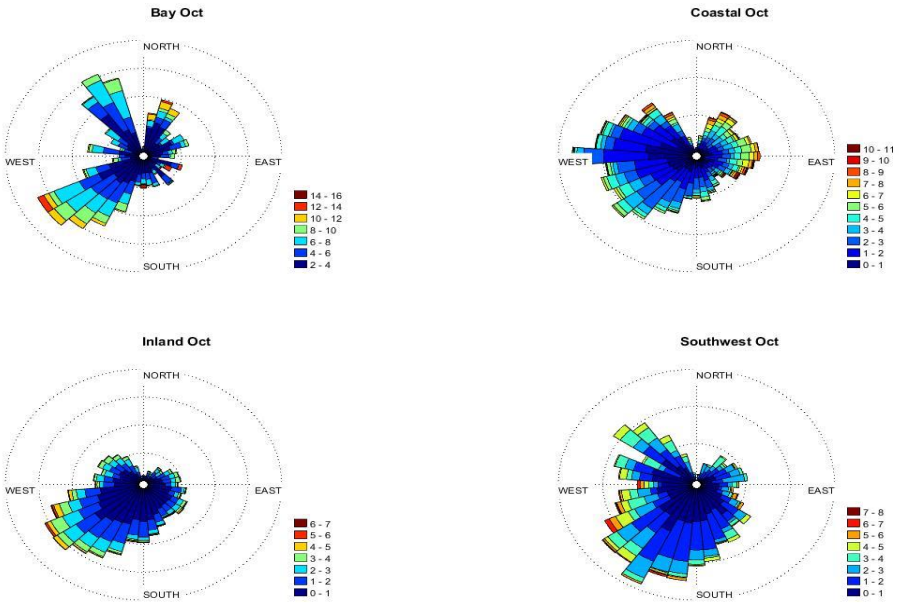

3.11d Fall (October) wind rose hourly mean wind speeds calculated for all corridors.

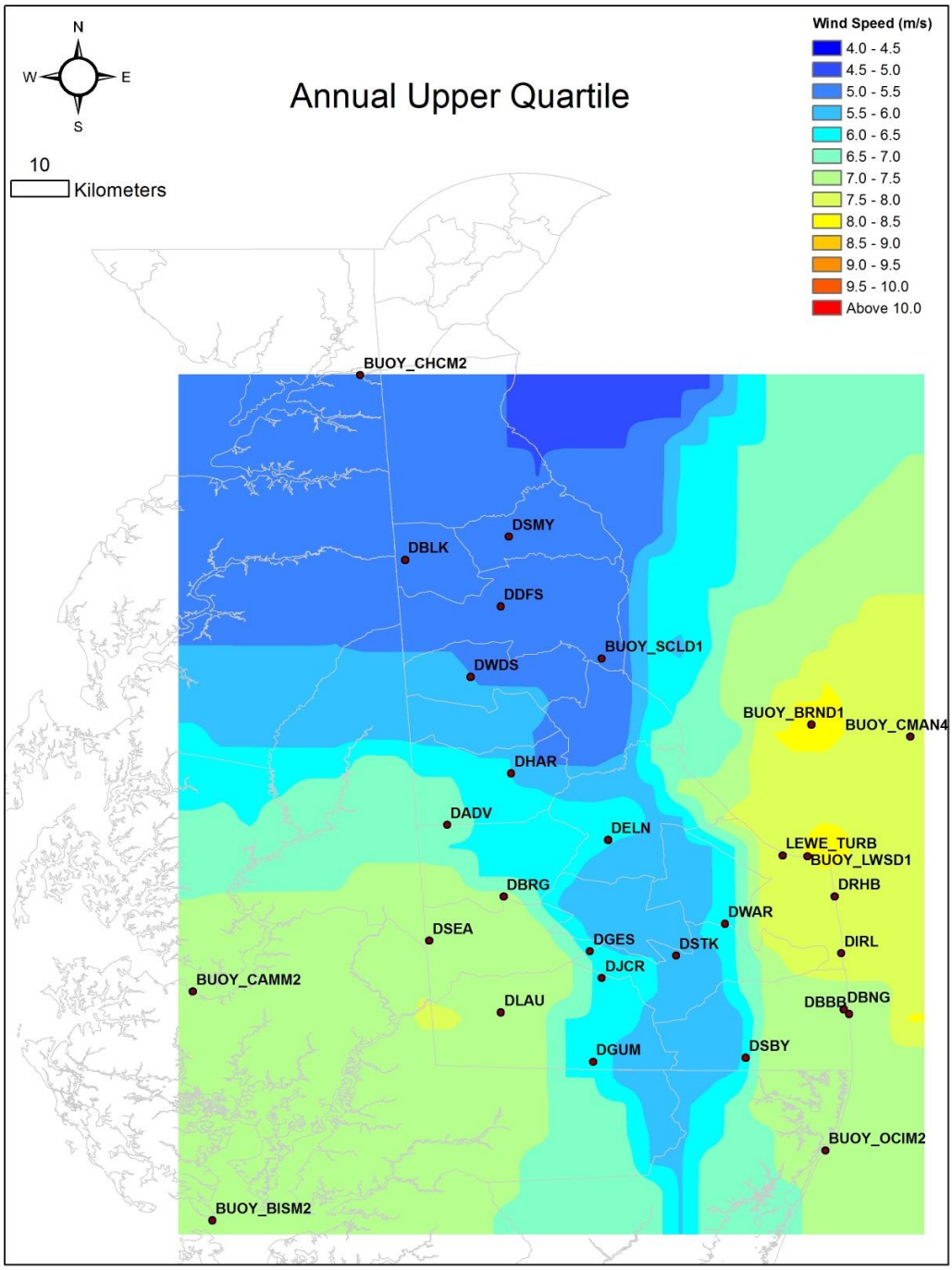

3.12 Upper quartile wind speed limit in m/s for the year 2015.

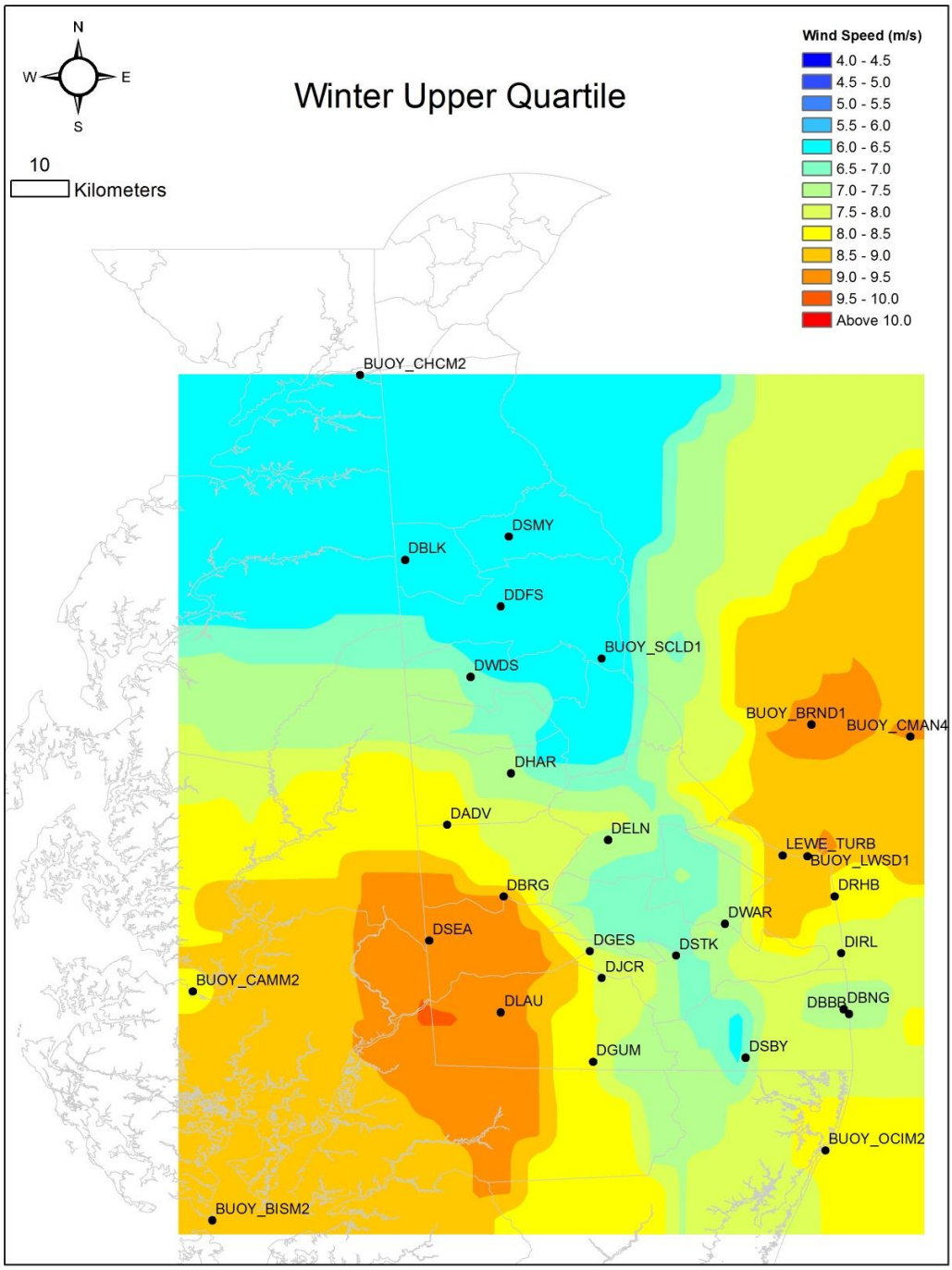

3.13a Upper quartile wind speed limit in m/s for the winter (January).

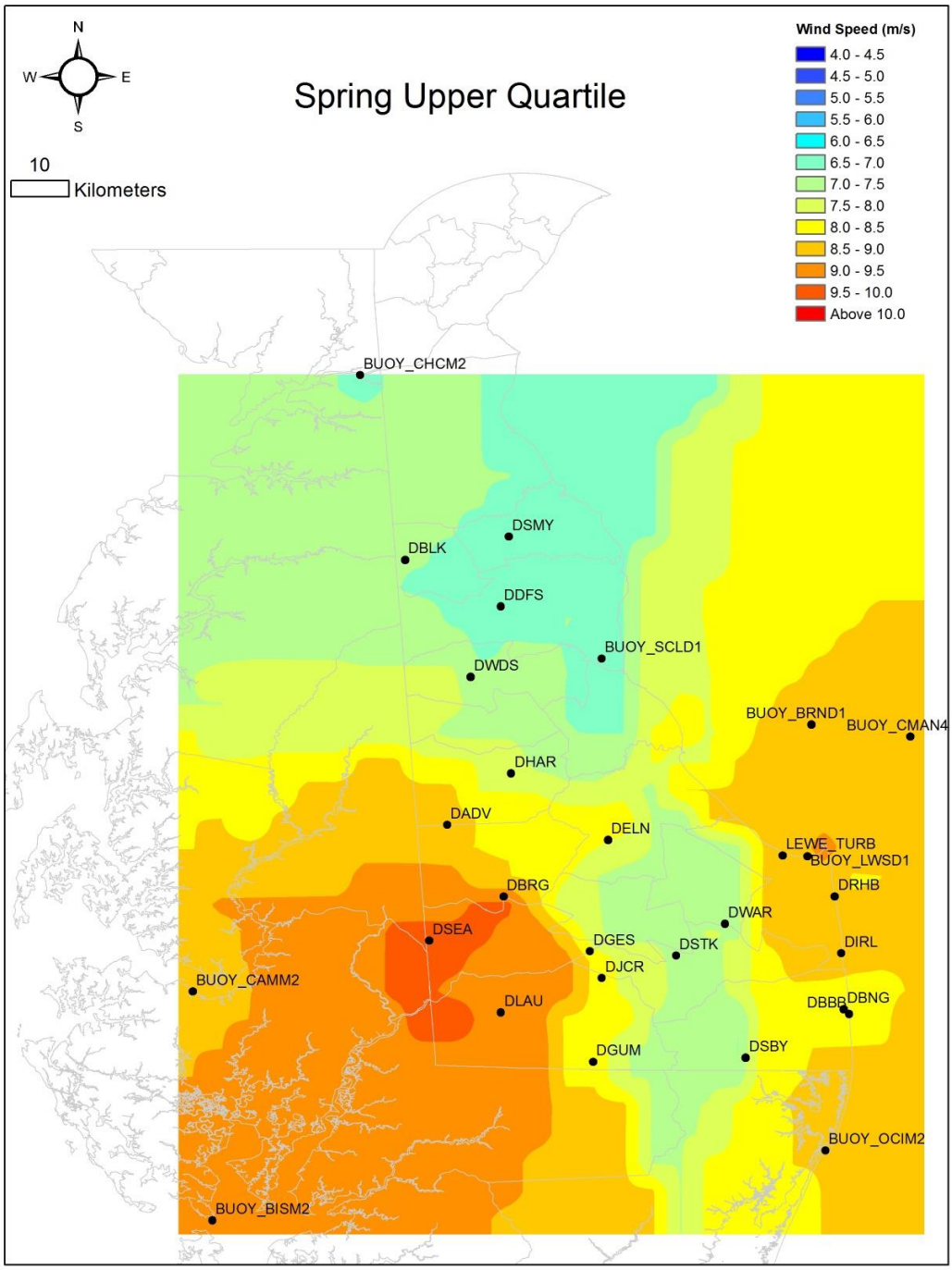

3.13b Upper quartile wind speed limit in m/s for the spring (April).

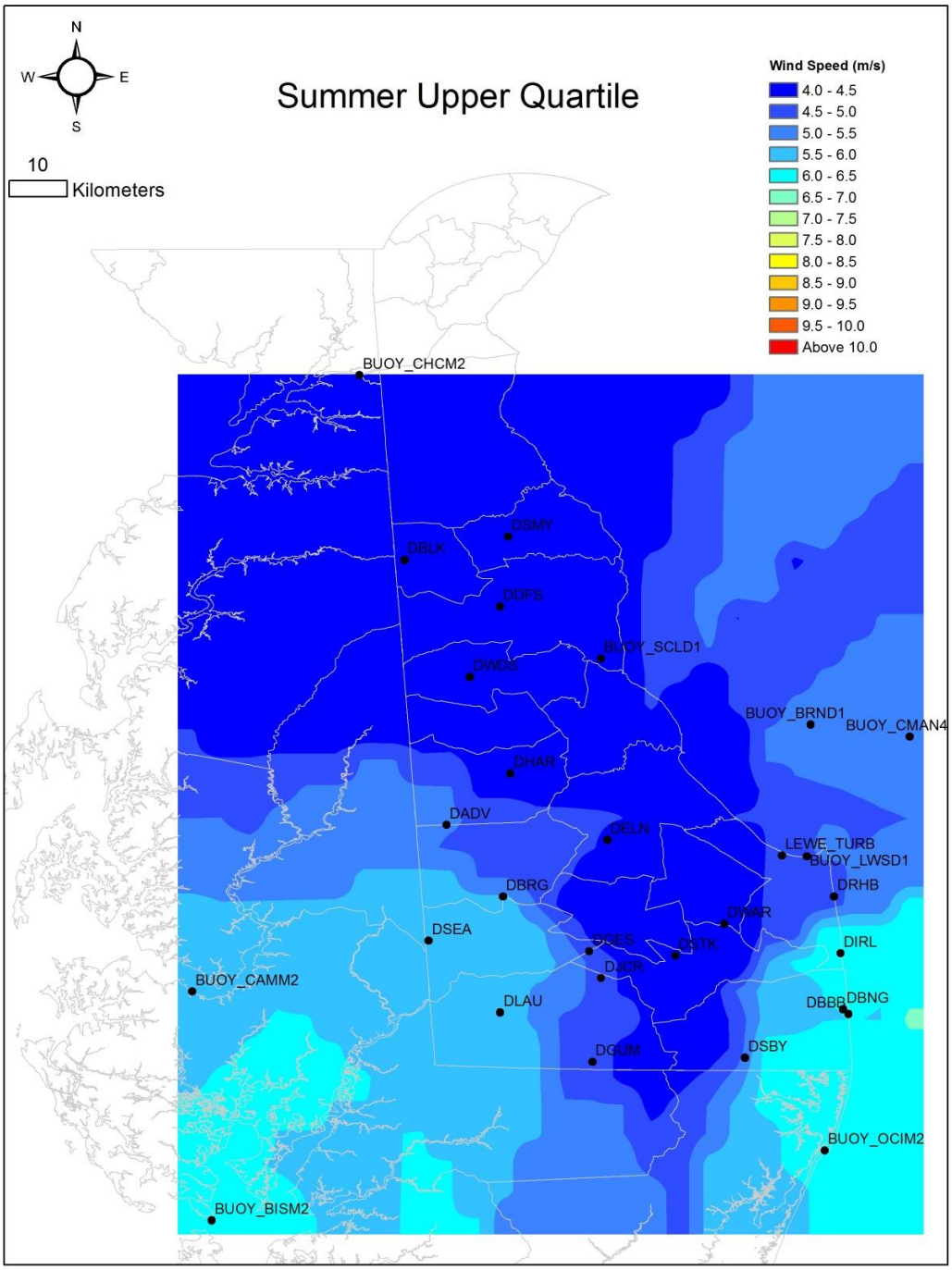

3.13c Upper quartile wind speed limit in m/s for the summer (July).

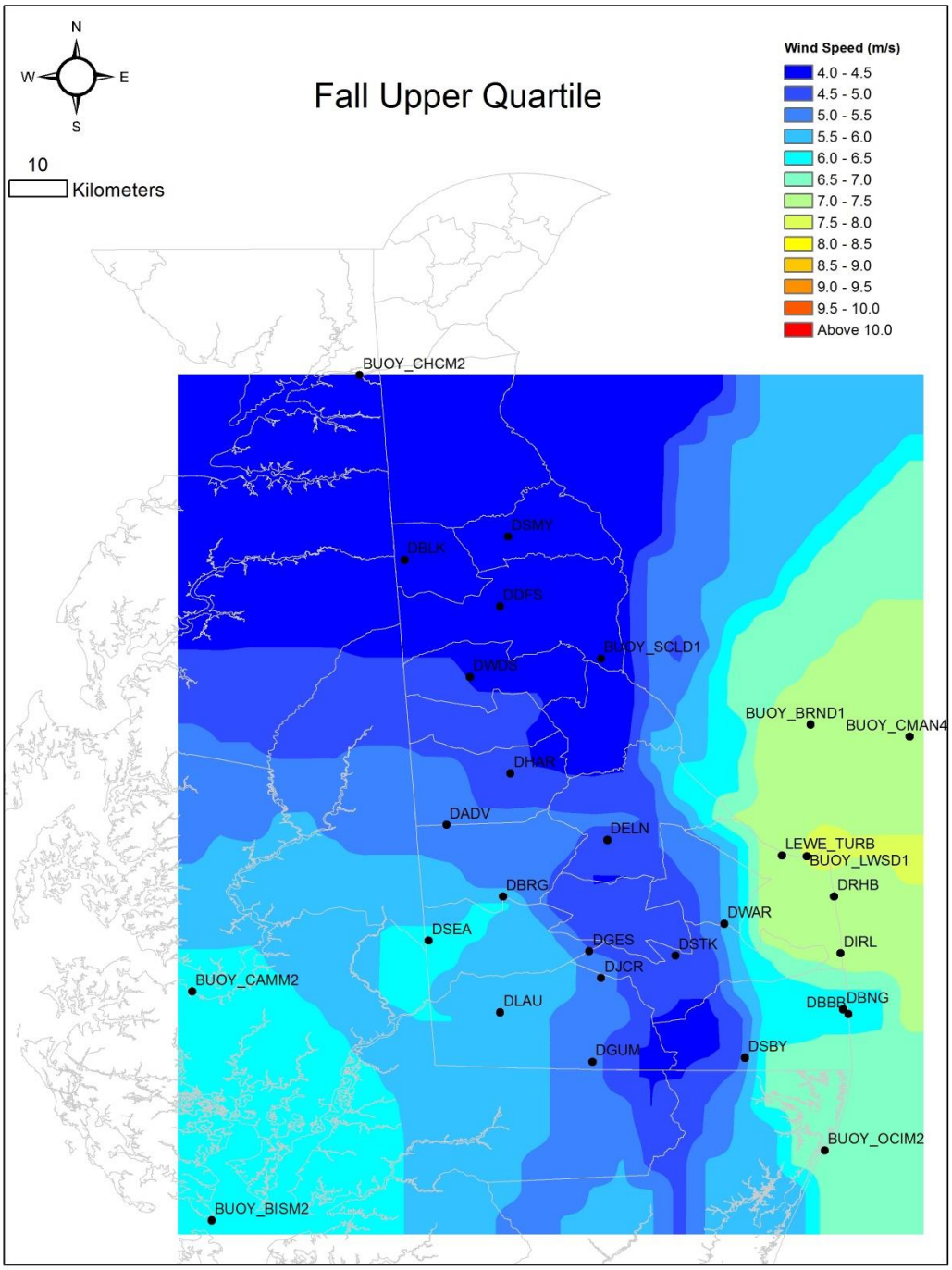

3.13d Upper quartile wind speed limit in m/s for the fall (October).

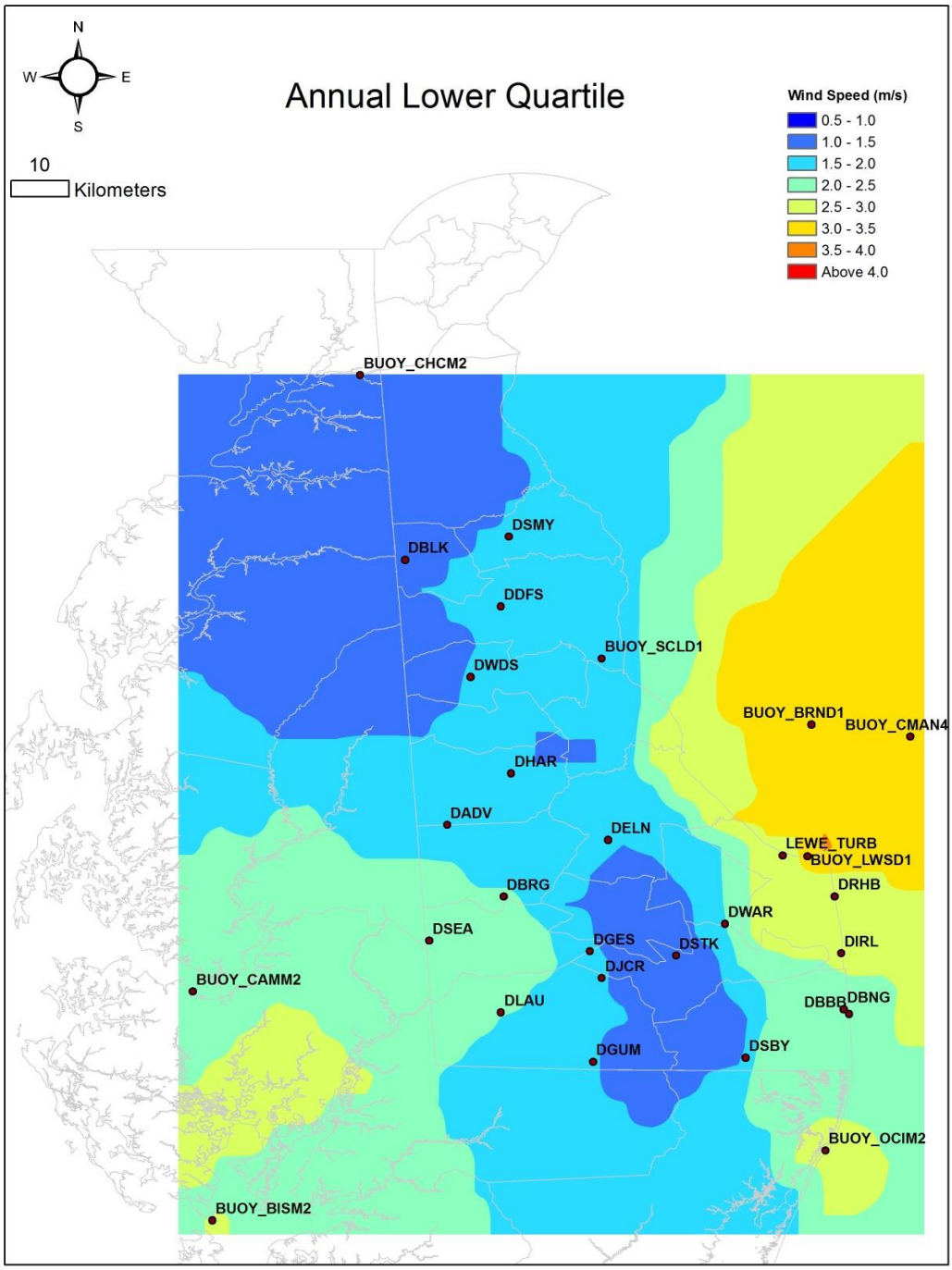

3.14 Lower quartile wind speed limit in m/s for the year 2015.

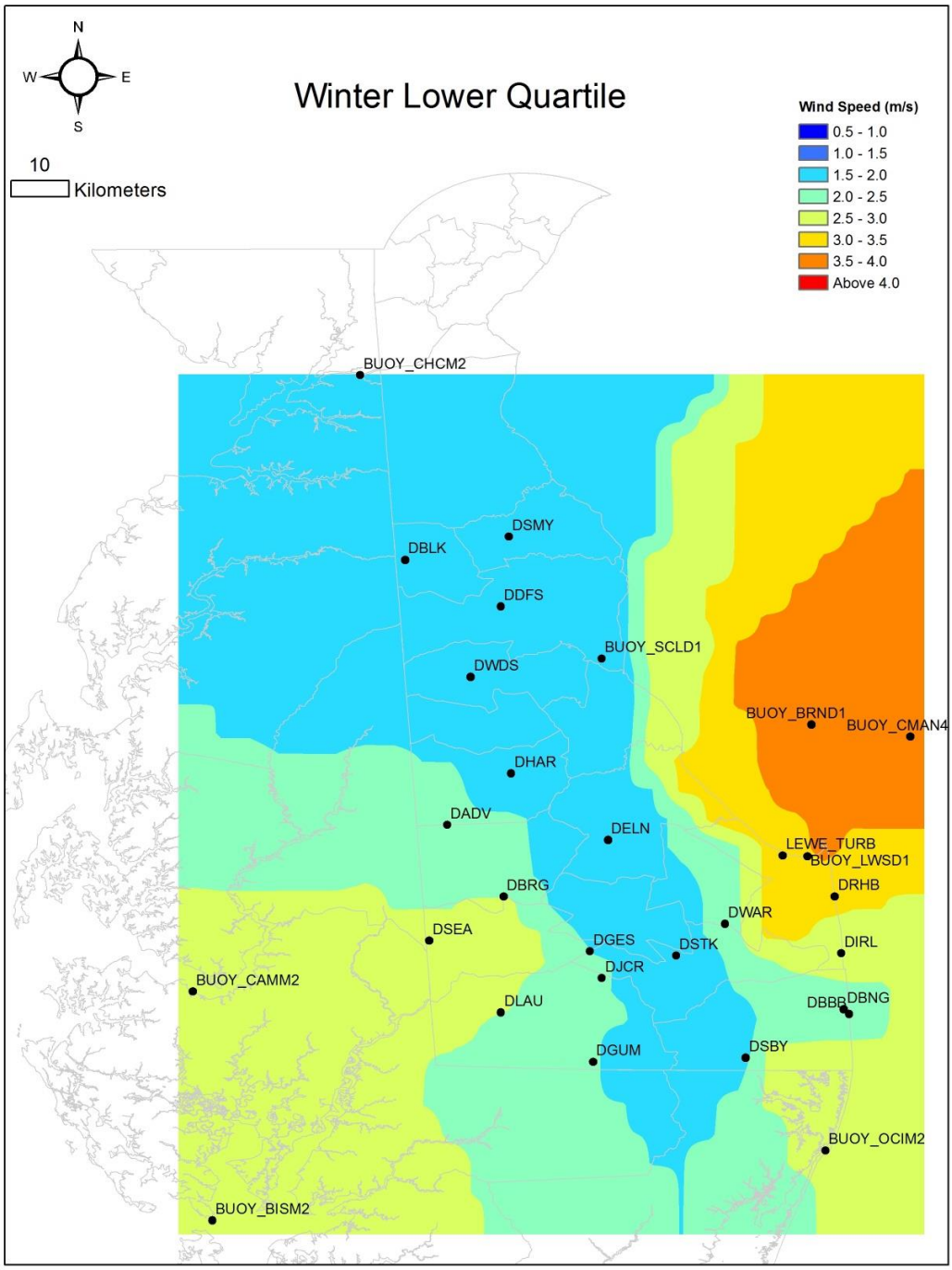

3.15a Lower quartile wind speed limit in m/s for the winter (January).

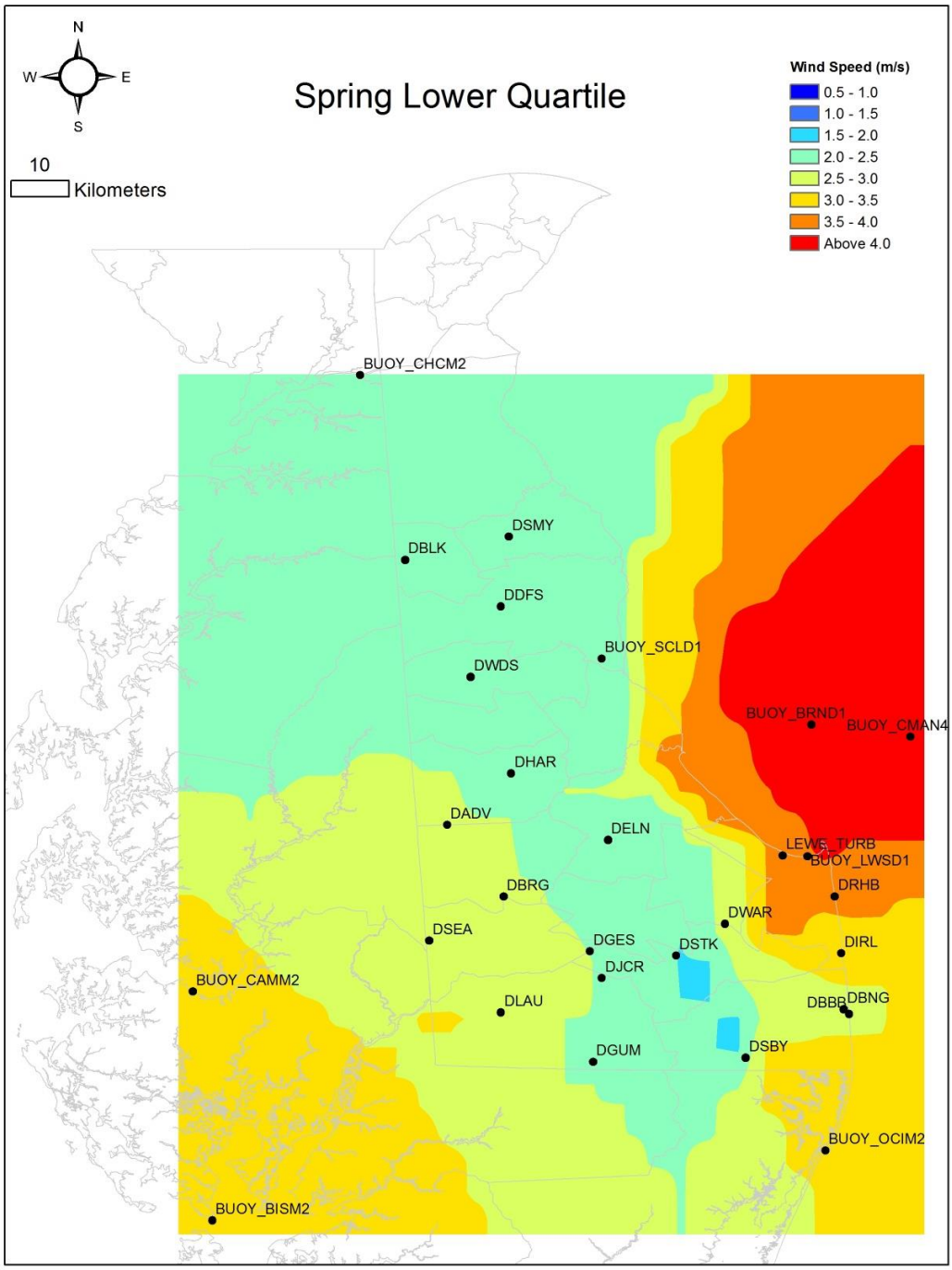

3.15b Lower quartile wind speed limit in m/s for the spring (April).

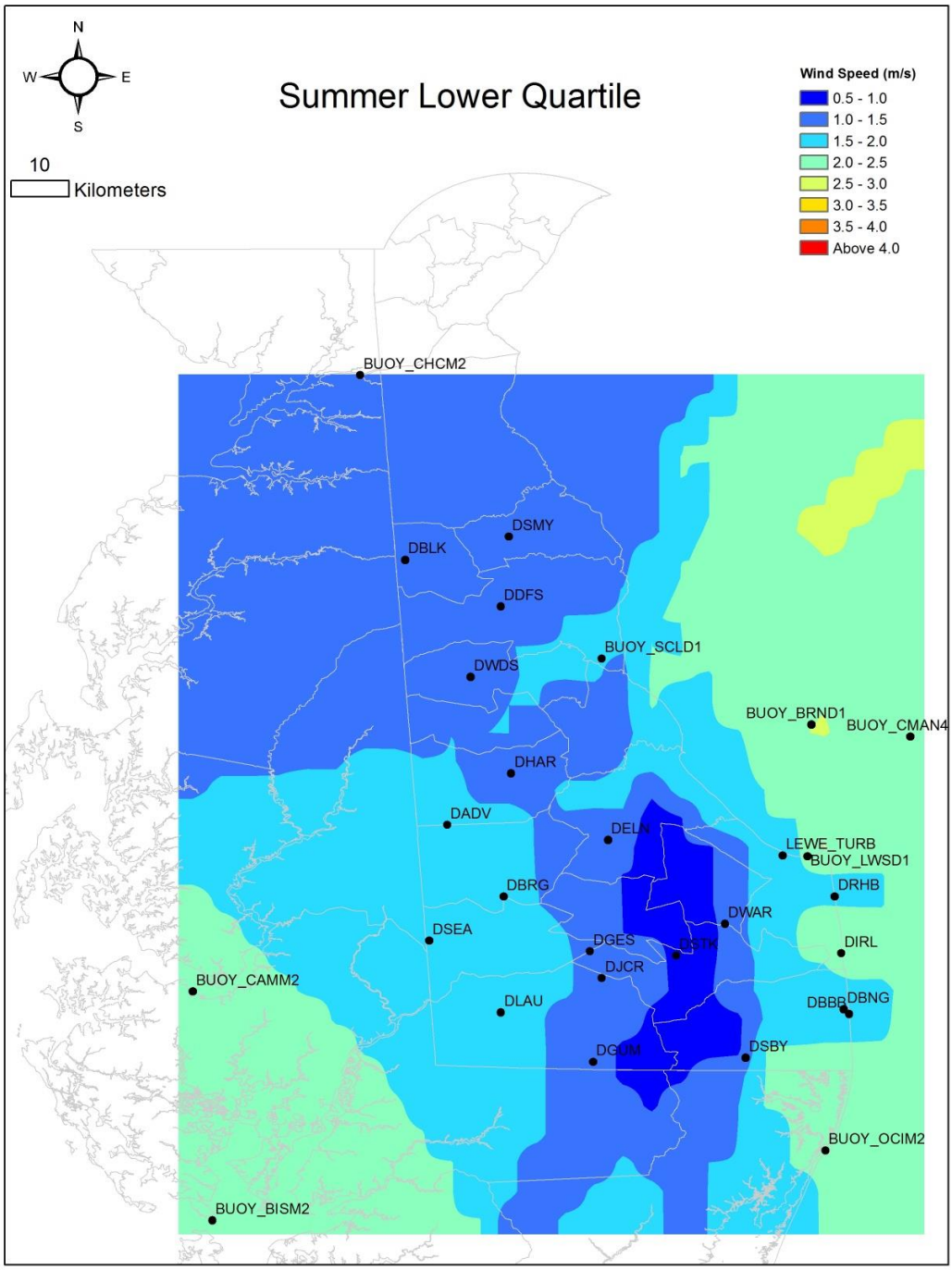

3.15c Lower quartile wind speed limit in m/s for the summer (July).

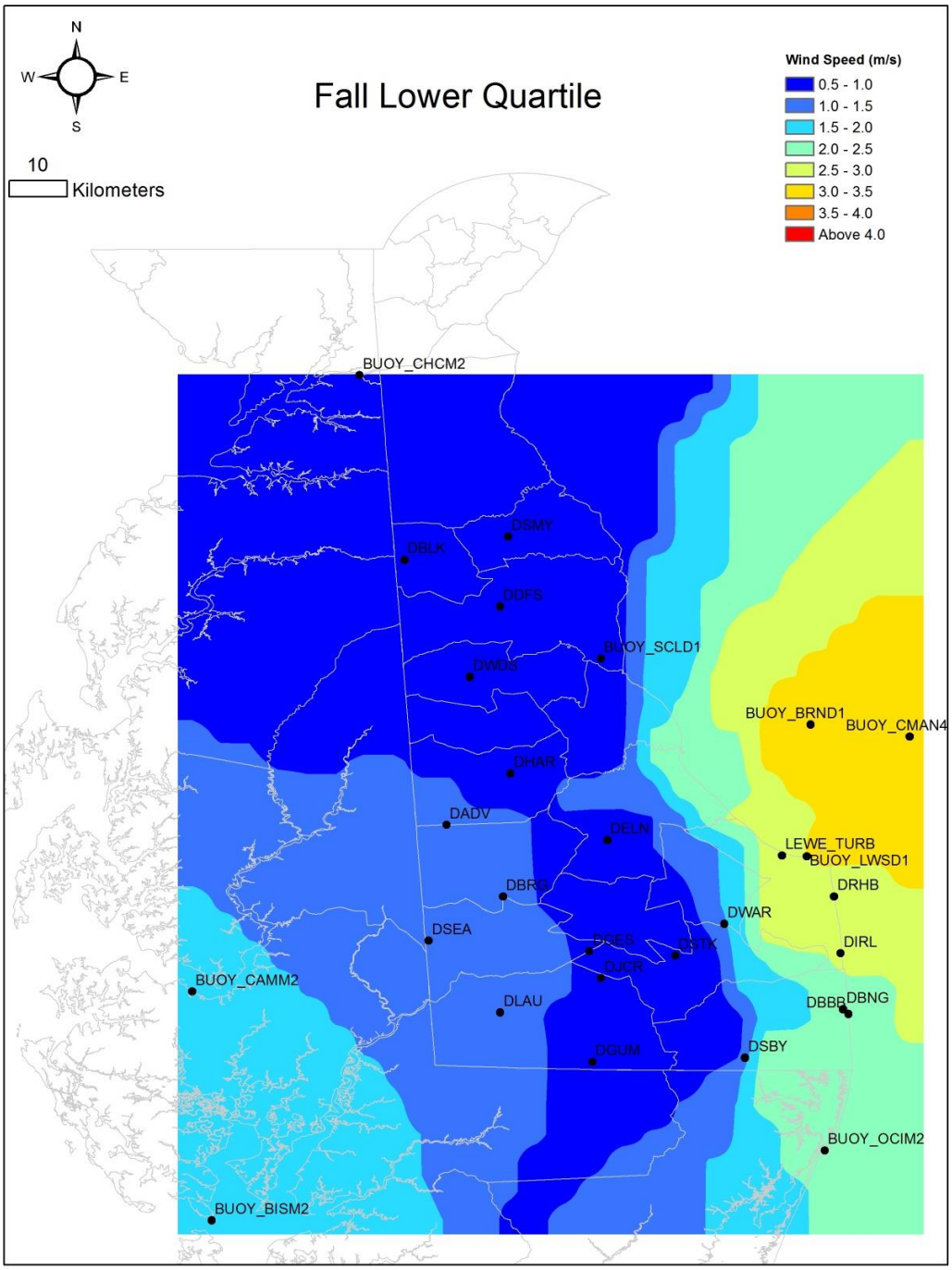

3.15d Lower quartile wind speed limit in m/s for the fall (October).

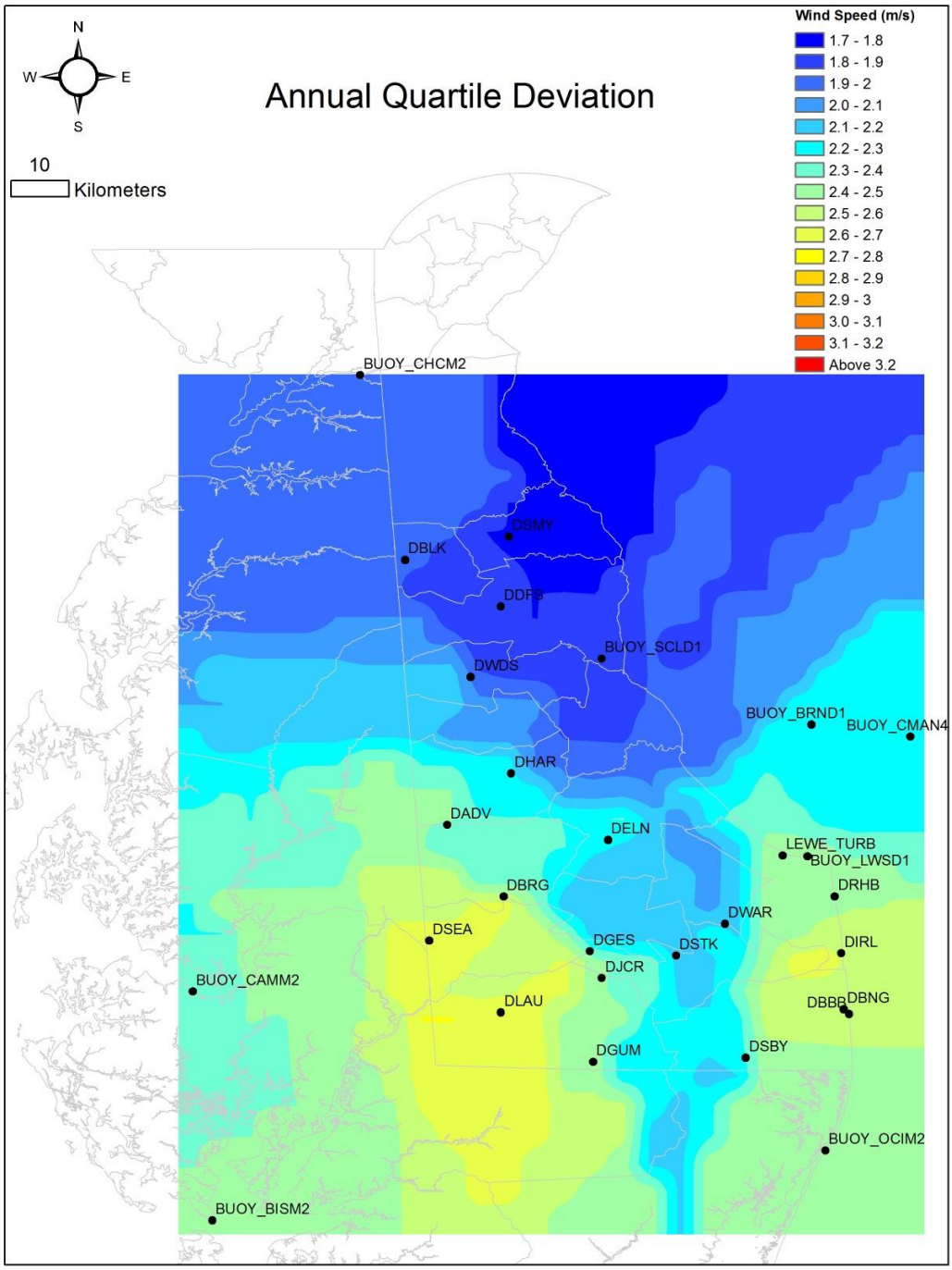

3.16 Wind speed quartile deviation in m/s for the year 2015.

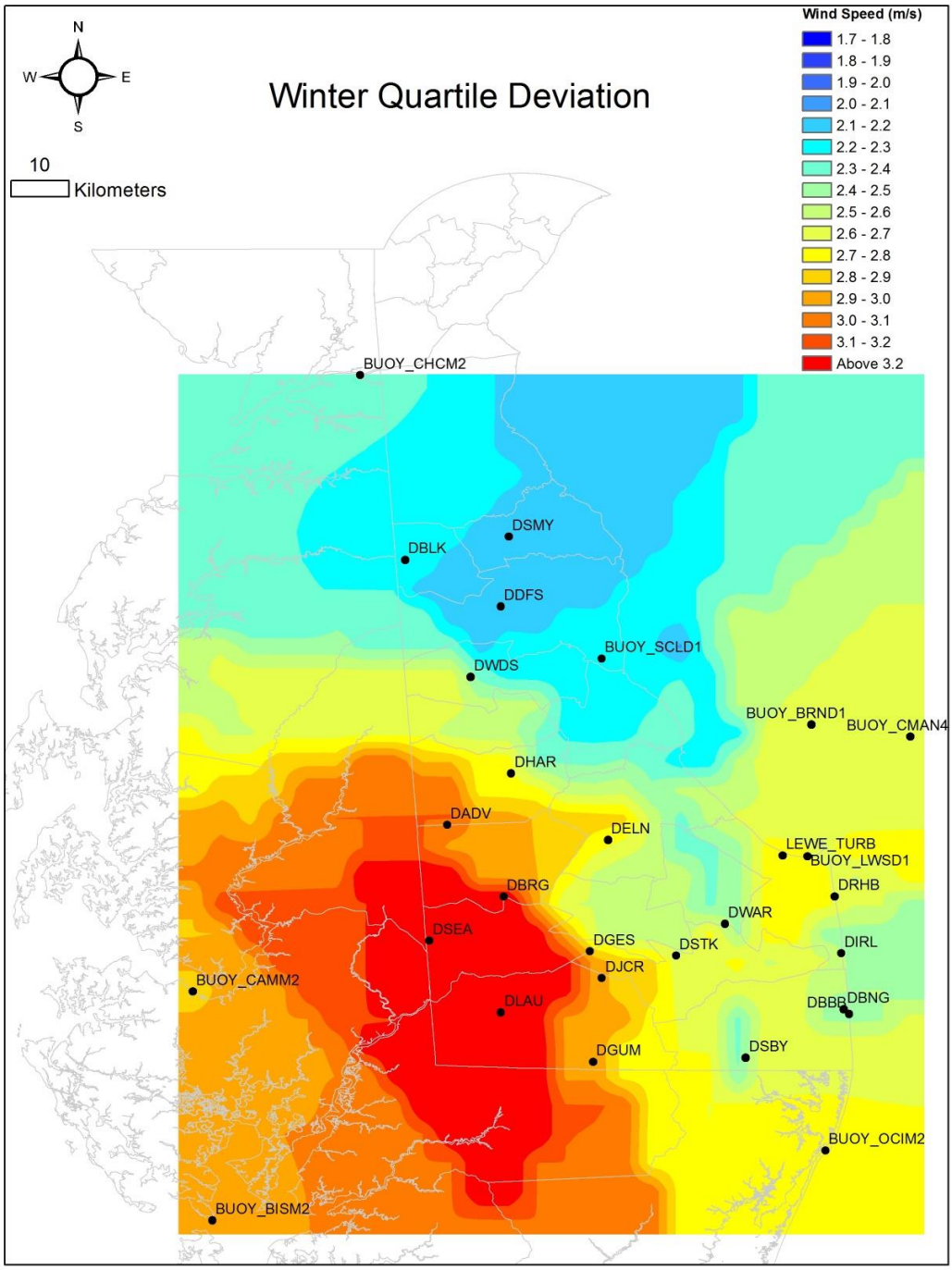

3.17a Wind speed quartile deviation in m/s for the winter (January).

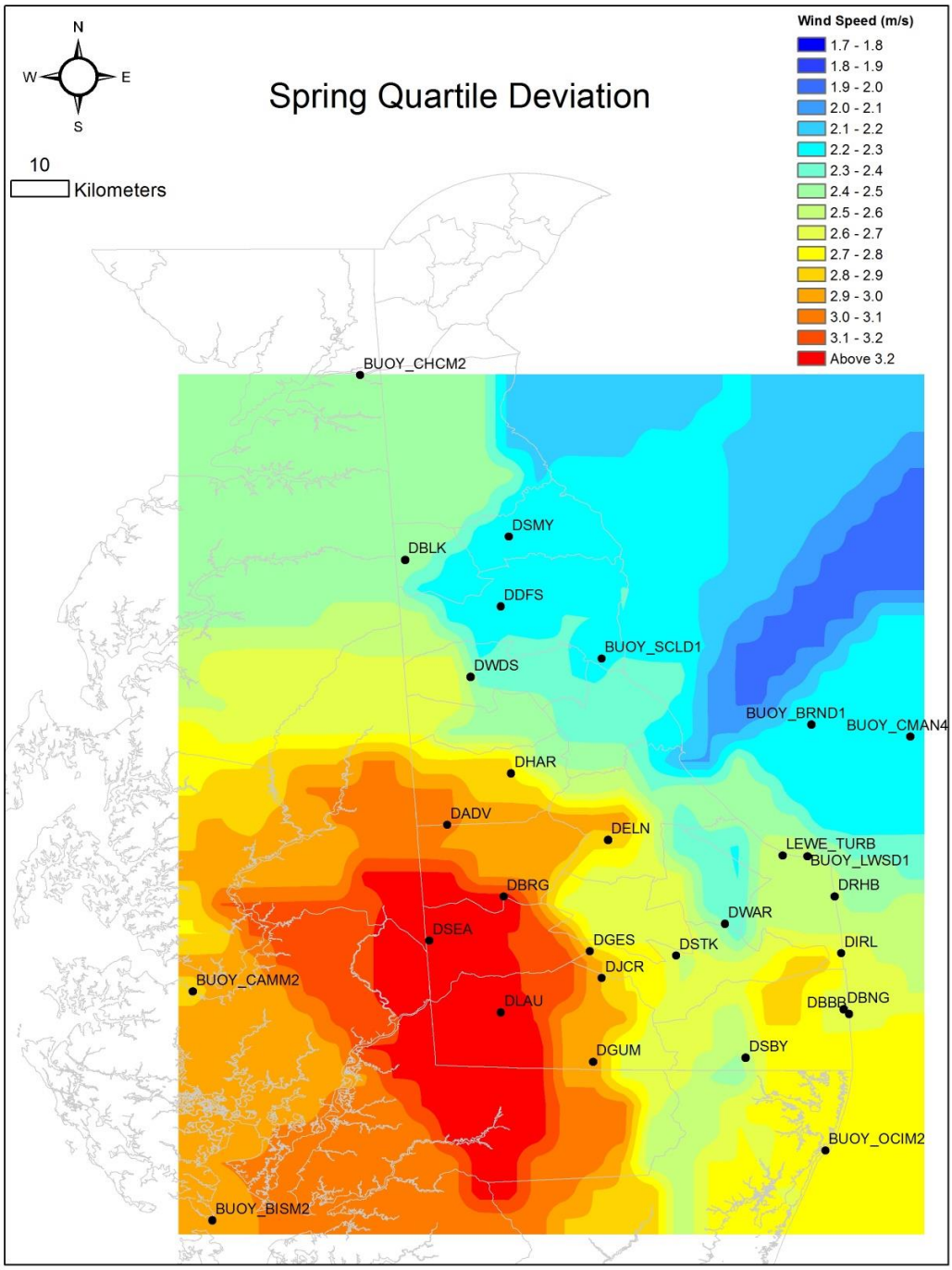

3.17b Wind speed quartile deviation in m/s for the spring (April).

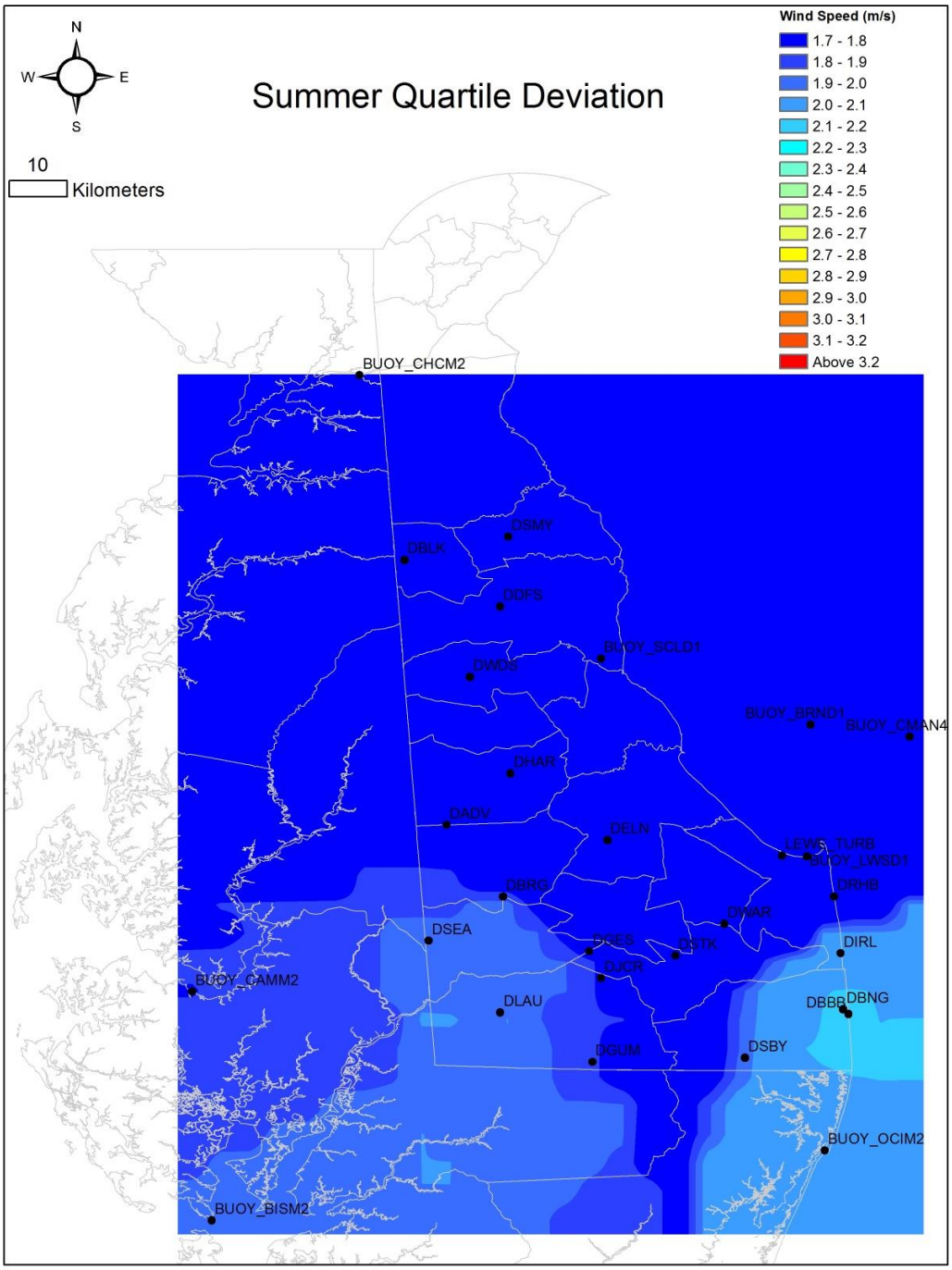

3.17c Wind speed quartile deviation in m/s for the summer (July).

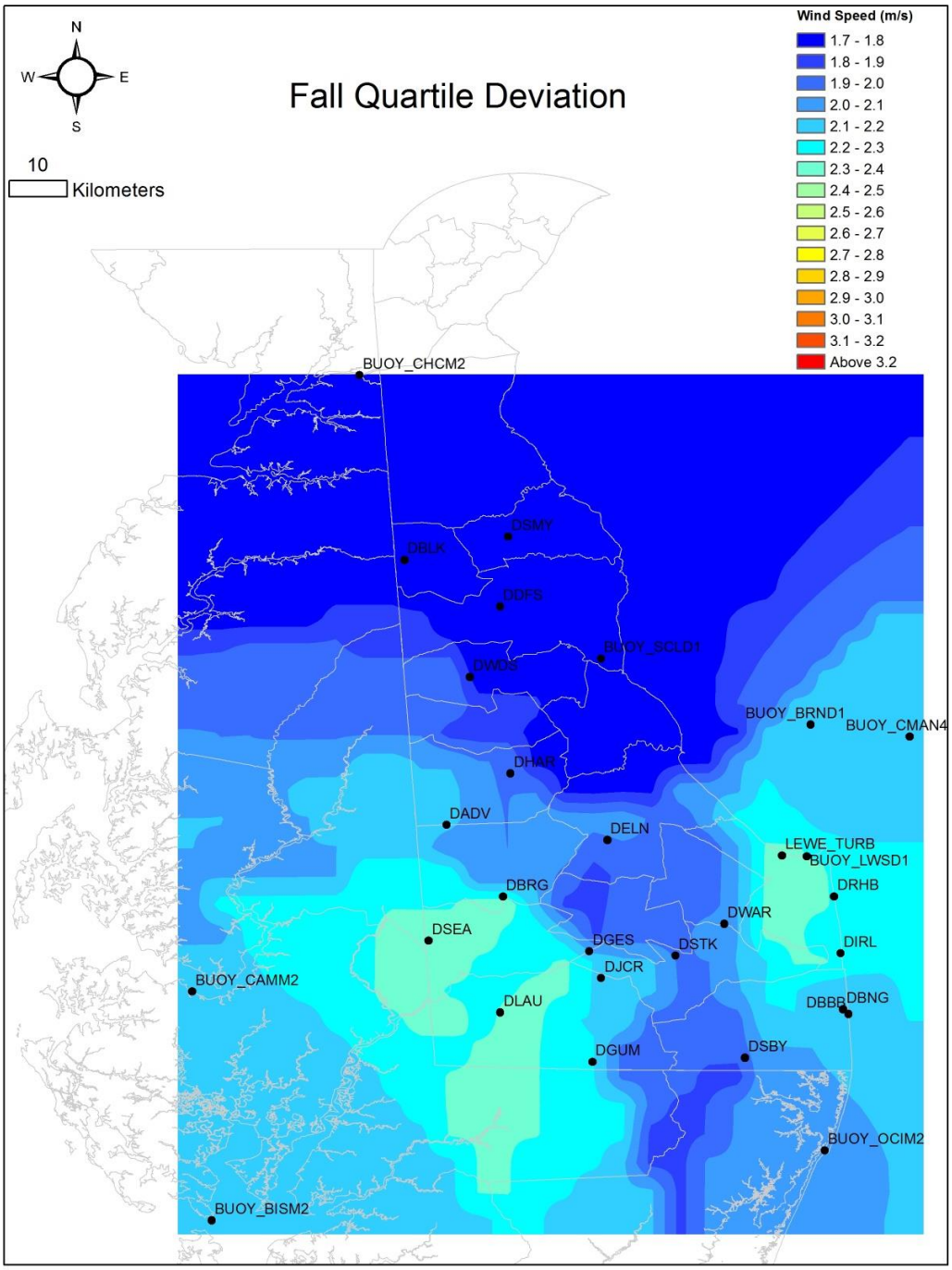

3.17d Wind speed quartile deviation in m/s for the fall (October).

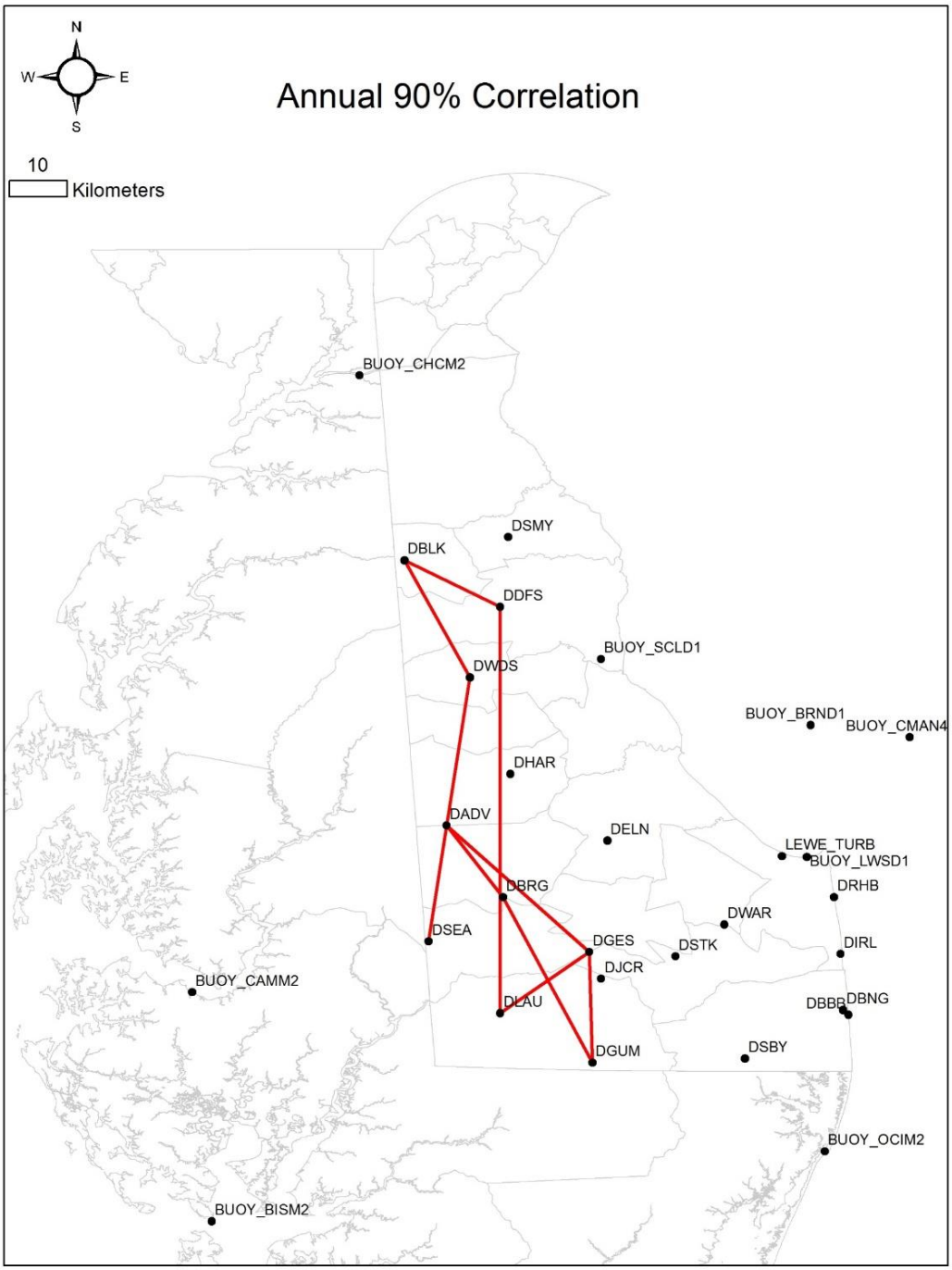

3.18a Pearson's autocorrelation shown for all stations with an R >90 %.

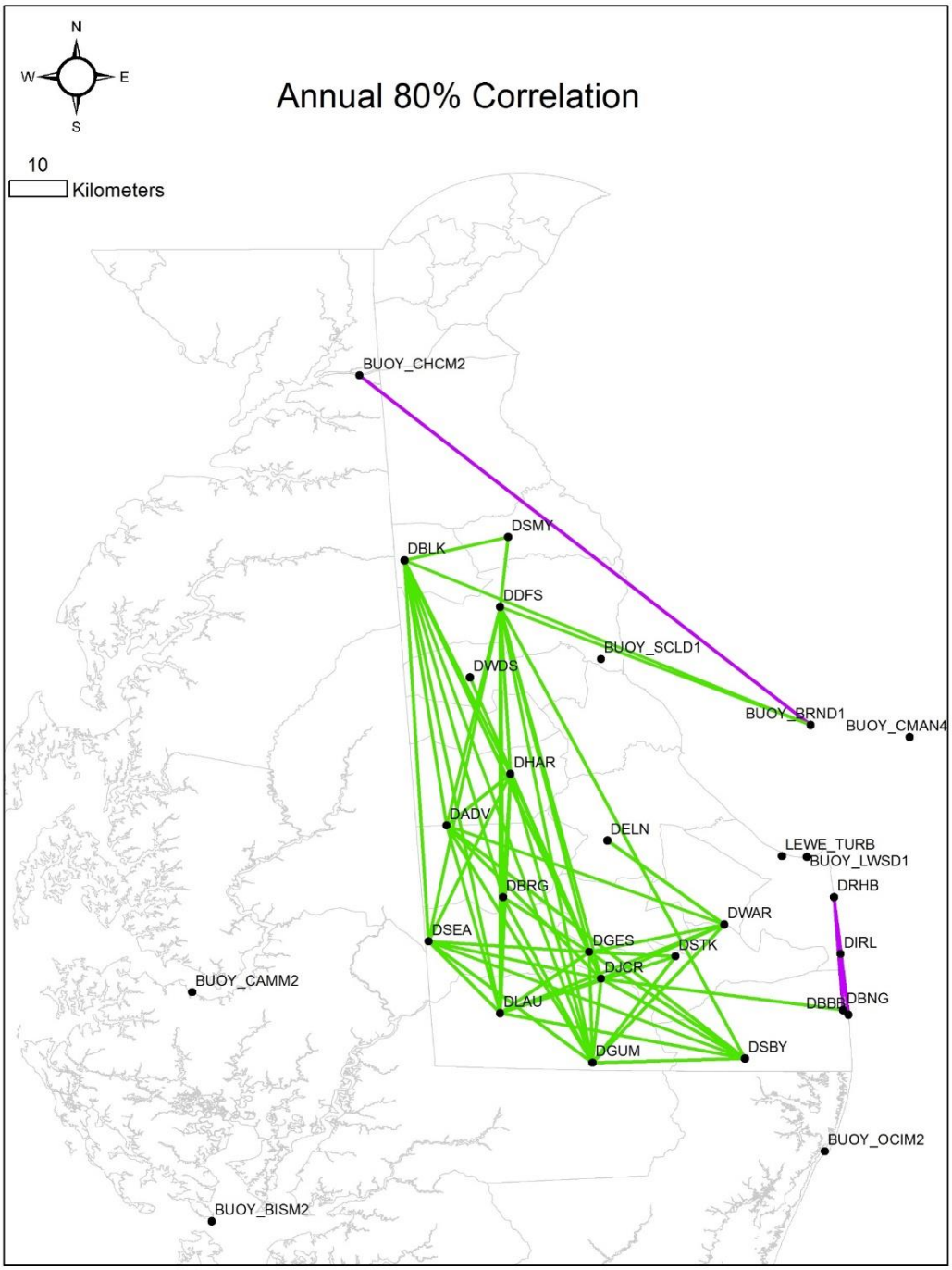

3. 18b Pearson's autocorrelation shown for all stations with an R > 80%.

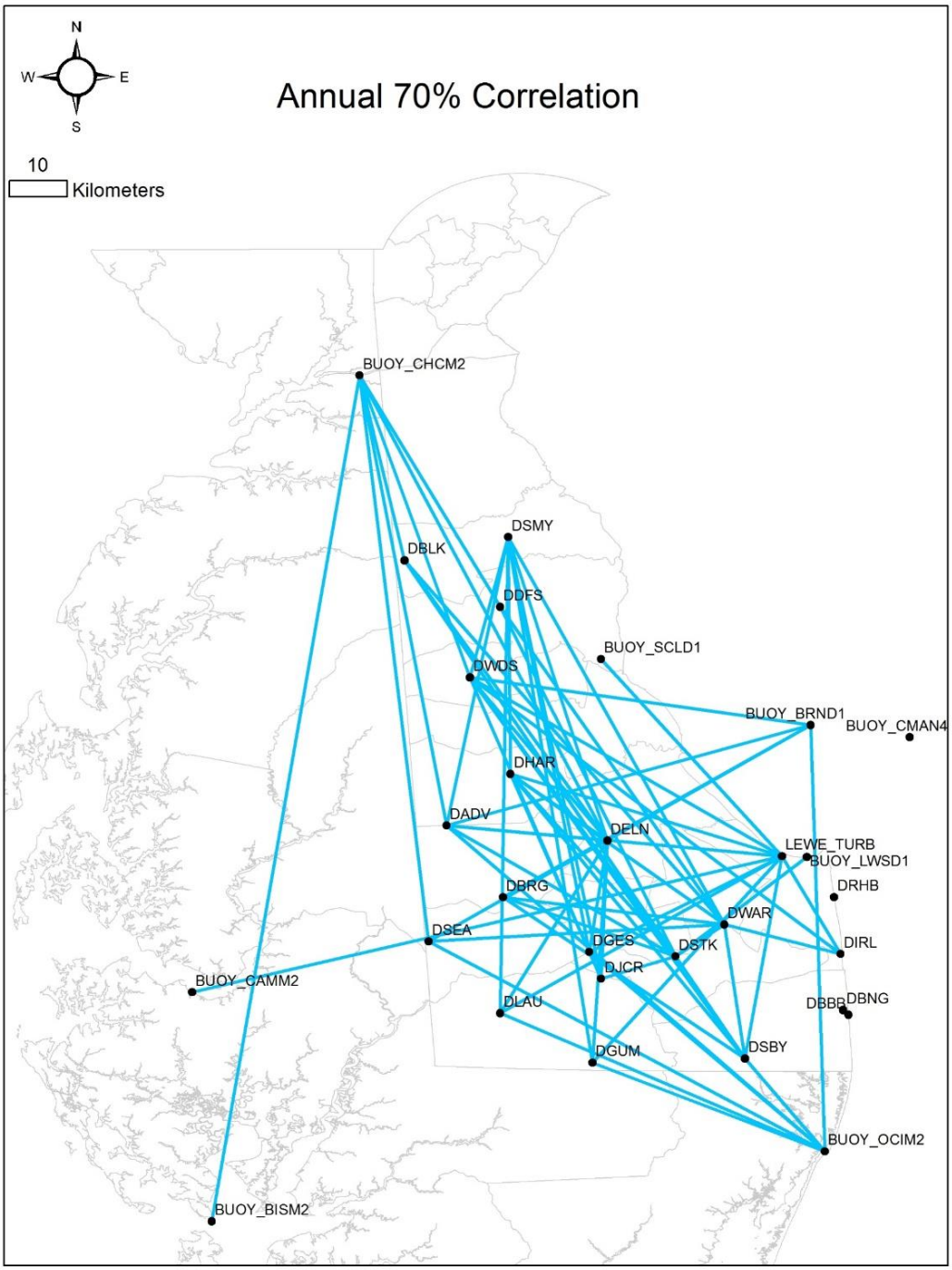

3. 18c Pearson's autocorrelation shown for all stations with an R > 70%.

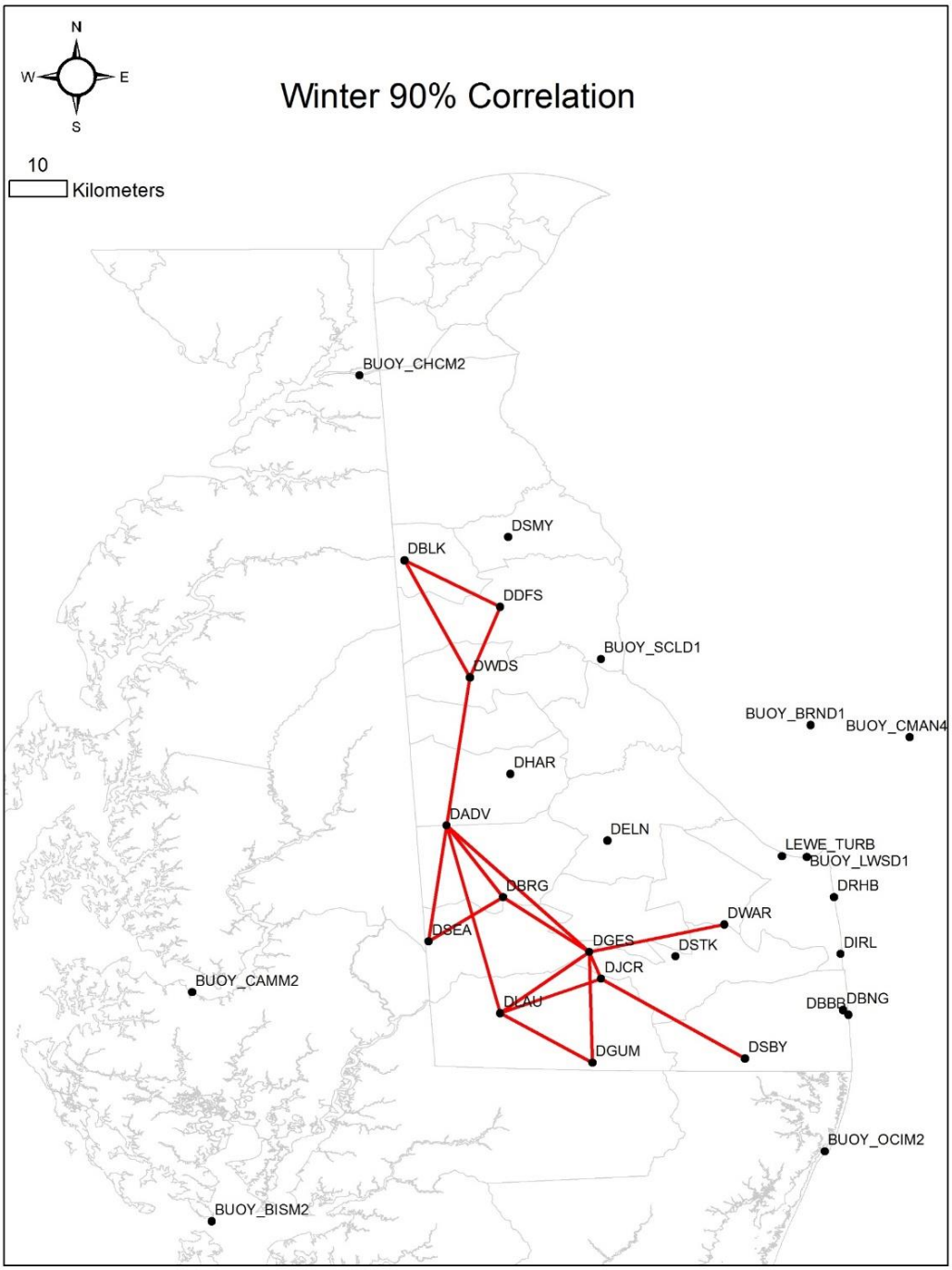

3.19a Pearson's autocorrelation shown for all stations with an R > 90% for the winter.

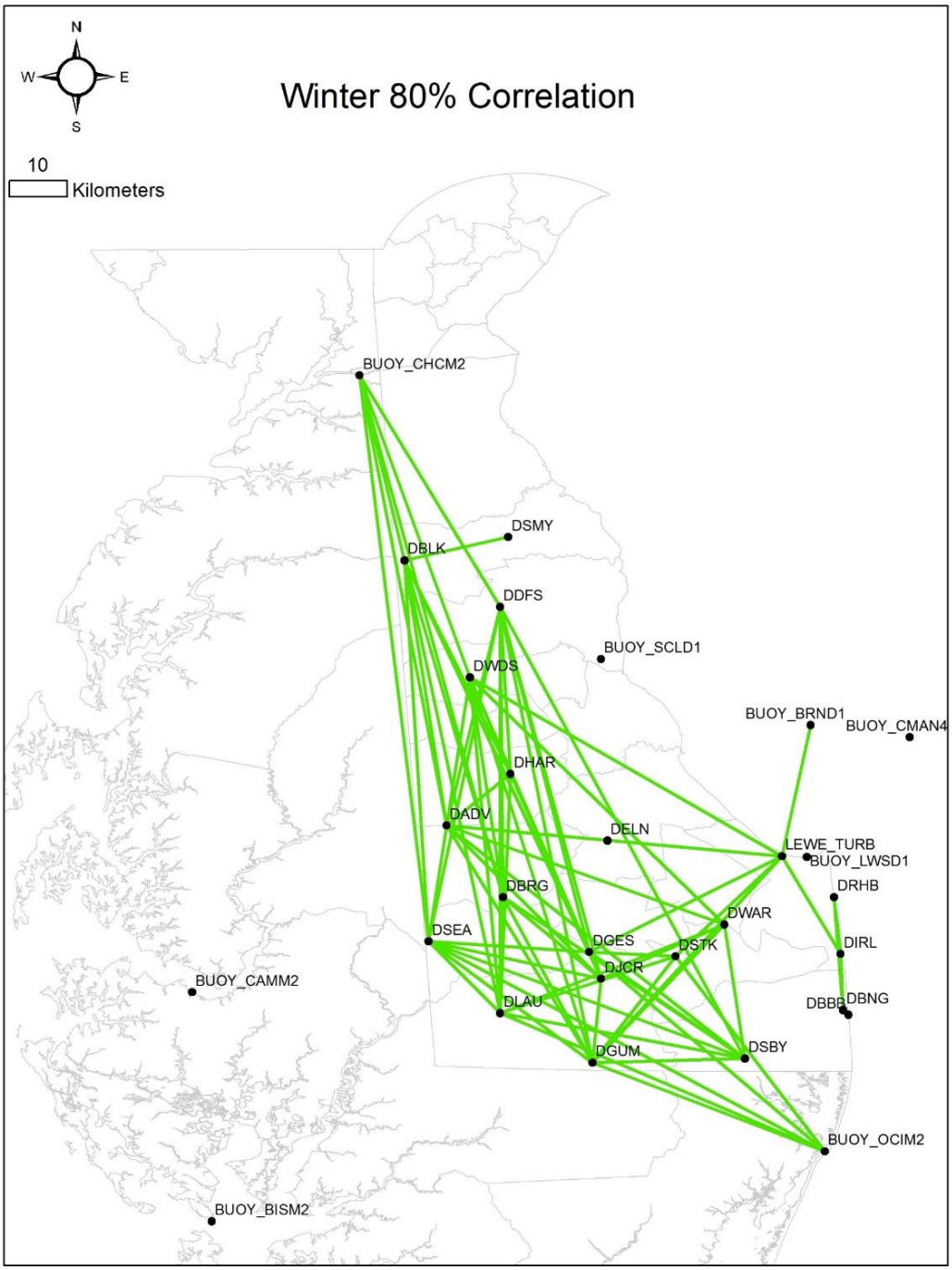

3.19b Pearson's autocorrelation shown for all stations with an R > 80% for the winter.

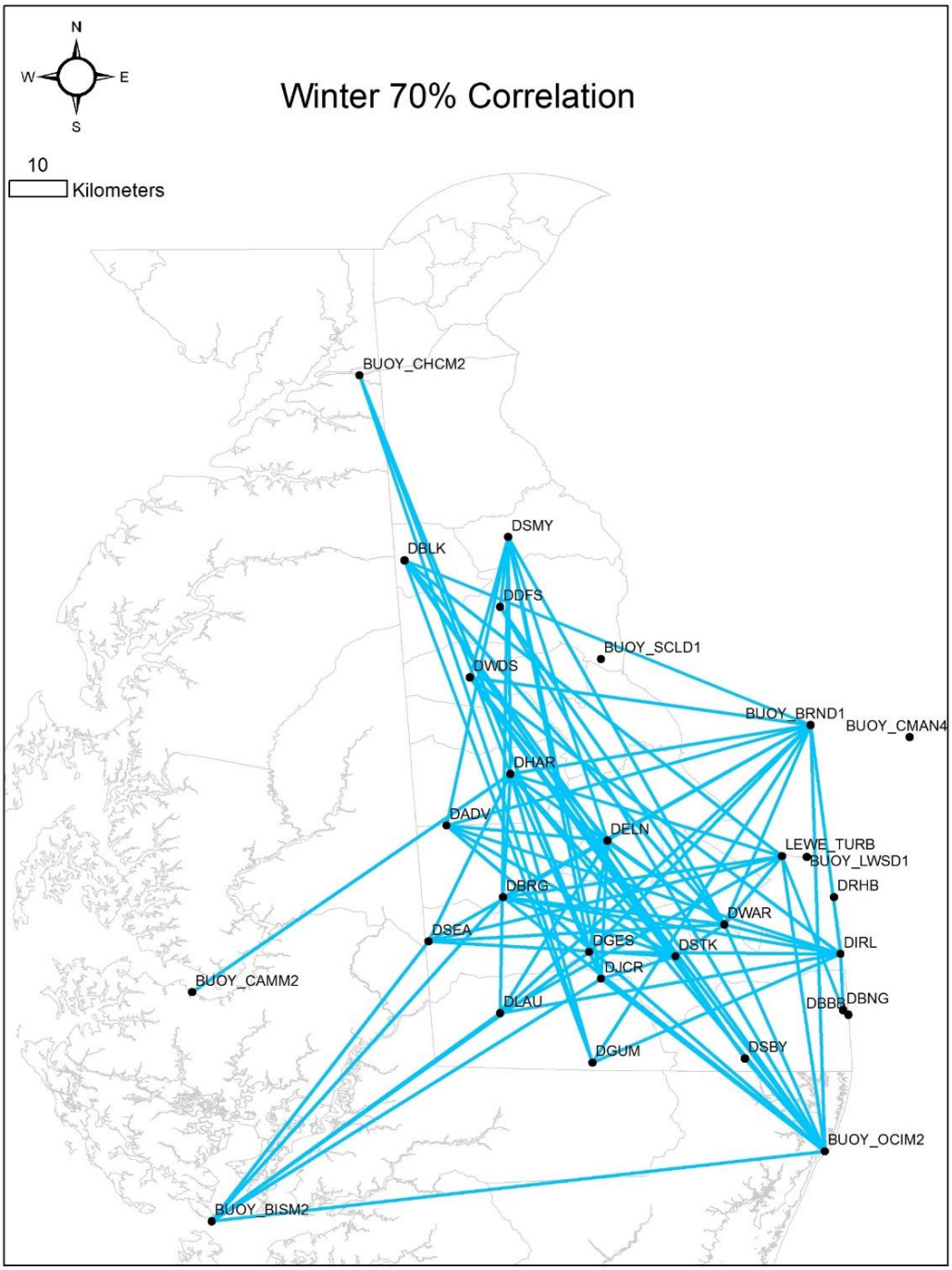

3.19c Pearson's autocorrelation shown for all stations with an R > 70% for the winter.

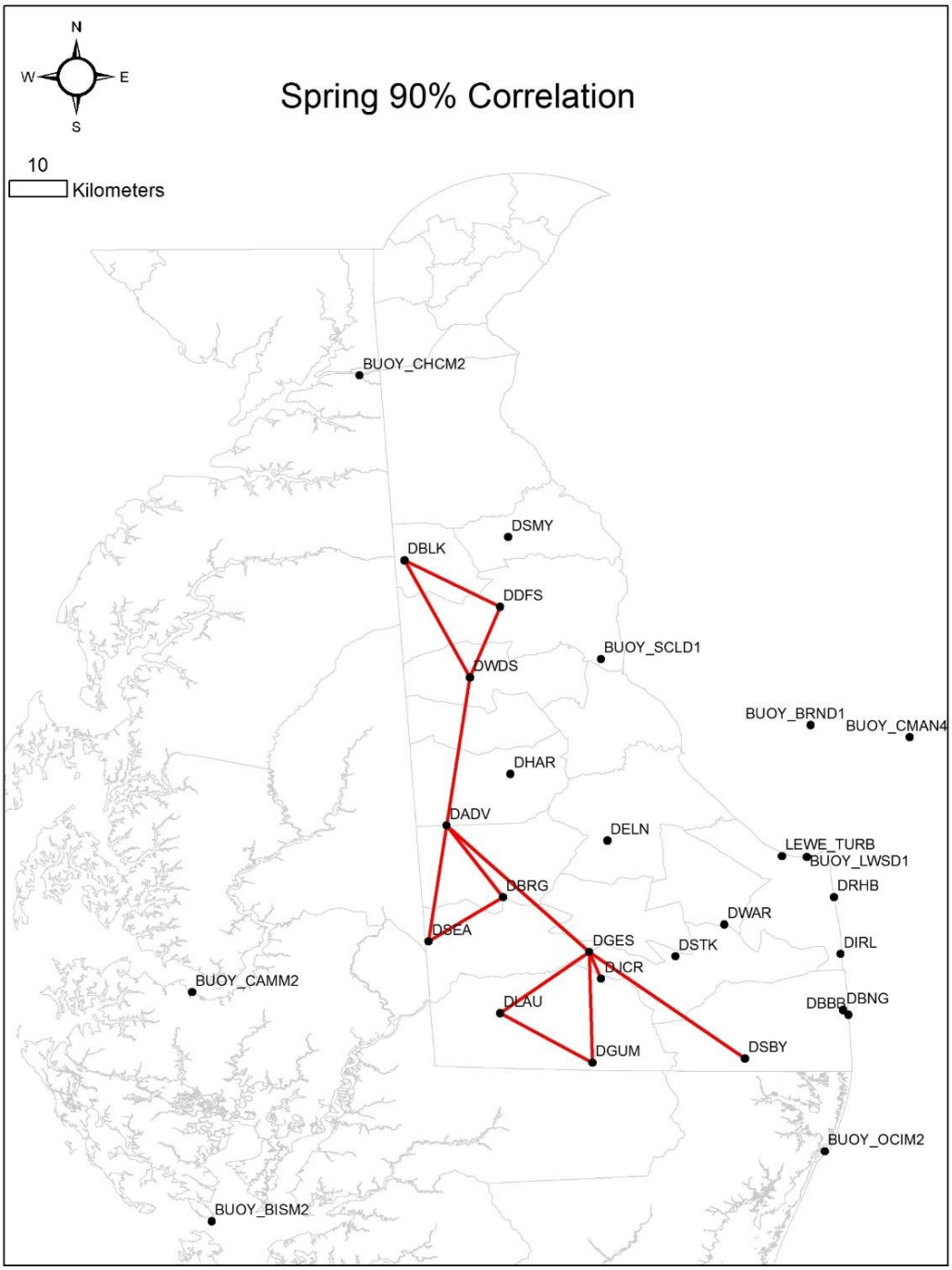

3. 20a Pearson's autocorrelation shown for all stations with an R > 90% for the spring.

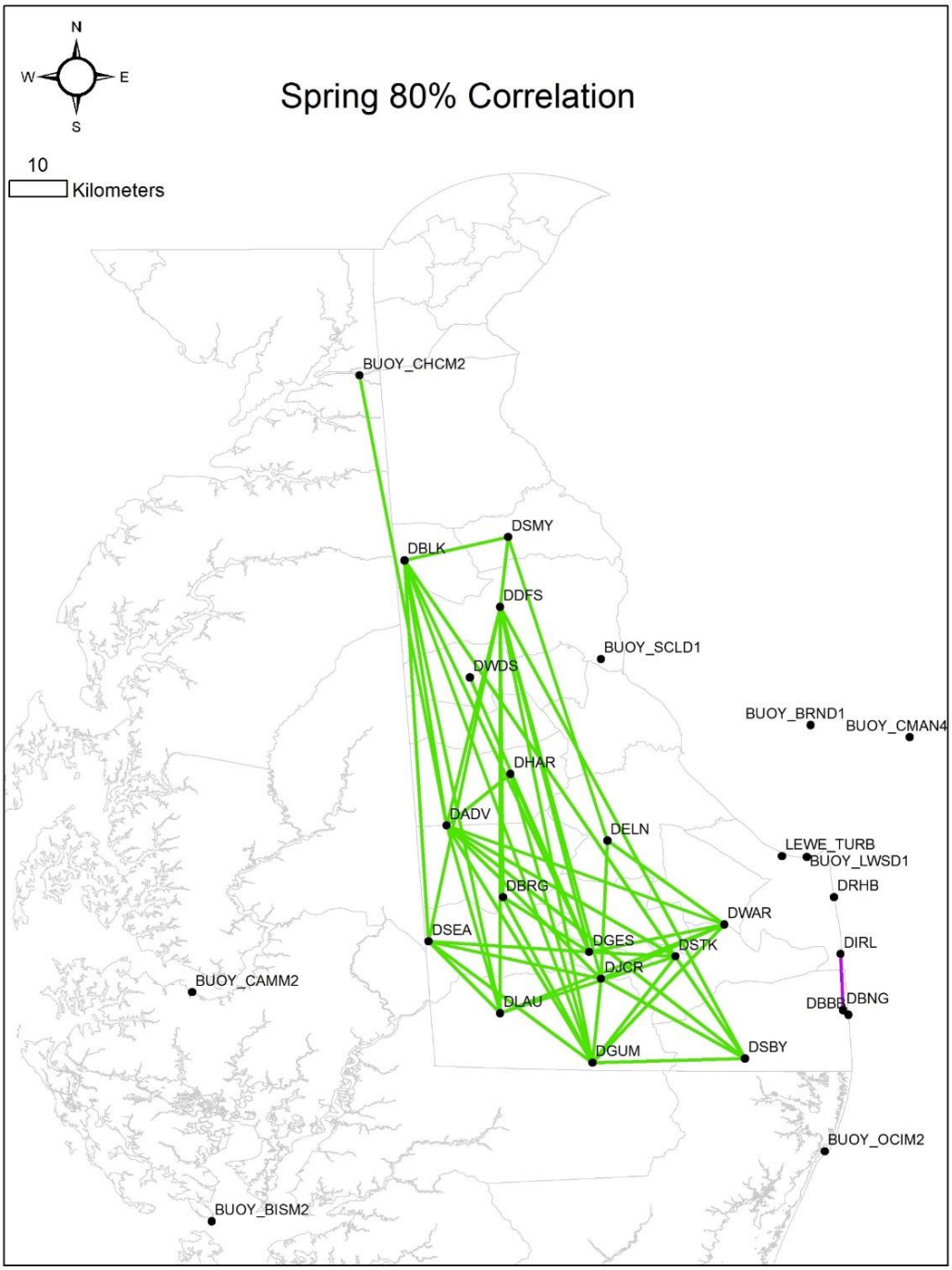

3. 20b Pearson's autocorrelation shown for all stations with an R > 80% for the spring.

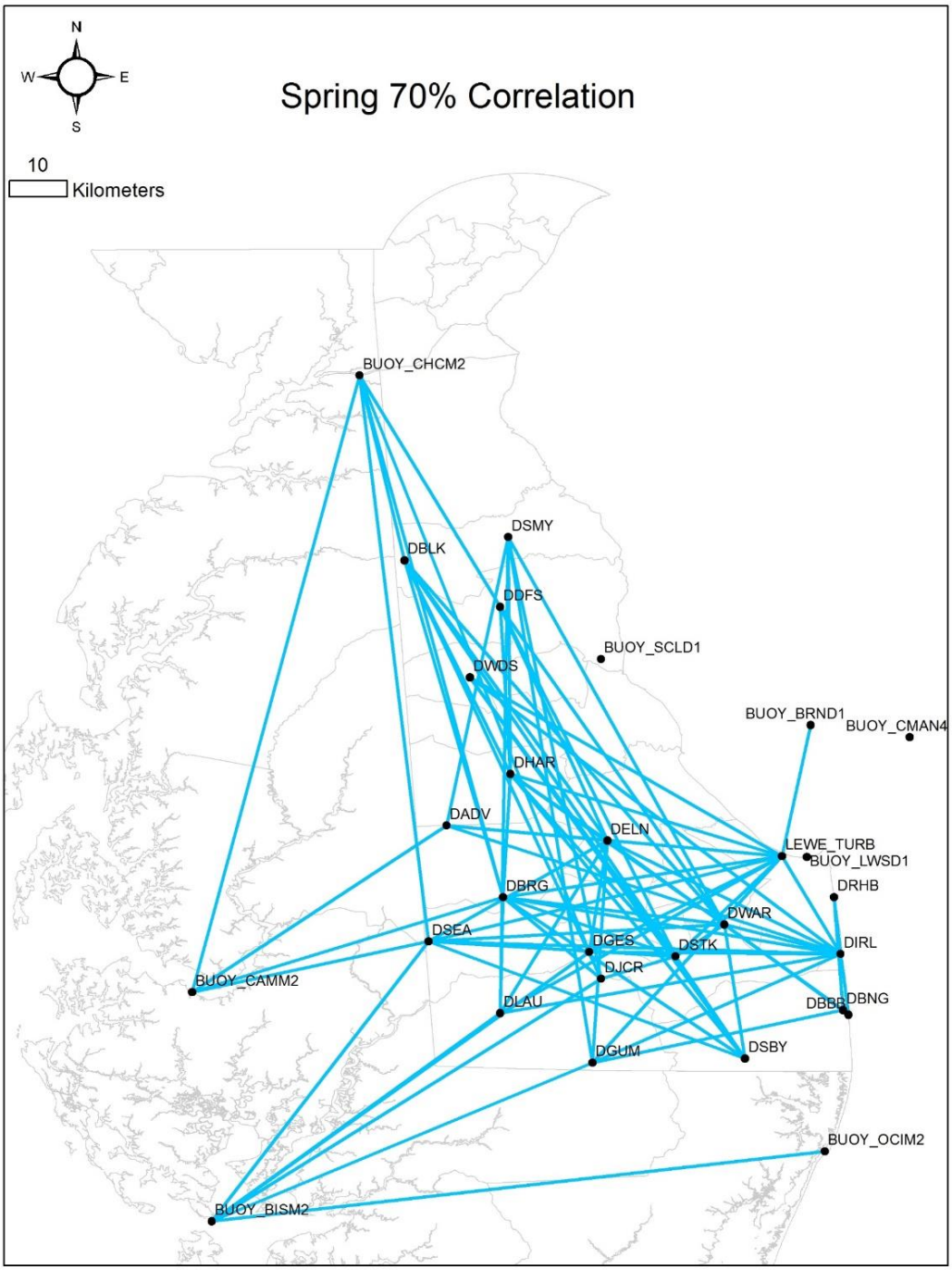

3.20c Pearson's autocorrelation shown for all stations with an R > 70% for the spring.

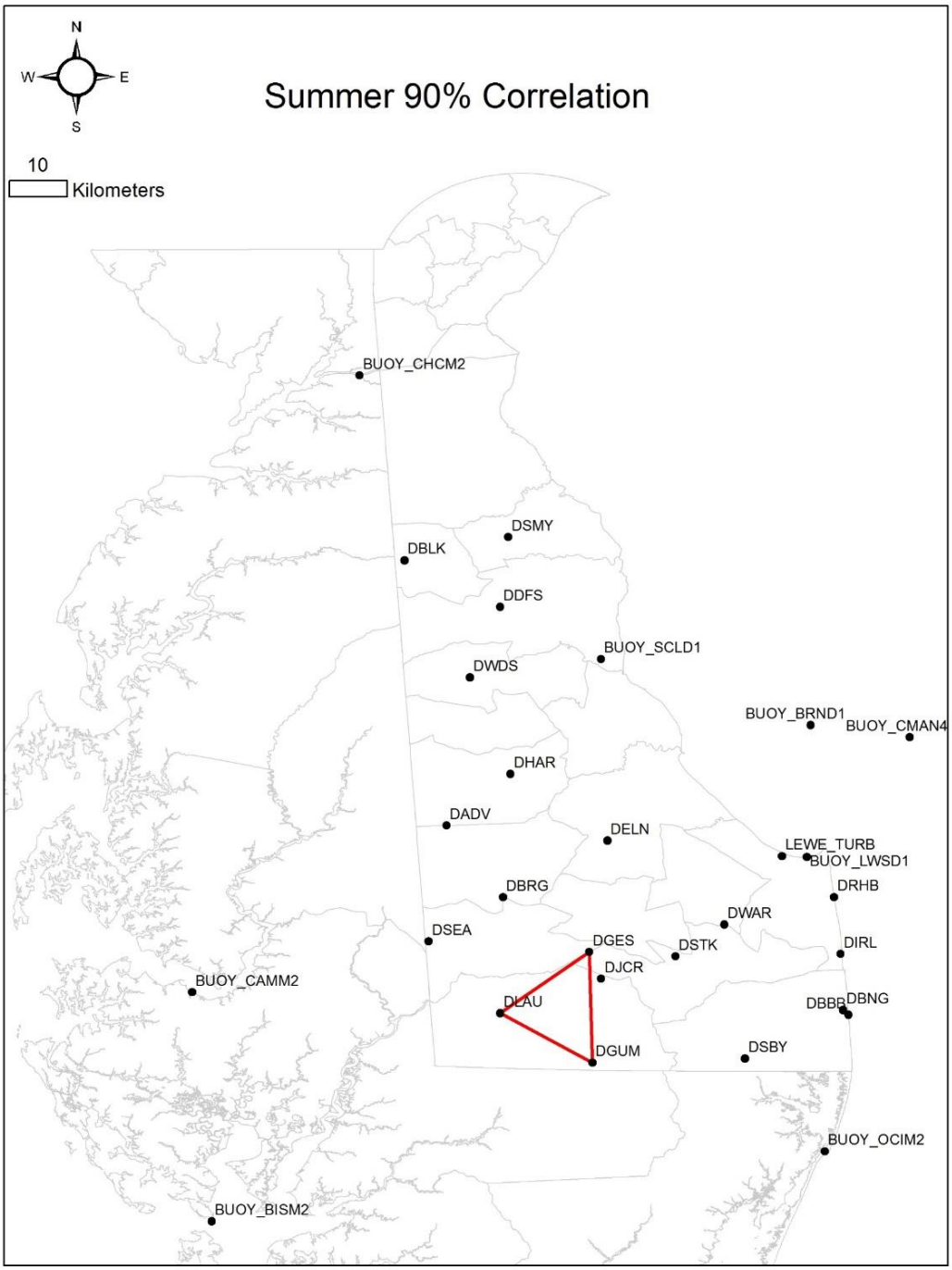

3.21a Pearson's autocorrelation shown for all stations with an R > 90% for the summer.

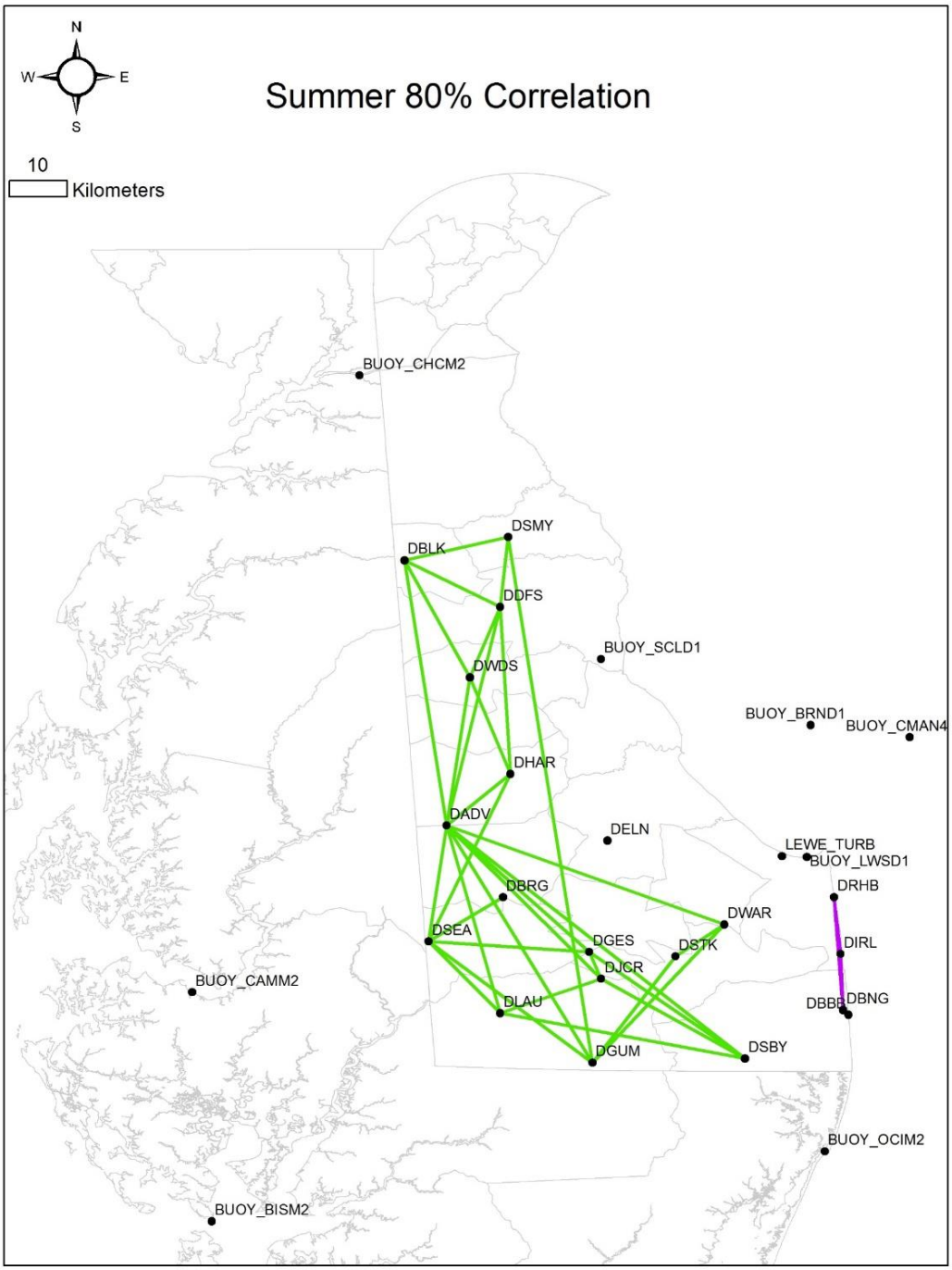

3. 21b Pearson's autocorrelation shown for all stations with an R > 80% for the summer.

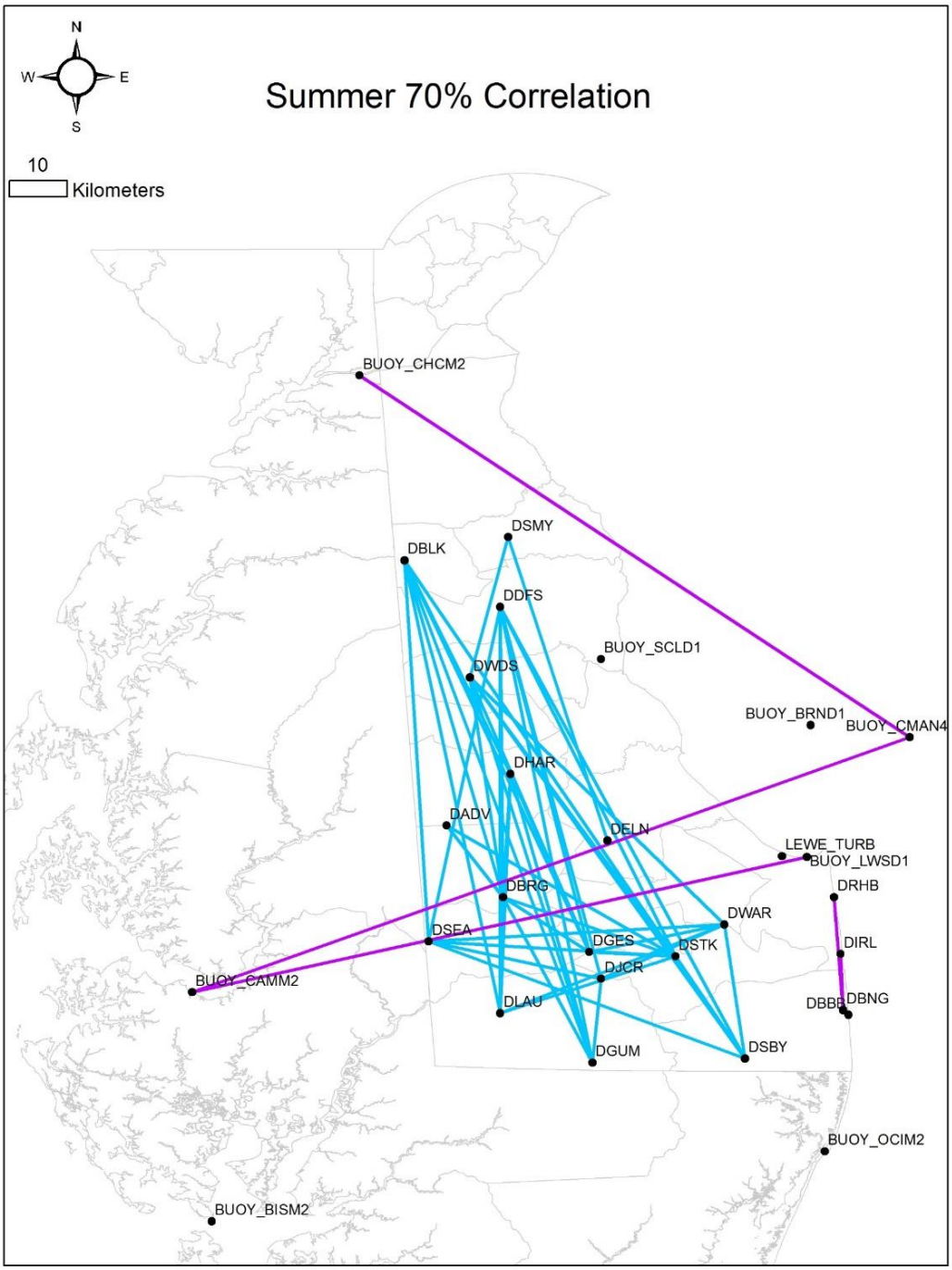

3. 21c Pearson's autocorrelation shown for all stations with an R > 70% for the summer.

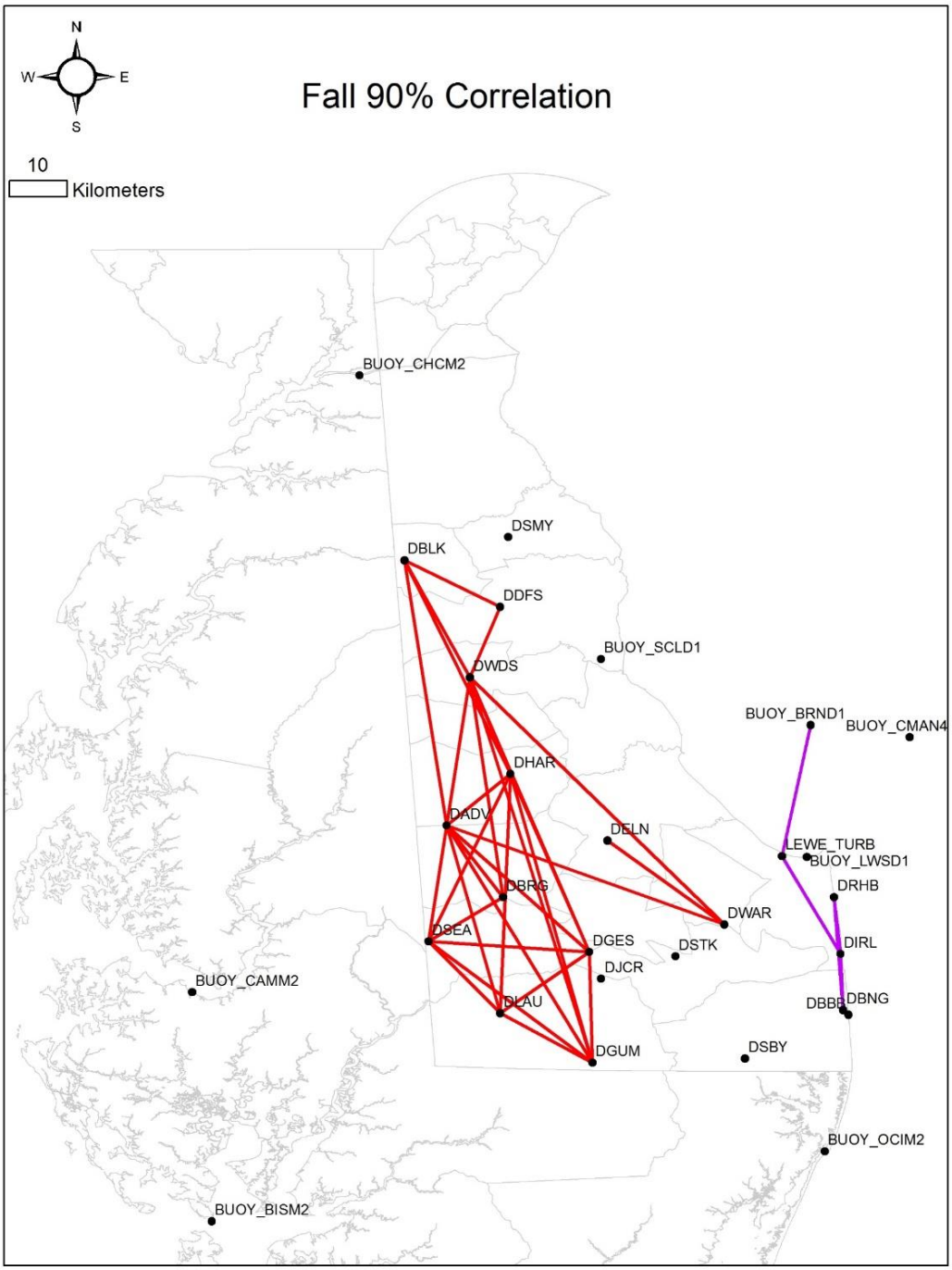

3.22a Pearson's autocorrelation shown for all stations with an R > 90% for the fall.

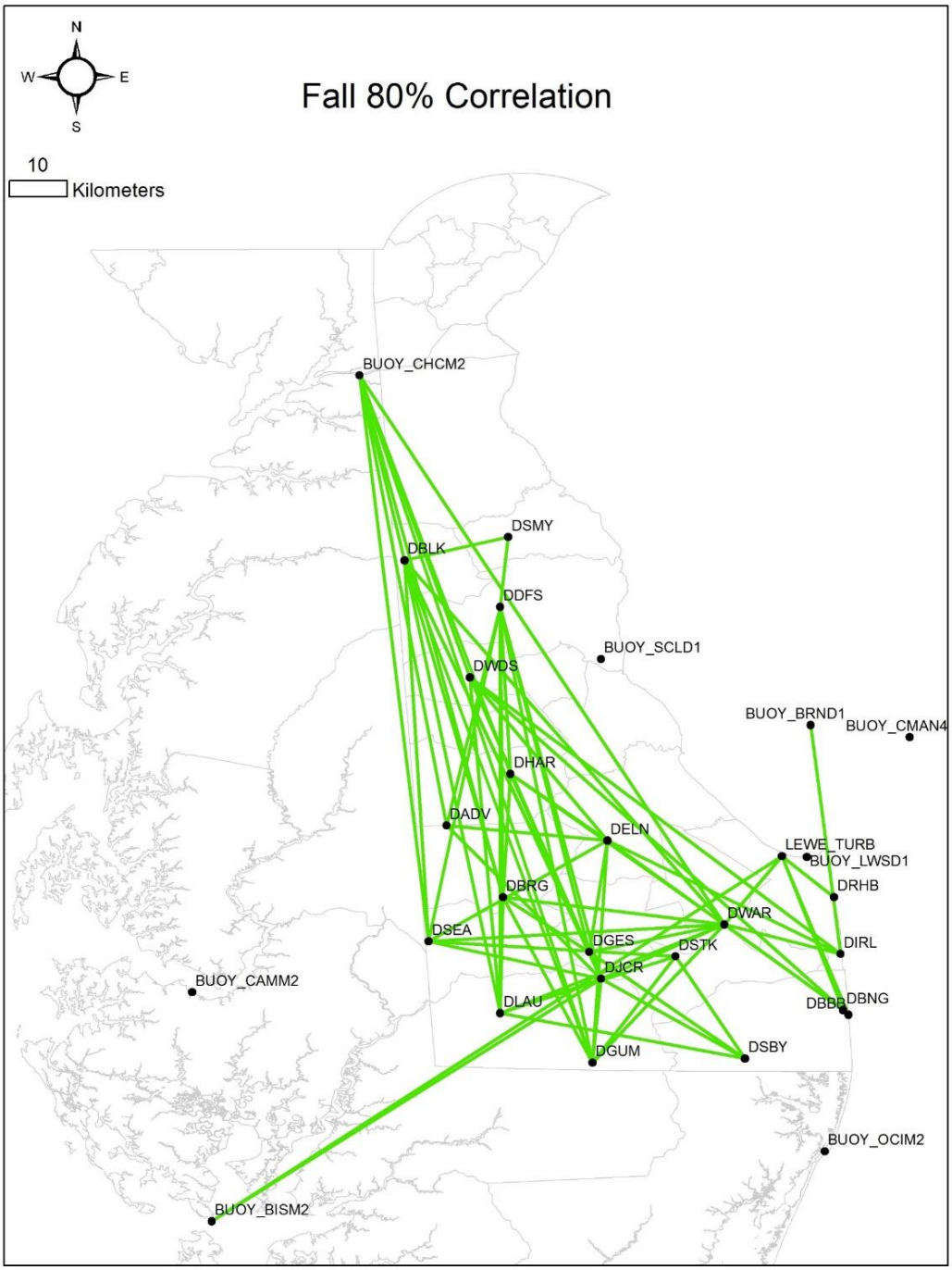

3.22b Pearson's autocorrelation shown for all stations with an R > 80% for the fall.

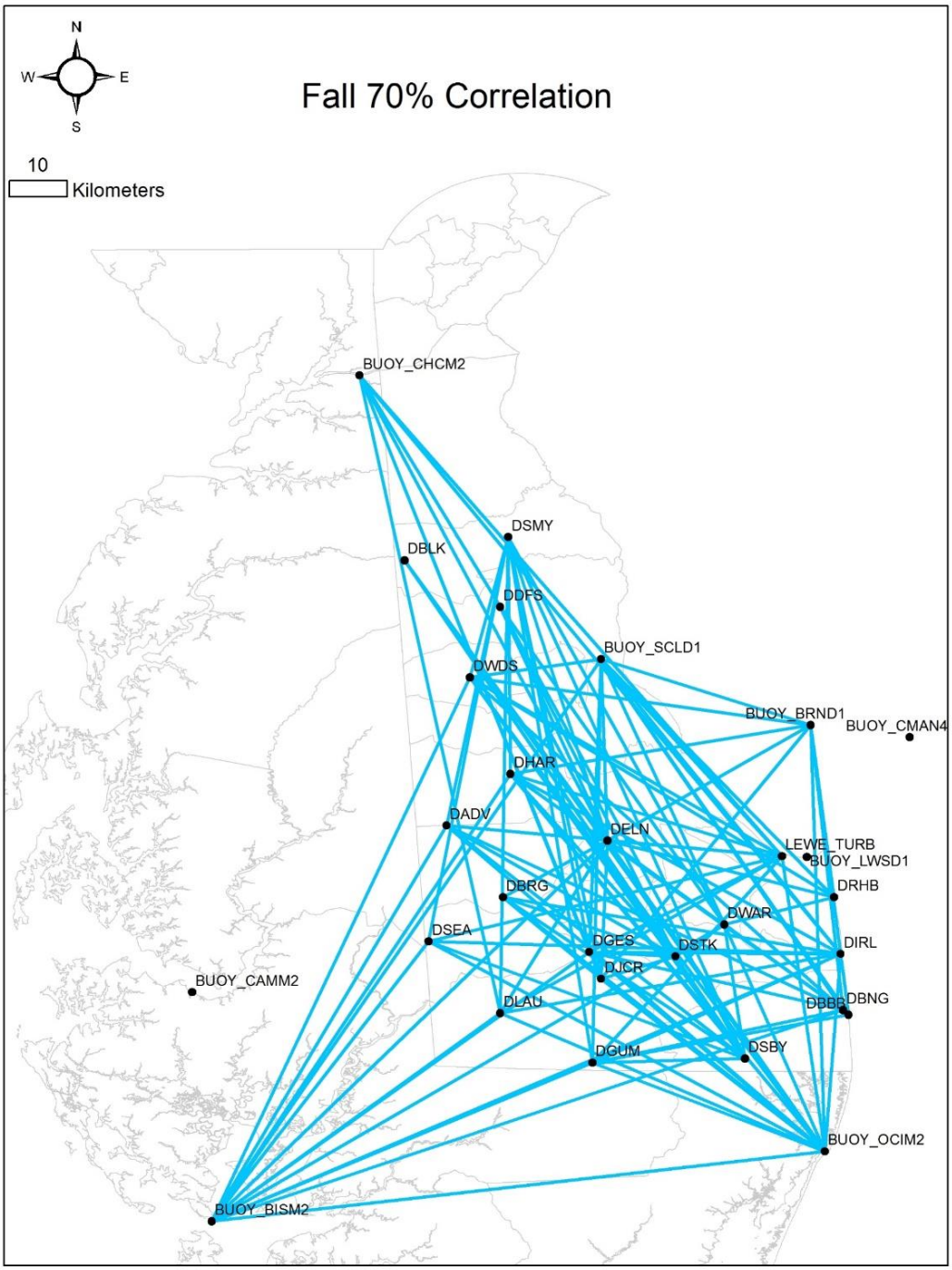

3.22c Pearson's autocorrelation shown for all stations with an R > 70% for the fall.

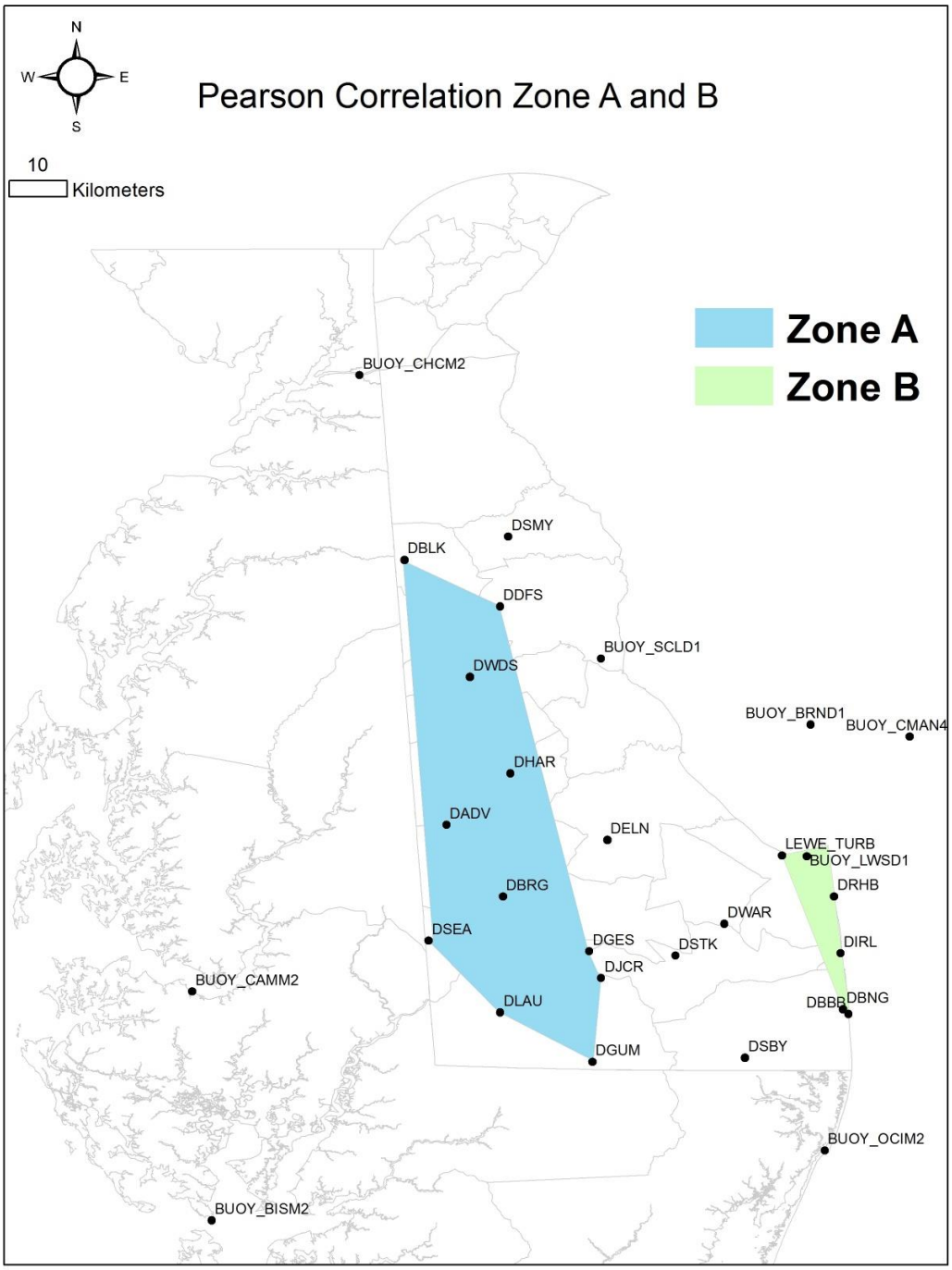

3.23 Pearson's autocorrelation areas.

Chapter 4

DISCUSSION

In this study winds across the lower two counties of Delaware were analyzed using various techniques and metrics such as: mean wind speed, median wind speed, wind roses, upper quartile (UQ), lower quartile (LQ), standard deviation, quartile deviation (QD), mean-median wind speed difference (MMD), skewness, Weibull and normal distributions, Pearson correlations and persistence autocorrelations. This study was done to better conceptualize wind variability in Delaware so as to assist wind farm planners in their initial site assessments of potential wind farms.

4.1 Discussion

Mean wind speeds were used as an initial indicator of winds in this study in the standard fashion (Rogers et al. 2005, Mirhosseini et al. 2011). Mean wind speeds are highest within the Bay corridor as was expected when inferring spatial variation from the determinations of Devorak et al. (2013) that few states possess the land based wind resources to meet 20% of their electrical needs. Coastal and Southwest corridor wind speeds alternate in intensity between seasons where Coastal corridor wind speeds are higher in fall and overall annually. However, Southwest corridor mean wind speeds exceed Coastal wind speeds in the winter, spring and summer. There is an area of low mean wind speed that overlaps the Inland corridor and extends into the Northern portion of Delaware and Southeastern part of Maryland This area of low mean wind speed varies in extent and intensity seasonally with the lowest mean wind speeds and largest extent present in the summer and the converse present in the spring. These patterns in intensity confirm the variability in wind speeds across the state of Delaware

first noticed by Garvine and Kempton (2008) in there study assessing the winds over East Coast Continental Shelf. One seasonal anomaly did occur in this study from prior assessments of the Delmarva Peninsula in that winter wind speeds were second highest to spring wind speeds, this is generally uncommon for wind patterns with few exceptions and should be further investigated (Archer and Jacobson 2013, Hughes and Veron 2015).

Wind rose analysis reveals wind frequently comes from the Southwest direction. This is in line with Maurmeyer's characterization of winds at the Wilmington airport (1978) which was later confirmed by Moffatt and Nichol (2007) who analyzed wind directions and intensities from airport weather observation stations located in the Indian River, Dover, and Sussex airports. Hughes and Veron (2015) cited both of these works and expanded these findings to include the Delaware Bay and the entire state of Delaware furthering acceptance of southwesterly winds dominating the region. Results from Hughes and Veron (2015) over the state of Delaware are validated in this study and further authenticated in that this study found the same results as Hughes and Veron (2015) and improved on these by using a denser network of weather observation stations. Winds coming from the southwest direction significantly affect portions of the study area that have open water to the southwest of them. This may result in providing the Southwest corridor with disproportionally high wind speeds relative to other coastal and inland regions. In addition, winds traveling from West to East across the state of Maryland will cross the Chesapeake Bay and accelerate due to the lower surface friction, while approaching the Eastern coastline of the Chesapeake Bay. Therefore, the Southwest corridor can attribute much of its high

mean wind speeds to large areas of limited surface roughness adjacent to its location in Maryland and surrounding water bodies.

Median wind speeds followed similar spatial patterns to mean wind speeds throughout the four seasons as well as annual. Median wind speeds were highest in the Bay corridor and second highest in the Southwest corridor except for the fall season where Coastal median wind speeds were the second highest median wind speeds observed. Inland median wind speeds were always the lowest wind speeds recorded and produced a region of low median wind speeds that range from the Northern section of the Inland corridor and proceeded through to the Southern portion of the Inland corridor. This Inland area of low wind speeds grew and diminished in size seasonally with larger extents in the summer and fall and smaller extents in the winter and spring. The area of this region was smaller than that observed in the mean wind speed fields. Median wind speeds were better able to represent the central point of all datasets over the mean as proposed by Wolf-Gerrit (2013) and his study accounting for wind uncertainty estimation in Scotland. Additionally, median wind speeds proved to be less susceptible to outlier influences than mean wind speeds (Leys et al. 2013); thus the utility of median wind speeds should be considered in representing wind data which can vary greatly between seasons (Archer and Jacobson 2013).

Mean-median difference (MMD) is a way of determining if the distribution of wind speeds is asymmetrical compared to a normal distribution (Brown et al. 1984). MMD, regardless of season, were always highest in the Coastal corridor. Overall MMD exhibited a few notable patterns that may be beneficial to the wind industry. MMDs, regardless of season, were always highest in the Coastal corridor indicating

that the wind speed probability distribution was not evenly distributed about the mean. MMDs varied seasonally and were strongest during the fall and weakest in the summer with moderate values in the winter and spring. MMD generally was proportionally higher during the winter and spring within the Bay and Southwest corridors. However, in the fall and summer, the MMDs were more intense in the Inland corridor. Therefore, Coastal corridor wind speeds are the least well represented by mean wind speed, while mean wind speeds represent the other 3 corridors variably well depending on the season of interest. These results are in agreement with Bludszuweit et al. (2008) in their analysis of the normal distribution, which assumes Gaussian characteristics about the mean; the normal distribution failed to accurately depict wind speed distributions. Thus, as Wolf-Gerrit (2013) proposed using the median to better represents wind speed distributions than the mean, the MMD emerges as a useful tool to assess the degree of inadequacy the mean wind speed metric assumes when representing a given dataset. Therefore, the MMD serves as a metric of symmetry of a given dataset.

Seasonal skewness, with the exception of the summer season, followed the same seasonal pattern as that observed in the MMD values (Table 3.4). Therefore, the skewness present in the dataset indicates lack in symmetry about the mean wind speed value (Harmel et al. 2002). Further, the data exhibit positive skewness, thus these distributions have large tails to the right of the distribution (Trauth 2015) because of disproportionate outlier occurrences inherent within the data set (Haan 1977). These results are in full agreement with the modern understanding of wind speed distributions in that winds are subject to high positive outliers (Fields et al. 2016).

Probability density functions of the observed wind speeds were calculated annually and for each season, for each corridor. Then, Weibull and Normal distributions were overlaid on the observed pdf's. It is clear that the Weibull distribution is a far more accurate representation of the data than the Normal distribution; this is in agreement with numerous studies including Jowder (2006), Justus et al. (1977), Celik (2004) and Pishgar-Komleh (2014). Weibull distributions provide good fits to most of the annual and seasonal wind data and support other findings throughout the study in that wind speeds had larger ranges during the winter and spring, and narrower ranges during the summer and fall seasons. Peak wind speeds are higher in the winter and spring and lower in the summer and fall, thus illustrating the trend that seasonally, wind speed and dispersion are related (Archer et al. 2016). The Normal distributions come closest to accurately representing the probability distribution of the data within the Bay corridor, although Weibull distributions are still slightly more effective representations. Seasonally, Normal distributions are most effective at representing the summer season, although again, fall short of the performance of the Weibull distributions. The normal distribution performs its relative best in the Bay corridor and during the summer season because this corridor and time period have the most consistent winds due to minimal surface roughness in the Bay corridor and due to overall low wind speeds in the summer season; this resulting in a more Gaussian distribution. Thus, the Normal distribution, which assumes Gaussian characteristics, performs best in the summer season and Bay corridor. Safari and Gaser (2010) explored the use of the Square Root Normal Distribution in an attempt to improve the use of the Normal distribution. Despite significantly improving on the applicability of the Normal distribution, similar to

findings of using the Standard Normal distribution in this study, the Weibull distribution still outperformed this version of the Normal distribution. Analyzing these results posits the conclusion that areas exposed to land and sea breeze effects will exhibit the most widely dispersed wind speeds compared to areas exposed to only one form of surface cover. This result is in accord with Hughes and Veron (2015).

The analysis of standard deviations described in Chapter 3 shows that the standard deviation for the wind data used in this study are extremely large, and although able to provide very broad generalizations, this metric is not adequate to address the variability within wind measurements as most wind speed distributions are not well represented by Normal distributions (Bludszuweit et al. 2008). This is in accord with Leys et al. (2012) where they found that standard deviation is a poor metric to use for datasets involving large outliers, such as those present in wind data. Chang and Bai (2001) also found standard deviation to be a poor metric of variability for positively skewed datasets, as did Harmel et al. (2002) in their research on simulating temperature with Normal distributions. For these reasons, alternative metrics were developed to cope with the unique variability present within wind observations, these metrics are upper quartile, lower quartile and quartile deviation metrics discussed below.

Upper and Lower Quartile analysis shows that the Southwest corridor is more likely to have a higher UQ threshold than the other corridors analyzed, however it has moderate LQ thresholds. The Bay corridor has a substantially higher LQ threshold than any other corridor for all seasons and has a high UQ limit as well. Additionally, the Bay corridor's UQ threshold is higher than the Southwest corridor's UQ threshold, although more than half the amount of difference between the Bay and Southwest

corridor's LQ values. This means that winds in the Southwest corridor are significantly more dispersed than winds in the Bay corridor because of the larger the distance between the upper and lower quartiles, the larger the dispersion of wind speed observations (Trauth 2015). Conversely, the high LQ threshold in the Bay corridor suggest higher-level wind speeds are present in this corridor more regularly than any other corridor; this assertion is supported by the high UQ limit found in the Bay corridor throughout all seasons. Quartiles, being a specific type of quantile (Trauth 2015), provide wind developers with better assessments of wind speeds in an area that are more applicable to the wind energy industry (Bremnes 2004). Bremnes (2006) further affirms the use of quantile metrics in wind energy forecasting in 2006. The applicability of quantiles is confirmed in this study in which it was found that UQ and LQ metrics provide additional information about the wind speed variability beyond the MMD.

Quartile Deviation (QD) throughout this study indicate levels of dispersion in the hourly average wind speed data similar to how Buller and McManus (1973) used QD to represent dispersion of glacial tills. Krumbein (1936) additionally used QD metrics to represent data due to its ability to geometrically represent data over other methods, such as mean or standard deviation, which rely on arithmetic principals to project representation. Due to the QD metrics geometric properties, it accounts for but is not overly influenced by outliers and thus provides useful and unique applications in wind energy planning. QD in the Southwest Corner is the highest of any corridor for all time periods analyzed. The second highest QD was present in the Coastal corridor and the lowest QD was present in the Bay corridor. QD analysis demonstrates that the

dispersion of winds will be greatest in areas that experience Land and Sea Breeze events and have at least 2 large terrain transitions (bay water and inland terrain), such as the Southwest and Coastal areas. Winds will be least dispersed in areas far removed from Land and Sea Breeze effects such as the Inland and Bay corridors. Winds will also be less dispersed in areas with minimal surface roughness; this explains the substantially lower QD consistently found in the Bay corridor which has minimal surface roughness. QD has not been extensively used in wind farm planning although it presents ample utility in its applications and should be considered in future wind resource assessments (Bremnes 2006).

Comparing mean wind speeds with QD, three potential wind farm locations were identified within the study area because of their high average wind speed and low wind variability. These viable locations are present within every season and are as follows, the Bay corridor, Southwest corridor and Coastal corridor. All three of these locations have average wind speeds of 5.2 m/s or greater and are therefore viable options for wind farm development (Gamesa 2015). Bay locations consistently presented the best option for wind farm development due to high wind speeds and wind speed consistency; however, the Southwest corridor provides similar opportunities to Bay locations as an alternative potential wind farm site. Southwest corridor mean wind speeds often overlapped and at times exceeded Bay wind speeds within this study. The main discrepancy between Bay and Southwest corridor locations was the difference in QD, which were 0.3 m/s annually and 0.7 m/s seasonally, respectivly. Therefore, Southwest corridor locations present a viable yet less attractive alternative to Bay corridor wind farm locations. This area was also identified by Burt and Firestone (2016) to be a potential site for wind farm

development based on site geology, economic feasibility and potential resource availability. Using both mean wind speed and QD provides developers with the ability to assess the potential resource of an area, while also discerning the variability within the area (Fields et al. 2016 and Fisher 1987).

Autocorrelation trends indicate that the Bay corridor area has the least persistent signal in winds, although this persistence at 6 hours is only 1 hour less than the remaining three corridors. The findings of this study in relation to persistence measured through autocorrelation techniques produced disappointing results in that persistence, here measured as explaining 25% of the variance or more, exhibited only a 6.75 hour signal. These findings, although disappointing are within expected results of other wind autocorrelations. Abdel-Aal et al. (2009) points out that current autocorrelation techniques, similar to the ones use in this study are in need of improvement and often poorly represent wind speed persistence. The poor performance of autocorrelation techniques is in part due to the ambiguity surrounding data interval size (Brokish and Kirtley 2009). This study is no exception to the disappointing results produced via persistence analysis, and thus it is recommended to use autoregressive Torres et al. (2005) or Neural Network (Alexiadis et al. 1999) models in the future as an alternative to persistence methods of predicting wind speeds. Kavasseri and Seetharaman (2009) further expanded the use of autoregressive modeling of persistence using *f*-ARIMA models. Autocorrelation methods used in assessing persistence within a wind signal have been proven obsolete; efforts now should be focused on determining the proper use and implementation of autoregressive modeling in wind persistence analysis.

The Pearson Correlation analysis revealed two predominant zones present throughout the study area that have coherence among stations. The two zones, Zone A and Zone B represented two notably different sections of the study area in which wind patterns differed significantly. Zone A appeared in all 90% correlations maps and was restrained to the western side of Delaware within the study area, and was the strongest showing zone. Zone B appeared only in 80% maps and occupied the coastal section of Sussex County, DE. The differences between these two zones may provide an opportunity similar to the one outlined in Katzenstein and Apt (2012) in which multiple sites may be suitable for wind farm development and would be able to provide interconnected benefits to aid in offsetting losses due to wind uncertainty resulting from variability. However, covariance tests between Zones A and B should be performed to confirm fluctuations in wind speeds are independent of one another. Potential wind farms in Delaware will be highly susceptible to pattern overlap due to the flat terrain and relatively small expanse of the state (Damousis et al. 2004). Apt (2007) found that even at a distance of 400 km which is a notably greater distance than present within the study area, wind farm's production may overlap significantly, although this trait diminishes significantly at the synoptic scale (Kempton et al. 2010).

Based on the results of this study, two metrics emerge that pose useful and reliable applications for categorizing variability within the wind. They may be useful for indicating the impact of wind variability on the wind resource to wind farm developers. These metrics are the mean-median difference (MMD) and the Quartile Deviation (QD). MMD provides a representation of how different a distribution of wind speeds is relative to a Normal distribution. Given that mean wind speed is the current gold standard in wind representation within an area, MMD adds additional

information about the distribution of the wind speeds around the peak in the distribution. Additionally, changes in MMD were shown to follow a seasonal pattern that was similar to that of skewness, thus lending weight to the validity of this simple metric as a way to indicate when the distribution is highly asymmetric with a large, positive tail. Therefore, in using the MMD, wind developers will have a way of discerning if wind variability needs to be characterized early on in their site studies.

QD is the second metric suggested as a way to simply characterize the variability in the wind resource. QD provides a measure of dispersion and characterizes the range between the highest and lowest 25% of wind speeds within a dataset. This may be more useful information than that provided by standard deviation. QD is a geometrically derived dispersion representation statistic and is therefore not vulnerable to outliers in the same way as standard deviation (Trauth 2015). Given that wind speed datasets tend to contain large outliers due to storminess, QD is selected as the preferred dispersion statistic. The use of the QD was illustrated in that it found Southwest and Coastal corridors to be the most dispersed, as did standard deviation (Figures 3.5 and 3.8).

4.2 Mean Wind Speed and Quartile Deviation Evaluation

Combining QD and mean wind speed metrics provides an effective assessment of an area's wind power potential and subsequent suitability for wind farm development. In assessing the mean wind speeds, MMD was used to gauge the applicability of the mean wind speeds to the datasets analyzed. The combination of mean wind speed and QD provides wind developers with the ability to assess total

potential power output of an area and represent some features of the wind variability, notably the data range.

Mean wind speed assessment shows that potential wind farm sites may exist within the Bay, Southwest and Coastal corridors with each corridor having annual mean wind speeds of 6.1 m/s, 5.2m/s, and 5.4 m/s. Wind farm development currently is not feasible within the Inland corridor due to its low wind speeds. Annual mean wind speeds indicate Bay wind resources present the most promising location to install a wind farm. The second most promising area is located within the Coastal corridor, after this corridor; the Southwest corridor presents the least desirable yet feasible potential wind farm site. MMD analysis of these three locations reveals that the mean is most accurate in representing wind speeds in the Bay and Southwest corridors, while slightly less reliable in the Coastal corridor. Annual QD assessments of the three potential wind farm sites reveal that Bay winds are the least variable and most concentrated winds within the entire study area with QD as low as 1.3 m/s in the spring and 2.3 m/s annually. The Coastal corridor has the second lowest variability of all potential wind farm sites with values ranging between 1.6 m/s and 2.6 m/s with an annual QD of 2.4 m/s. Thus, the Coastal corridor wind resource will have more variability and dispersion than Bay corridor winds. The area with the most variable and dispersed winds that provides a viable location for wind farm siting is found in the Southwest corridor. The Southwest corridor has QD ranging between 2.0 m/s and 3.3 m/s seasonally with an annual QD of 2.6 m/s. Based on the available wind resource and its reliability, the Bay corridor area is the most promising potential site for future wind farm development. Coastal and Southwest corridor areas also provide

opportunities for wind farm development, although the wind resources at these locations will be less intense and more variable.

Seasonal analysis of mean wind speeds revealed the same three potential locations suitable for wind farm siting as annual assessments. These areas are the Bay corridor, the Southwest corridor and the Coastal corridor. These potential locations were also assessed using the QD metric and it was found that seasonal patterns mimicked annual patterns, although in varied intensities with respect to wind speed.

Chapter 5

CONCLUSIONS

5.1 Conclusions

This study aimed to characterize the variability of winds within Delaware by analyzing hourly winds within the 2015 calendar year using 29 weather observation stations pulled from four weather-monitoring networks; these networks are the Delaware Environmental Observing System, the National Data Buoy Center, the National Estuary Research Reserve System and the WeatherBug Monitoring System. The methods reviewed and pioneered within this study were done in such a way as to explore methods of wind resource characterization. Current preliminary wind energy assessment is done using highly detailed annual mean wind maps. This study suggests that additional maps of QD and MMD may be very helpful in this preliminary stage.

The data provided were quality controlled for consistency and standardized to hourly average observations. Additionally, station location roughness was assessed using the Danish Wind Industry land roughness criteria and wind speeds were projected to a height of 114 meters using the Log Law. These projected station wind speed values were then interpolated onto the study area using the Inverse Distance Weighting technique through ESRI ArcMap. Wind speed interpolations were made for the following metrics; mean, median, mean-median difference (MMD), Upper Quartile, Lower Quartile and Quartile Deviation (QD). Normal and Weibull distributions, skew and standard deviation calculations and wind roses were also produced using the mean wind speed metric. Finally, autocorrelations and Pearson correlations were conducted to determine station self-similarity and station-to-station similarity.

Findings of this study show that the MMD metric is a useful tool in assessing the applicability of mean wind speed's accuracy at representing a given area's winds. Weibull distributions are much better representations of the wind speed probability distributions in most seasons and corridors, due to their ability to model non-negative positively skewed data. QD is a simple, reliable method for representing the range of wind speeds. Geographically, the Bay corridor presents the highest and most consistent winds within the study area and is meteorologically best suited for wind farm installation. Coastal and Southwest corridors also present suitable meteorological conditions for wind farm development, although the Inland corridor presents a poor choice for wind farm development. Pearson Correlation results further proved that multiple wind farm installation within the state is possible, and might be able to counterbalance times of high and low energy production between sites.

The Southwest corridor emerged as an unexpected finding within this study in that it boasted higher wind speeds much like the Coastal corridor, and at times outperformed Coastal corridor wind speeds. The Southwest corridor simultaneously possessed some of the highest variability within the study area.

Further study should be conducted to assess the cost benefit ratio of all three proposed wind farm locations, Bay, Coastal and Southwest corridors, to determine the best location to install Delaware's first commercial wind farm. This future study should account for installation and maintenance costs, energy transmission costs, land value and acquisition costs, public opinion and opposition costs, and environmental costs.

REFERENCES

Abdel-Aal, R. E., Elhadidy, M. A., and S. M., Shaahid, 2009: Modeling and Forecasting the Mean Hourly Wind Speed Time Series Using GMDH-Based Abductive Networks. *Renewable Energy*, **34**, 7, 1686-1699, doi.org/10.1016/j.renene.2009.01.001.

Albani, A., Ibrahim, M. Z., and K. H., Yong 2011: Investigation on Wind Energy Potential at Sabah State of Malaysia; *Proc. University Malaysia Terengganu 10th International Annual Symposium (UMTAS 2011)*, Kuala Terengganu, Terengganu, Malaysia, Faculty of Science and Technology, 104-108 pp, http://s3.amazonaws.com/zanran_storage/www.umt.edu.my/ContentPages/2526533317.pdf.

Alexiadis M. C., Dokopoulos, P. S., and H. S., Sahsamanoglou, 1999: Wind Speed and Power Forecasting Based on Spatial Correlation Models, *IEEE Transactions on Energy Conversion*. **14**, 3, doi:10.1109/60.790962.

American Wind Energy Association (AWEA), 2017: U.S. Wind industry Fourth Quarter 2016 Market update. Fact Sheet. 2 pp, Available online at http://www.awea.org/4q2016.

Apt, J., 2007: The Spectrum of Power from Wind Turbines, *Journal of Power Sources*, **169**, 369-374, doi:10.1016/j.jpowsour.2007.02.077.

Archer, C. L., and M. Z., Jacobson, 2003: Spatial and temporal distributions of US winds and wind power at 80 m derived from measurements. *Journal of Geophysical Research: Atmospheres* **108**, D9, doi:10.1029/2002JD002076.

Archer, C. L., and M. Z., Jacobson, 2013: Geographical and Seasonal Variability of the Global "Practical" Wind Resources, *Applied Geography*, **45**, 119-130, doi.org/10.1016/j.apgeog.2013.07.006.

Archer, C. L., Colle, B. A., Veron, D. L., Veron, F., and M. J., Sienkiewicz, 2016: On the Predominance of Unstable Atmospheric Conditions in the Marine Boundary Layer Offshore of the U.S. Northeastern Coast, *Journal of Geophysical Research: Atmospheres*, **121**, 8869–8885, doi:10.1002/2016JD024896.

Bañuelos-Ruedas, F., Camacho Á. C., and S., Rios-Marcuello, 2011, Methodologies Used in the Extrapolation of Wind Speed Data at Different Heights and Its Impact in the Wind Energy Resource Assessment in a Region. *Wind Farm: Technical Regulations, Potential Estimation and, Siting Assessment*, G. O. Suvire, InTech.

Barthelmie, R. J., (1999), The Effects of Atmospheric Stability on Coastal Wind Climates, *Meteorol. Appl.*, **6**, 1, 39–47. doi:10.1017/S1350482799000961.

Bechrakis, D. A., Deane, J. P., and E. J., McKeogh 2004, Wind Resource Assessment of an Area Using Short Term Data Correlated To a Long Term Data Set, *Solar Energy*, **76**, 725-732, doi:10.1016/j.solener.2004.01.004.

Blanc, T. V., 1987: Accuracy of Bulk-Method-Determined Flux, Stability, and Sea Surface Roughness, Journal of Geophysical Research, **92**, C4, 3867-3876, doi:10.1029/JC092iC04p03867.

Bludszuweit, H., Domínguez-Navarro, J. A., and A., Llombar, 2008: Statistical Analysis of Wind Power Forecast Error, *IEEE Transactions on Power Systems*, **23**, 3, 983-991, doi:10.1109/TPWRS.2008.922526.

Bourassa, M. A., and Coauthors, 2009: Remotely Sensed Winds and Wind Stresses for Marine Forecasting and Ocean Modeling, 17 pp, http://hdl.handle.net/10261/81433.

Bremnes, J. B., 2004: Probabilistic Wind Power Forecasts Using Local Quantile Regression, *Wind Energy*, **7**, 1, 47-54, doi:10.1002/we.107.

Bremnes, J. B., 2006: A Comparison of a Few Statistical Models for Making Quantile Wind Power Forecasts, *Wind Energy*, **9**, 1-2, 3-1, doi:10.1002/we.182.

Brokish, K., and J., Kirtley, 2009: Pitfalls of Modeling Wind Power Using Markov Chains. *Proc.* Power Systems Conference and Exposition, 2009. PSCE '09. IEEE/PES, 1-6, doi:10.1109/PSCE.2009.4840265.

Brown, B. G., Katz, R. W., and A. H., Murphy, 1984: Time Series Models to Stimulate and Forecast Wind Speed and Wind Power, *Journal of Climate and Applied Meteorology*, **23**, 1184-1195, doi:10.1175/1520-0450(1984)023<1184:TSMTSA>2.0.CO;2.

Buller, A. T., and J., McManus, 1973: The Quartile-Deviation/Median- Diameter relationships of Glacial Deposits, *Sedimanetary Geology*, **10**, 135-146, file:///C:/Users/mbrianik/Desktop/Thesis/Read/114-%20QD.pdf.

Burt, M., and J., Firestone, 2016: Tall Towers, Long Blades and Manifest Destiny: The Migration of Land-based Wind from the Great Plains to the First State, Marine Science and Policy, 42 pp, https://www.ceoe.udel.edu/File%20Library/Research/Wind%20Power/Publication%20PDFs/Tall-Towers-Report-Sept-2016.pdf.

Carta J. A., Ramírez P., and S., Velázquez, 2008: A Review of Wind Speed Probability Distributions Used in Wind Energy Analysis: Case Studies in the Canary Islands. *Renewable and Sustainable Energy Reviews*, **13**, 933-955, doi:10.1016/j.rser.2008.05.005.

Celik, A. N., 2004: A Statistical Analysis of Wind Power Density Based on the Weibull and Rayleigh Models at the Southern Region of Turkey, *Renewable Energy*, **29**, 593-604, doi:10.1016/j.renene.2003.07.002.

Chang, A. T. C., and T. T., Wilheit, 1979: Remote Sensing of Atmospheric Water Vapor, Liquid Water, and Wind Speed at the Ocean Surface by Passive Microwave Techniques From the Nimbus 5 Satellite, *Radio Science*, **14**, 5, 793-802, 10.1029/RS014i005p00793.

Chang, Y. S., and D. S., Bai, 2001: Control Charts for Positively-Skewed Populations with Weighted Standard Deviations, *Quality and Reliability Engineering International*, **17**, 397-406, doi:10.1002/qre.427.

Crum, R. M., Anthony, J. C., Bassett, S. S., and M. F., Folstein, 1993: Population-Based Norms for the Mini-Mental State Examination by Age and Educational Level, *Journal of American Medical Association*, **269**,18, 2386-2391, doi:10.1001/jama.1993.03500180078038.

Damousis, I. G., Alexiadis, M. C., Theocharis, J. B., and P. S., Dokopoulos, 2004: A Fuzzy Model for Wind Speed Prediction and Power Generation in Wind Parks Using Spatial Correlation, *IEEE Transactions on Energy Conversion*, **19**, 2, doi:10.1109/TEC.2003.821865.

Danish Wind Industry Association (DWIA), 2003: Wind Energy Reference Manual Part 1: Wind Energy Concepts. Accessed 17 March 2017. [Available online at http://xn--drmstrre-64ad.dk/wp-content/wind/miller/windpower%20web/en/stat/unitsw.htm#roughness]

Davy, R. J., Woods, M. J., Russell, C. J., and P. A., Coppin, 2010: Statistical Downscaling of Wind Variability from Meteorological Fields, *Boundary-Layer Meteorol*,**135**, 161-175, doi:10.1007/s10546-009-9462-7.

Delaware Environmental Observing System (DEOS), 2016: About Us. Accessed 3 November 2016. [Available online at http://www.deos.udel.edu]

Delaware-Map, 2015: Delaware Topo Map. Delaware-Map.org, Accessed 7 March 2017. [Available online at http://www.delaware-map.org/topo-map.htm]

Dvorak, M. J., Corcoran, B. A., Hoeve, J. E. T., McIntyre, N. G., and M. Z., Jacobson, 2013: US East Coast Offshore Wind Energy Resources and Their Relationship to Peak-Time Electricity Demand. *Wind Energy*, **16**, 977-997, doi:10.1002/we.1524.

ESRI, 2016: How IDW Works. Accessed 21 March 2017. [Available online at http://desktop.arcgis.com/en/arcmap/10.3/tools/3d-analyst-toolbox/how-idw-works.htm]

European Wind Energy Association (EWEA), 2009: The Annual Variability of Wind Speed, Accessed 28 March 2017. [Available online at https://www.wind-energy-the-facts.org/the-annual-variability-of-wind-speed.html]

Everitt, B. S., and A., Skrondal, 2010, *The Cambridge Dictionary of Statistics: Fourth Edition*, Cambridge University Press, Cambridge University Press, 1-480.

Feijóoa, A., Villanuevaa, D., Pazos, J. L., and R., Sobolewski, 2011: Simulation of Correlated Wind Speeds: A Review, *Renewable and Sustainable Energy Reviews*, **15**, 2826-2832, doi:10.1016/j.rser.2011.02.032.

Fields, J., Tinnesand, H., and I., Baring-Gould, 2016: Distributed Wind Resource Assessment: State of the Industry. National Renewable Energy Laboratory / Contract No. DE-AC36-08GO28308 /TP-5000-66419/ 36 pp, [Available online at http://www.nrel.gov/docs/fy16osti/66419.pdf]

Fisher, N. I., 1987: Problems With Current Definitions of the Standard Deviation of Wind Direction, *Journal of Applied Climate and Meteorology*, **26**, 1522-1529, doi.org/10.1175/1520-0450(1987)026<1522:PWTCDO>2.0.CO;2.

Gamesa, 2015:Gamesa 2.0-2.5 MW Technological Evolution, Gamesa Corporation, Accessed 2 November 2016. [Available online at http://www.gamesacorp.com/recursos/doc/productos-servicios/aerogeneradores/catalogo- g9x-20-mw-eng.pdf]

Garmashov, A. V., and A. B., Polonskii, 2011: Wind Variability in the Northwestern Part of the Black Sea from the Offshore Fixed Platform Observation Data, *Russian Meteorology and Hydrology*, **36**, 12, 811-818, doi:10.3103/S1068373911120065.

Garvine, R. W., and W., Kempton, 2008: Assessing the Wind Field Over the Continental Shelf as a Resource for Electric Power. *Journal of Marine Research*, **66**, 751-773, doi:10.1357/002224008788064540.

Gilhousen, D. B., 1987: A Field Evaluation of NDBC Moored Buoy Winds. *Journal of Atmospheric and Oceanic Technology*, **4**, 94-104, doi.org/10.1175/1520-0426(1987)004<0094:AFEONM>2.0.CO;2.

Haan, C. T., 1977: *Statistical Methods in Hydrology*. The Iowa State Press, 378 pp.

Hall, F. F., Huffaker, R. M., Hardesty, .R. M., Jackson, M. E., Lawrence, T. R., Post, M. J., Richter, R. A., and B. F., Weber, 1984: Wind Measurement Accuracy of the NOAA Pulsed Infrared Doppler Lidar, *Applied Optics*, **23**,14, 2503-2506, doi.org/10.1364/AO.23.002503.

Hansen F. V., 1993: Surface Roughness Lengths, Final Report ADA274550, 51 pp, Accessed 20 February 2017. [Available online at http://www.dtic.mil/dtic/tr/fulltext/u2/a274550.pdf]

Harmel, R. D., Richardson, Hanson, C. L., and G. L., Johnson, 2002: Evaluating the Adequacy of Simulating Maximum and Minimum Daily Air Temperature with the Normal Distribution, *Journal of Applied Meteorology*, **41**, doi.org/10.1175/1520-0450(2002)041<0744:ETAOSM>2.0.CO;2.

Hasager, C. B., Peña, A., Christiansen, M. B., Astrup, P., Nielsen, M., Monaldo, F., Thompson, D., and P., Nielsen, 2008: Remote Sensing Observation Used in Offshore Wind Energy, *IEEE Journal of Selected Topics in Applied Earth Observations and Remote Sensing*, **1**,1, 67-79, doi:10.1109/JSTARS.2008.2002218.

Hennessey, J. P. Jr, 1977: Some Aspects of Wind Power Statistics, *Journal of Applied Meteorology*, **16**, 2, 119-128, http://journals.ametsoc.org/doi/pdf/10.1175/1520-0450(1977)016%3C0119:SAOWPS%3E2.0.CO%3B2.

Hiester, T. R., and W. T., Pennell, 1981: Strategies for Wind Turbine Siting, 512 pp. https://searchworks.stanford.edu/view/11126097.

Hodge, B. M., Lew, D., Milligan, M., Holttinen H., Sillanpää, S., Gómez-Lázaro, E., Scharff, R., Söder, L., Larsén, X. G., Giebel, G., and K. D., Flynn, 2012: Wind Power Forecasting Error Distributions: An International Comparison, DE-AC36-08GO28308, 9, file:///C:/Users/mbrianik/Desktop/Thesis/Read/109-nrel%20skew.pdf.

Holden, M. C., and J. F., Wedman, 1993: Future Issues of Computer-Mediated Communication: The Results of a Delphi Study, *Educational Technology Research and Development*, **41**, 4, 5-24, doi:10.1007/BF02297509.

Holttinen, H., Milligan, M., Kirby, B., Acker, T., Neimane, V., and T., Molinski, 2008: Using Standard Deviation as a Measure of Increased Operational Reserve Requirement for Wind Power. *Wind Engineering*, **32**,4, 355-377, http://citeseerx.ist.psu.edu/viewdoc/download?doi=10.1.1.176.4558&rep=rep1&type=pdf

Hsu, S. A., Eric A. Meindl, and D. B. Gilhousen, 1994: Determining the Power-Law Wind-Profile Exponent Under Near-Neutral Stability Conditions at Sea. *Journal of Applied Meteorology*, **33**, 6, 757-765, doi.org/10.1175/1520-0450(1994)033<0757:DTPLWP>2.0.CO;2.

Huffaker, R. M., and R. M., Hardesty, 1996: Remote Sensing of Atmospheric Wind Velocities Using Solid-State and CO/Sub 2/Coherent Laser Systems, *Proceedings of the IEEE*, **84**, 2, 181-204, doi:10.1109/5.482228.

Hughes, C. P., and D. E., Veron, 2015: Characterization of Low-Level Winds of Southern and Coastal Delaware. *American Meteorological Society*, **1**, 77-93, 10.1175/JAMC-D-14-0011.1.

International Electrotechnical Commission (IEC): 2017. 61400-12-1-2017. 558pp, https://webstore.iec.ch/publication/26603

International Encyclopedia of the Social Sciences (IESS), 2008: Normal Distribution. Encyclopedia.com. Accessed 21 March 2017, [Available online at http://www.encyclopedia.com/science-and-technology/mathematics/mathematics/normal-distribution#3]

Jagdish, P. K., and R. B., Campbell, 1996: Limit Theorems and Expansions, *Handbook of the Normal Distribution*, Owen, D.B., Cornell, R.G., Marcel Dekker, Inc. 145-184.

Johnson G.L., 2006, Wind Characteristics, *Wind Energy Systems*, Prentice Hall PTR, 2.1-2.62.

Jowder, F. A. L., 2006: Weibull and Rayleigh Distribution Functions of Wind Speeds in Kingdom of Bahrain, *Wind Engineering*, **30**, 5, 439-446, doi:10.1260/030952406779502650.

Justus, C. G., Hargraves, W. R., Mikhail, A., and D., Graber, 1977: Methods for Estimating Wind Speed Frequency Distributions, *Journal of Applied Meteorology*, **17**, 350-353, doi.org/10.1175/1520-0450(1978)017<0350:MFEWSF>2.0.CO;2.

Kahn, E., 1979: The Reliability of Distributed Wind Generators, *Electric Power Systems Research*, **2**, 1, 1-14, doi.org/10.1016/0378-7796(79)90021-X.

Katzenstein, W., and J., Apt, 2012: The Cost of Wind Power Variability, *Energy Policy*, **51**, 233-243, doi.org/10.1016/j.enpol.2012.07.032.

Kavasseri, R. G., and K., Seetharaman, 2009: Day-Ahead Wind Speed Forecasting Using F-ARIMA Models, *Renewable Energy*, **34**, 5, doi.org/10.1016/j.renene.2008.09.006.

Kempton, W., Pimenta, F. M., Veron, D. E., and B. A., Colle, 2010: Electric Power from Offshore Wind Via Synoptic-Scale Interconnection, *Proceedings of the National Academy of Sciences of the United States of America*; **107**, 16, 7240-7245, doi:10.1073/pnas.0909075107.

Klink, K., and C. J., Willmott, 1988: Principal Components of the Surface Wind Field in the United States: A Comparison of Analyses Based Upon Wind Velocity, Direction, and Speed, *International Journal of Climatology*, **9**, 293-308, doi:551.552:551.553.6(73):519.23.

Koeneman, B., and K., Link, 2017: New York Just Approved The Nation's Largest Offshore Wind Farm. 23ABC News, Accessed 9 March 2017. [Available online at http://www.turnto23.com/newsy/new-york-just-approved-the-nations-largest-offshore-wind-farm]

Korb, L. C., Gentry, B. M., and S. L., Xingfu, 1997, Edge Technique Doppler Lidar Wind Measurements with High Vertical Resolution, *Applied Optics*, **36**, 24, 5978-5983, doi.org/10.1364/AO.36.005976.

Krumbein W. C., 1936: The Use of Quartile Measures in Describing and Comparing Sediments. *American Journal of Science*, **32**, 98-111, doi:10.2475/ajs.s5-32.188.98.

Lambert, W. C., Merceret, F. J., Taylor, G. E., and J. G., Ward, 2003: Performance of Five 915-MHz Wind Profilers and Associated Automated Quality Control Algorithm in an Operational Environment, *Journal of Atmospheric and Oceanic Technology*, **20**, 1488-1495, doi:10.1175/1520-0426(2003)020<1488:POFMWP>2.0.CO;2.

Lange, M., 2004: On the Uncertainty of Wind Power Predictions—Analysis of the Forecast Accuracy and Statistical Distribution of Errors, *Journal of Solar Energy Engineering*, **127**, 2, doi:10.1115/1.1862266.

Leys, C., Ley, C., Klein, O., Bernard, P., and L., Licata, 2012: Detecting outliers: Do not Use Standard Deviation Around the Mean, Use Absolute Deviation Around the Median. *Journal of Experimental Social Psychology*, **49**, 764-766, 10.1016/j.jesp.2013.03.013.

Louie, H., 2014: Correlation and Statistical Characteristics of Aggregate Wind Power in Large Transcontinental Systems, *Wind Energy*, **17**, 793-810, doi:10.1002/we.1597.

Luo, W., Taylor, M. C., and S. R., Parker, 2008: A Comparison of Spatial Interpolation Methods to Estimate Continuous Wind Speed Surfaces Using Irregularly Distributed Data From England and Wales, *International Journal of Climatology*, **28**, 947-959, doi:10.1002/joc.1583.

Manwell, J. F., McGowan, J. G., and A. L., Rogers, 2010: *Wind Energy Explained: Theory, Design and Application Second Edition*, Wiley, 689 pp.

Maurmeyer, E. M., 1978: Geomorphology and Evolution of Transgressive Estuarine Washover Barriers Along The Western Shore of Delaware Bay. Ph.D. Dissertation, University of Delaware, 546 pp.

MidAmerica Energy, 2017: Wind Energy, Accessed 21 February 17, [Available online at https://www.midamericanenergy.com/wind-energy.aspx]

Mirhosseini, M., Sharifi, F., and A., Sedaghat, 2011: Assessing The Wind Energy Potential Locations In Province of Semnan In Iran, *Renewable and Sustainable Energy Reviews*, **15**, 1, 449-459, doi.org/10.1016/j.rser.2010.09.029.

Moffatt, J., and F. Nichol, 2007: Sediment Management plan: Rehoboth Bay, Sussex County, Delaware. DNREC Final Rep., 132 pp. [Available online at http://www.dnrec.delaware.gov/swc/Shoreline/Documents/Regional%20Sediment%20Management% 20Plan%20-%20Rehoboth%20Bay.pdf]

National Data Buoy Center (NDBC), 2016: Home. Accessed 14 November 2016 [Available online at http://www.ndbc.noaa.gov]

National Estuarine Research Reserve System (NERRS). 2015. System-wide monitoring program, Accessed 7 Apr 2015. [Available online at http://www.nerrsdata.org/]

National Renewable Energy Laboratory (NREL), 2017: Wind, Accessed 02 February 2017. [Available online at https://www.nrel.gov/wind/]

New York State Energy Research and Development Authority (NYSERDA), 2010: Wind Resource Assessment Handbook. Final Report/10-30, 203 pp, [Available online at file:///C:/Users/mbrianik/Downloads/wind-resource-assessment-toolkit%20(2).pdf]

Newman, J. F., and Klein, P. M., 2014: The Impacts of Atmospheric Stability on the Accuracy of Wind Speed Extrapolation Methods, *Resources*, **3**, 1, doi:10.3390/resources3010081.

Office of Efficiency & Renewable Energy (OERE), 2016: Grid Integration. Accessed 10 April 2017. [Available online at https://energy.gov/eere/wind/grid-integration]

Oswald, J., Raine, M., and H., Ashraf-Ball, 2008: Will British Weather Provide Reliable Electricity? *Energy Policy*, **36**, 3202-3215, doi:10.1016/j.enpol.2008.04.033.

Ozelkan, E., Chen, G., and B. B., Ustundag, 2016: Spatial Estimation of Wind Speed: A New Integrative Model Using Inverse Distance Weighting and Power Law, *International Journal of Digital Earth*, **9**, 8, 733-747, doi: 10.1080/17538947.2015.1127437.

Paulson, C. A., 1970: The Mathematical Representation of Wind Speed and Temperature Profiles in the Unstable Atmospheric Surface Layer. *Journal of Applied Meteorology*, **9**, 6, 857-861, doi.org/10.1175/1520-0450(1970)009<0857:TMROWS>2.0.CO;2.

Pimenta, F., Kempton, W., and R., Garvine, 2008, Combining Meteorological Stations and Satellite Data to Evaluate the Offshore Wind Power Resource of Southeastern Brazil, *Renewable Energy*, **33**, 11, 2375–2387, doi.org/10.1016/j.renene.2008.01.012.

Pishgar-Komleh, S. H., Keyhani, A., and P., Sefeedpari, 2014: Wind Speed and Power Density Analysis Based on Weibull and Rayleigh Distributions (A Case Study: Firouzkooh County of Iran), *Renewable and Sustainable Energy Reviews*, **42**, 313-322, doi.org/10.1016/j.rser.2014.10.028.

Rogers, A. L., Rogers, J. W., and J. F., Manwell, 2005: Comparison of The Performance of Four Measure–Correlate–Predict Algorithms, *Journal of Wind Engineering and Industrial Aerodynamics*, **93**, 243–264, doi:10.1016/j.jweia.2004.12.002.

Rosa, M. C, Anthony, J. C., Bassett, S. S., and M. F., Folstein, 1993: Population-Based Norms for the Mini-Mental State Examination by Age and Educational Level, *Journal of the American Medical Association*, **269** 2286-2391, doi:10.1001/jama.1993.03500180078038.

Rosenberg, B. V., 1983: *Microclimate: The Biological Environment,* Wiley-Interscience, *495 pp.*

Safari, B., and J., Gasore, 2010: A Statistical Investigation of Wind Characteristics and Wind Energy Potential Based on the Weibull and Rayleigh Models in Rwanda, *Renewable Energy*, **35**, 2874-2880, doi:10.1016/j.renene.2010.04.032.

Sorensen, P., Hansen, A. D., Andre, P., and C., Rosas, 2002: Wind Models for Simulation of Power Fluctuations from Wind Farms, *Journal of Wind Engineering and Industrial Aerodynamics*, **90**, 1381–1402, doi.org/10.1016/S0167-6105(02)00260-X.

Tagle, F., Castruccio, S., Crippa, P., and M. G., Genton, 2017: Assessing Potential Wind Energy Resources in Saudi Arabia with a Skew-t Distribution, *Pre*, 1-20, [Available online at: https://arxiv.org/pdf/1703.04312.pdf.]

Tennekes, H., 1972: The Logarithmic Wind Profile, *Journal of Atmospheric Sciences*, **30**, 234-238, doi:10.1175/1520-0469(1973)030<0234:TLWP>2.0.CO;2

To, A. P., and K. M., Lam, 1995: Evaluation of Pedestrian-Level Wind Environment Around a Row of Tall Buildings Using a Quartile-Level Wind Speed Descriptor, *Journal of Wind Engineering and Industrial Aerodynamics*, **54**, 55, 527-541, doi.org/10.1016/0167-6105(94)00069-P.

Torres, J. L., García, A., De Blas, M., and A., De Francisco, 2005: Forecast of Hourly Average Wind Speed With ARMA Models In Navarre (Spain), *Solar Energy*, **79**, 1, 65-77, doi.org/10.1016/j.solener.2004.09.013.

Trauth, M. H., 2015, MATLAB Recipes for Earth Sciences: Fourth Edition, Springer Science & Business Media, 436 pp.

United States Department of Energy (USDE), 2015: Wind Vision: A New Era for Wind Power in the United States. DOE/GO-102015-4557. 110 pp, [Available online at https://energy.gov/eere/wind/maps/wind-vision]

Weekes S. M., and A. S., Tomlin, 2014: Comparison Between the Bivariate Weibull Probability Approach and Linear Regression for Assessment of the Long-Term Wind Energy Resource Using MCP, *Renewable Energy*, **68**, 529-539, doi.org/10.1016/j.renene.2014.02.020.

Wind Exchange, US Department of Energy, 2010: Utility Scale Land-Based 80-Meter Wind Maps. Accessed 10 march 2017. [Available online at http://apps2.eere.energy.gov/wind/windexchange/wind_maps.asp]

Wiser, R., and M., Bolinger, 2015: 2015 Wind Technologies Market Report. 102 pp, [Available online at https://energy.gov/sites/prod/files/2016/08/f33/2015-Wind-Technologies-Market-Report-08162016.pdf]

Wolf-Gerrit. F., 2013: Long-Term Wind Resource and Uncertainty Estimation Using Wind Records from Scotland as Example, *Renewable Energy*, **50**, 1014-1026, doi.org/10.1016/j.renene.2012.08.047.

Yunus, K., Thiringer, T., and P., Chen, 2016: ARIMA-Based Frequency-Decomposed Modeling of Wind Speed Time Series, *IEEE Transactions on Power Systems*, **31**, 4, 2546-2556, doi:10.1109/TPWRS.2015.2468586.

Zoumakis, N. M., 1992: The Dependence of the Power-law Exponent on Surface Roughness and Stability in a Neutrally and Stably Stratified Surface Boundary Layer, *Atmópshera*, **6**, 79-83, http://www.ejournal.unam.mx/atm/Vol06-1/ATM06105.pdf.